

UV-B radiation affects plant volatile emissions and shade avoidance responses

UV-B straling beïnvloedt de emissie van vluchtige stoffen en het ontwijken van schaduw door planten
(met een samenvatting in het Nederlands)

Proefschrift

ter verkrijging van de graad van doctor aan de Universiteit Utrecht op gezag van de rector magnificus, prof.dr. G.J. van der Zwaan, ingevolge het besluit van het college voor promoties in het openbaar te verdedigen op woensdag 2 september 2015 des middags te 2.30 uur

door

Paulien Gankema
geboren op 22 augustus 1984 te Emmen

Promotoren: Prof.dr. L.A.C.J. Voesenek

Prof.dr. R. Pierik

Contents

Chapter 1	General introduction	5
Chapter 2	A plant chamber system with PTR-TOF-MS to study the effects of pollution on plant volatile emissions	15
Chapter 3	Ultraviolet-B radiation alters tomato volatile emissions	27
Chapter 4	UV-B regulates volatile emission in <i>Arabidopsis thaliana</i> independent from the UV-B photoreceptor UVR8	43
Chapter 5	Crosstalk between UV-B and R:FR signalling pathways regulates elongation in <i>Arabidopsis thaliana</i>	49
Chapter 6	General discussion	65
References		69
Nederlandse samenvatting		80
Dankwoord		82
Curriculum vitae		85

General introduction

As sessile organisms, plants have to deal with the challenges their environment provides. Often, this environment includes other plants growing in close proximity. Since these neighbours have access to the same pool of resources as the focal plant they are direct competitors for resources such as light, water and nutrients. To optimise their fitness, plants have evolved intricate signalling pathways to process a variety of cues from their environment and subsequently display optimal growth and survival strategies. These cues can be visual (light quality and quantity), olfactory (volatile emissions), chemical (root and microbial exudates), based on nutrients (water, minerals) or actual tactile contact with other organisms (touching or invasive). The signal transduction networks that process these cues are complex, involving hormones and proteins, regulating gene expression and often balanced by (multiple) negative feedback loops. Moreover, these signalling networks interact. This thesis investigates how ultraviolet (UV)-B radiation affects (i) the emission of volatiles and (ii) shade avoidance response to changes in light quality. This chapter introduces these visual and olfactory signals and shortly reviews current knowledge on the associated physiological and signalling responses, before laying out the structure of this thesis.

Volatiles

All plants seem to emit volatile organic compounds (VOCs; Niinements *et al.*, 2004; Arimura *et al.*, 2005), resulting in global yearly emissions of over 1000 Tg C year⁻¹ (Guenter *et al.*, 2006). Plants emit VOCs constitutively as well as in an inducible fashion (Scutareanu *et al.*, 2003) from floral and vegetative plant parts (Unsicker *et al.*, 2009). VOC blends consist mainly of terpenes and green leaf volatiles, in addition to volatile plant hormones like ethylene and methyl salicylate and damage-associated methanol (Von Dahl *et al.*, 2006). Green leaf volatiles (GLVs) are a group of six-carbon aldehydes and alcohols and their respective esters that are derived from fatty acids and embody the typical smell of freshly-mowed grass. Terpenes are usually classified based on the amount of carbons in their backbone into hemiterpenes (C₅), monoterpenes (C₁₀), sesquiterpenes (C₁₅), diterpenes (C₂₀) and homoterpenes (>C₂₀). These volatile terpenes have been investigated frequently because of their role in ecological interactions (Heil 2008). Their biosynthesis and regulation is discussed in the following sections, after which the induction, ecology and evolution of VOC emissions are covered.

Biosynthesis of volatile terpenes

Volatile terpenes, or terpenoids, are synthesised (Fig 1.1) from two five-carbon precursors: isopentenyl diphosphate (IPP) and its isomer dimethylallyl diphosphate (DMAPP; McGarvey and Croteau 1995). IPP and DMAPP are synthesised by the compartmentally separated mevalonic (MVA) and methylerythritol 4-phosphate (MEP) pathways. The plastidic MEP pathway produces DMAPP and IPP from pyruvate and glyceraldehyde 3-phosphate for synthesis of monoterpenes (C₁₀) and diterpenes (C₂₀; reviewed by Lichtenthaler 1999). The MVA pathway produces DMAPP and IPP from acetyl-CoA for synthesis of sesquiterpenes (C₁₅), although this separation of precursor pools is not absolute (Hemmerlin *et al.*, 2003; reviewed by Hemmerlin *et al.*, 2012). Together, DMAPP and IPP form prenyl diphosphates, which serve as building blocks for the formation of larger terpenes. Monoterpenes are synthesised from geranyldiphosphate (GPP) formed by GPP synthase (GPS; Burke and Croteau 2002a), sesquiterpenes are synthesised from farnesyldiphosphate (FPP) formed by FPP synthase (FPS; Matsushita *et al.*, 1996), and diterpenes are synthesised from geranylgeranyldiphosphate (GGPP) formed by GGPP synthase (GGPS; Burke and Croteau 2002b). Terpene synthases (TPSs) convert these precursors into specific terpene products, creating a great diversity of terpenes with many species-specific compounds. TPSs can often use multiple substrates or create multiple products, at least *in vitro* (Degenhardt *et al.*, 2009). Terpene diversity is further increased by enzymes that modify the initial products, thereby often enhancing volatility or altering olfactory properties (Dudareva *et al.*, 2004). Besides volatile terpenoids, other terpenoids with a wide range of functions are produced from the same IPP and DMAPP precursor pools.

These include chlorophylls, carotenoids, membrane sterols and terpenoid hormones like brassinosteroids, gibberellins and abscisic acid (McGarvey and Croteau, 1995; Lange and Ghassemian 2003).

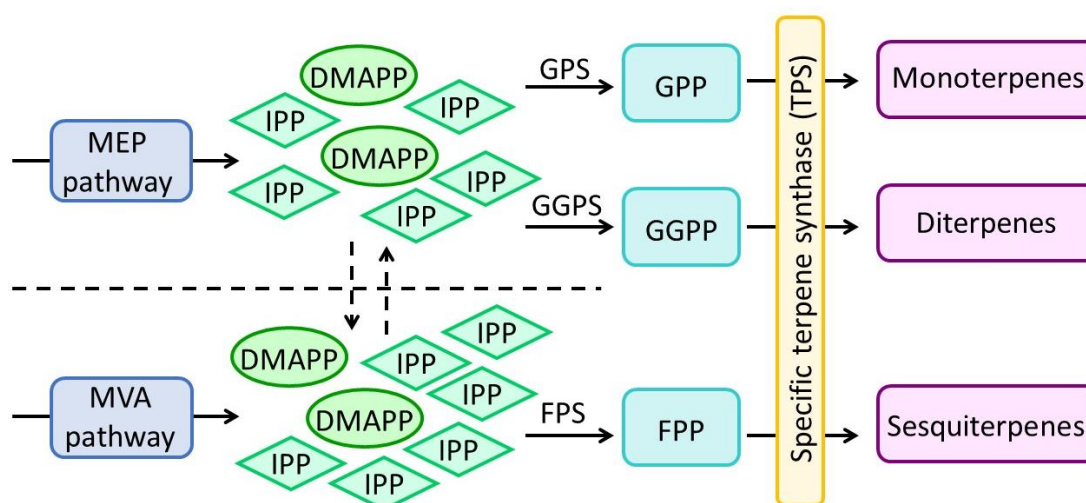


Figure 1.1 Schematic overview of volatile terpene biosynthesis. The MVA and MEP pathways form IPP and DMAPP. These five-carbon precursors are used to form prenyl diphosphate building blocks for larger terpene products. Monoterpenes are synthesised from GPP formed by GPS, diterpenes from GGPP formed by GGPS, sesquiterpenes from FPP formed by FPS, each by specific terpene syntases. Abbreviations: MVA, mevalonic acid; MEP, methylerythritol 4-phosphate; IPP, isopentenyl diphosphate; DMAPP, dimethylallyl diphosphate; GPP, geranyldiphosphate; GPS, GPP synthase; FPP, farnesyldiphosphate; FPS, FPP synthase; GGPP, geranylgeranyldiphosphate; GGPS, GGPP synthase.

Regulation of volatile terpene biosynthesis and emission

Transcriptional regulation of *TPS* genes plays an important role in controlling volatile terpene biosynthesis (Dudareva *et al.*, 2013). Up-regulation of *TPS* genes is found in practically all studied species, where this induction usually also correlates with increased emission of the terpene product, e.g. in tomato (Van Schie *et al.*, 2007), maize (Shen *et al.*, 2000; Schnee *et al.*, 2002), spruce (Miller *et al.*, 2005), lotus (Arimura *et al.*, 2004b) and poplar (Arimura *et al.*, 2004a). In addition, herbivore-induced volatile emissions are causally linked with elevated levels of the herbivore defence hormone jasmonic acid (JA; Walling 2000; Ament *et al.*, 2004). Furthermore, changes in volatile emissions related to developmental stage are mainly regulated at the level of gene expression (Dudareva *et al.*, 2000; McConkey *et al.*, 2000; Muhlemann *et al.*, 2012). Theoretically, specific regulation of volatile terpenoid biosynthesis will likely occur downstream of the IPP and DMAPP precursors, since volatile terpenes represent only a fraction of the total amount of metabolites produced from these shared precursor pools. However, *TPS* induction may not always be sufficient and an increased flux through the entire pathway might be required for significant induction of terpene production. Herbivore-induced expression of precursor biosynthesis genes (Hui *et al.*, 2003; Kant *et al.*, 2004; Ament *et al.*, 2006) is consistent with transcriptional regulation of volatile terpenoid production upstream of *TPS* genes.

Once synthesised, most volatile terpenes are probably promptly emitted. As described above, terpene emissions often correlate with induced *TPS* expression. Besides, most higher plant species lack specialised storage structures for terpenoids (Niinements *et al.*, 2004) and although limited amounts of terpenes can be stored in leaves, the volatility of most mono and sesquiterpenes is high enough to allow significant release into the air (Dudareva *et al.*, 2004). This will certainly be the case for induced emissions, where *de novo* synthesis will result in steep diffusion gradients (Paré and Tumlinson 1997; Miller *et al.*, 2005). Potential physiological and physiochemical constraints on VOC emissions are discussed elaborately by Niinements *et al.* (2004).

Induction of volatile emissions

Besides being emitted constitutively (Farag and Paré 2002; Leitner *et al.*, 2005; Blande *et al.*, 2010), volatile emissions are inducible by various biotic and abiotic environmental factors.

Herbivore species, whether directly attacking the plant or merely ovipositing their eggs (Wegener *et al.*, 2000; Heil 2008), are well-known to elicit plant volatile responses. Examples of herbivores inducing plant VOC emissions include aphids in birch and alder trees (Blande *et al.*, 2010), weevils in pine (Heijari *et al.*, 2011), spider mites in lotus and tomato (Arimura *et al.*, 2004b; Kant *et al.*, 2004) and caterpillars in cotton, *Arabidopsis* and tomato (Paré and Tumlinson 1997; Van Poecke *et al.*, 2001; Farag and Paré 2002). The qualitative composition of the induced blend depends on the type of herbivory (Leitner *et al.*, 2005) or even on the species attacking (Dicke 1999). Damaging the plant mechanically often induces a somewhat similar but much less complex volatile blend (Arimura *et al.*, 2005). Microbes can also induce plant volatiles emission, whether they are pathogenic or symbiotic (Leitner *et al.*, 2008). Examples include *Pseudomonas* in tobacco and bean (Croft *et al.*, 1993; Huang *et al.*, 2003) and the fungus *Sclerotium* in peanut (Cardoza *et al.*, 2002).

Abiotic factors also greatly affect plant VOC emissions. Volatile emissions generally increase with increasing temperature (Staudt and Bertin 1998; Loreto and Schnitzler 2010) and light intensity (Takabayashi *et al.*, 1994a; Loughrin *et al.*, 1994; Turlings *et al.*, 1995). The effect of light intensity can differ per volatile compound (Gouinguéné and Turlings 2002), thus altering the VOC blend, but is independent of the circadian rhythm (Arimura *et al.*, 2008). Changes in light quality can also affect VOC emissions; a decrease in the red to far-red ratio reduces plant emissions (Kegge *et al.*, 2013), while UV-B differentially affects volatile compounds and plant species. For example, UV-B increases VOC emissions in basil and oak as well as in subarctic peatland in a three-year field experiment (Harley *et al.*, 1996; Johnson *et al.*, 1999; Tiiva *et al.*, 2007); its effect is species and VOC-type specific in Mediterranean shrubs (Llusià *et al.*, 2012); whereas UV-B does not affect the emission of any VOC type in soy bean (Winter and Rostás 2008). Other abiotic factors that can alter plant volatile emissions include drought (Takabayashi *et al.*, 1994a; Gouinguéné and Turlings 2002; Llusià and Peñuelas 1998), elevated CO₂ and ozone (O₃; reviewed by Loreto and Schnitzler 2010).

Variation in information

As described in the previous section, emitted VOC blends depend on many environmental factors, including abiotic factors like temperature, light, CO₂ and O₃, as well as biotic factors like herbivore and pathogen attack. Besides, volatile blends differ between plant species and even between accessions and cultivars (Takabayashi *et al.*, 1991; Scutareanu *et al.*, 2003; Snoeren *et al.*, 2010). They can even depend on leaf developmental stage (Takabayashi *et al.*, 1994b). Although blends emitted by the same species attacked by different herbivores are less diverse than blends from different species (Takabayashi *et al.*, 1991; Dicke 1999), the variation is sufficient for specialised predators to distinguish between them (De Moraes *et al.* 1998; Drukker *et al.*, 2000). It is therefore clear that plant volatile blends contain intricate putative information about plant identity and environmental conditions, which could be 'read' by any receiving organism that is able to sense the variation of the blend.

Ecological functions of volatiles

A well-known function of plant volatiles is the attraction of pollinators. Floral scent is the most important channel of communication between flowering plants, their pollinators and enemies that even drives the evolution of these species (Raguso 2008). In this thesis, however, we confine to volatiles emitted by vegetative plant parts.

A function of VOCs that has recently received renewed attention is their potential to quench oxygen radicals *in planta* (Peñuelas and Llusià 2003). Monoterpenes could protect a plant against these radicals

Chapter 1

created upon abiotic stress by stabilising membranes or acting directly as antioxidants, taking over this role from isoprene (Monson *et al.*, 2013). Such a protective role for monoterpenes was already shown in *Quercus ilex* upon ozone damage (Loreto *et al.*, 2004) and is discussed in detail by Vickers *et al.* (2009).

Besides their potential quenching properties, VOCs can function as signals. Their role as signals between plants and higher trophic levels has been long established. Herbivore-induced volatile blends can repel subsequent attackers, from aphids, spider mites and thrips (Dicke and Dijkman 1992; Bernasconi *et al.*, 1998; Delphia *et al.*, 2007) to ovipositing adults, thereby fending off the next generation of herbivores (De Moraes *et al.*, 2001). Moving up one trophic level, herbivore-induced volatiles can attract a wide array of prey-seeking predators. Sabelis and van de Baan (1983) already demonstrated that volatiles of spider mite-infested leaves attract predatory mites, which was subsequently confirmed in many other plant species (Dicke and Sabelis 1988). It is now clear that besides predators, also parasitoids (Wegener *et al.*, 2000; Van Poecke *et al.*, 2001) and even birds (Mäntylä *et al.*, 2008) use herbivore-induced volatiles as signals to locate their prey. Since the emitted blends are very specific, specialised predators can distinguish between plants infested with prey and non-prey, or host and non-host, herbivores (De Moraes *et al.*, 1998).

A relatively new direction of research focuses on the role of volatiles in plant-pathogen relations. As described above, pathogen attack can induce volatile emissions. In return, volatiles can increase resistance against pathogens like *Botrytis cinerea* (Kishimoto *et al.*, 2005), potentially by inducing resistance-related gene expression (Arimura *et al.*, 2000).

VOCs have also increasingly been shown to function as signals within and between plants. Emitted volatiles can relay information between the branches of a plant, instead of or in addition to signals travelling through the vasculature, as shown in lima bean, poplar and blueberry (Heil and Silva Bueno 2007; Frost *et al.*, 2007; Rodriguez-Saona *et al.* 2009). Volatiles can also act in hostile plant-plant relations, leading parasitic plants to their host plant (Runyon *et al.*, 2006), or inhibiting germination (Gardner *et al.*, 1990; Karban 2007). Furthermore, plants can ‘eavesdrop’ on their neighbours: volatile signals from wounded or attacked plants activate herbivore defence genes and increase volatile emission in neighbouring plants (Arimura *et al.*, 2000; Arimura *et al.*, 2001; Engelberth *et al.*, 2004; Conrath *et al.*, 2006). This effect is often only measurable upon subsequent attack (Ton *et al.*, 2006; Kessler *et al.*, 2006). The eavesdropping plant that is ‘primed’ by its neighbours’ volatiles is significantly better protected against herbivores: their increased VOC emissions attract predators more strongly (Bruin *et al.*, 1992), they receive less herbivore damage (Karbon *et al.*, 2000) and herbivore populations grow slower on these plants (Hildebrand *et al.*, 1993; Kessler *et al.*, 2006). Although a sensory mechanism has never been identified, plants seem to be able to detect volatile signals very well: responses to neighbours can be cultivar-dependent (Peterson *et al.*, 1999) and single synthetic volatiles can partially activate, but never evoke the complete response (Bate and Rothstein 1998; Arimura *et al.*, 2001).

Evolution of volatile emission

Evolutionary theories on plant volatile signals in a multitrophic context have been discussed extensively (Dicke and Van Loon 2000; Arimura *et al.*, 2005; Dicke and Baldwin, 2010). Although it is clear how plant volatile emissions benefit neighbouring plants and higher trophic levels, this does not explain how these emissions evolved. In fact, if volatile signals benefit plant competitors and herbivores, this provides a selective pressure against those signals. As for the beneficial effects of attracting predators to act as ‘bodyguards’, and the potential positive effect on next-of-kin neighbours, these forces are disputable in shaping the evolution of the focal plant. In contrast, a function as within-plant signals does provide a positive selective pressure for the evolution of such signals. In this respect, an important outstanding question is to what extent plants can distinguish between volatile blends: are plants able to respond to their own and not to a neighbouring plants VOC blend? (Dicke *et al.*, 2003). In addition, the property of volatiles to quench oxygen radicals clearly benefits the producing plant (Vickers *et al.*, 2009). VOCs could

also have multiple functions, which would lower evolutionary costs, potentially shifting the balance to the positive (Nielson *et al.*, 2013). Certainly, both mechanistic experimental studies as well as long-term field trials are needed to test evolutionary theories and reveal the fitness value of plant volatiles (Frost *et al.*, 2008).

Sensing changes in the light environment

Light is the key source of energy for plant life. On the short-wavelength side of the solar light spectrum (Fig 1.2), there is ultraviolet (UV) radiation: UV-C (100-280 nm), UV-B (280-315 nm) and UV-A (315-400 nm). Blue (B) light is at 400-500 nm, then comes green (G) light (500-600 nm), followed by red (R: 600-700 nm). Finally, far-red is on the long-wavelength side of the visual spectrum (FR: 700-800 nm). The part of the spectrum that a plant can use for photosynthesis, is commonly called photosynthetically active radiation (PAR: 400-700 nm). Plants mainly use B and R for photosynthesis. However, in addition to B and R, they can also detect UV-B and changes in FR with specialised photoreceptors. B is perceived via three distinct receptor families: cryptochromes and phototropins, of which multiple versions exist to work optimal at low or high fluence rates, and ZTL/FKF1/LKP2 (Kami *et al.*, 2010). In addition, phytochromes can also absorb B, but are especially effective at signalling R and FR. Perception of FR by the active form of the phytochrome converts the receptor into its inactive form, which in turn can absorb R to convert back into the active form (Quail 2002). Relative phytochrome activity thus directly reflects the R:FR ratio, with low R:FR ratios resulting in a relatively large pool of inactive phytochrome. UV-B light is perceived by the photoreceptor UV RESISTANCE LOCUS 8 (UVR8; Rizinni *et al.*, 2011). The structure of this seven-bladed β -propeller protein uniquely forms its own UV-B chromophore from dedicated tryptophan residues at the interface of two UVR8 molecules forming a dimer (Christie *et al.*, 2012, Wu *et al.*, 2012). Excitation of this chromophore by UV-B absorption quickly monomerises the protein (Voityuk *et al.*, 2014), which leads to a signalling cascade activating UV-B responses (Heijde and Ulm 2012). A detailed account of the structure and molecular interactions of UVR8 is given by Jenkins (2014).

The following sections describe the physiological responses of plants to low R:FR ratios and UV-B light and their corresponding signal transduction networks.

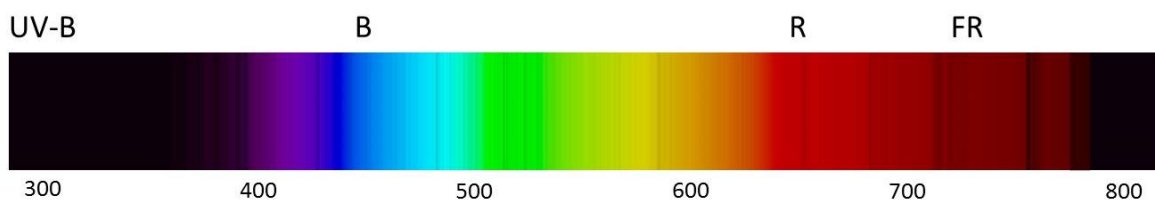


Figure 1.2 The solar spectrum, with ultraviolet (UV)-B, blue (B), red (R) and far-red (FR) light indicated at their respective wavelengths (in nm).

UV-B

UV-B levels on the Earth's surface

UV-B levels vary over time and space. The solar angle largely determines the radiation level, creating the highest UV-B levels in summer and around solar noon. For the same reason, UV-B levels vary with latitude. In addition, solar UV-B increases modestly with elevation above sea level: about 4 to 18 % per 1000 m elevation. Furthermore, the stratospheric ozone layer, which absorbs a significant portion of solar UV-B, has a natural latitudinal gradient; it is thinnest at the equator and thickest at the poles. Therefore, geographically, the highest UV-B levels are observed at the equator and at high altitude (Caldwell *et al.*, 1989). The last 50 years have seen increased concern over potential changes in UV-B levels at the Earth's

surface that are still relevant today. Concern over the consequences of stratospheric ozone depletion and concomitant impacts on individuals and ecosystems originates in the late 1960s, with the Antarctic ozone hole first noted in 1985 (Solomon 1990). Because of the successful implementation of the 1987 Montreal Protocol, recovery of the stratospheric ozone layer was projected for the second half of this century (McKenzie *et al.*, 2011). However, (i) synergistic effects between ozone depletion and global warming could substantially delay the recovery of the ozone layer (Hartmann *et al.*, 2000), (ii) climate change will lead to longer droughts and reduced cloud cover in agronomically important regions like the Mediterranean, South-West U.S.A. and Australia, increasing UV-B doses in these regions (IPCC 2007) and (iii) decreased vegetation cover due to desertification and deforestation will also enhance UV-B doses (UNEP 2011). Many organisms and ecosystems will thus experience an enhanced UV-B radiation environment in the next decades, with important consequences for terrestrial ecosystems (Ballaré *et al.*, 2011).

UV-B levels in the Netherlands were about $8 \text{ kJ m}^{-2} \text{ d}^{-1}$ in June 1993, and were expected to rise (Van de Staaij *et al.*, 1993). This is consistent with measurements of UV-B and PAR levels in the spring and summer of 2014 at Utrecht Science Park, the Netherlands, which add up to a daily UV-B dose of about $13 \text{ kJ m}^{-2} \text{ d}^{-1}$ (Fig 1.3).

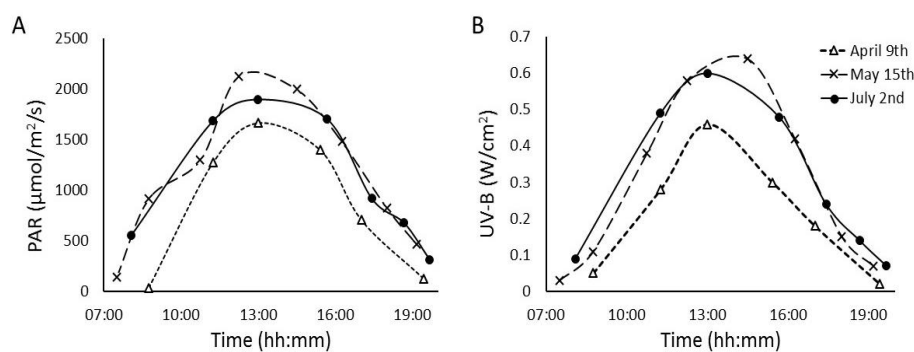


Figure 1.3 (A) Photosynthetically active radiation (PAR) and (B) UV-B radiation at Utrecht Science Park, the Netherlands, in the spring and summer of 2014.

UV-B damages plants

When the high-energy photons of UV-B radiation hit live plant material, this inevitably causes damage, either directly or indirectly through the formation of radicals. Most notably, UV-B causes damage to DNA and the photosystems, thus impairing photosynthesis. UV-B damage to DNA leads specifically to the formation of pyrimidine dimers that block transcription (Britt 1996). These can be removed by (i) specific light-dependent photoreactivation by photolyases (directly reversing the pyrimidine dimers), or (ii) general nucleotide excision repair that can also happen in the dark (Britt 1996). Despite these repair mechanisms, mutations still persist and accumulate over time (Ries *et al.* 2000). Although in some cases UV-B increases chlorophyll levels, UV-B negatively affects photosynthesis in species across the plant kingdom, including in a three-year field experiment (Ziska *et al.*, 1992; Mark and Tevini 1997; Deckmyn and Impens 1997; Hao *et al.*, 2000; Moon *et al.*, 2011; Albert *et al.*, 2012; Hui *et al.*, 2013).

Physiological responses to UV-B

The physiological effects of UV-B are well described in a wide range of plants, from tomato and rice to sunflower (Huang *et al.*, 1997; Mark and Tevini 1997; Hao *et al.*, 2000). UV-B-exposed plants have decreased height, shorter internodes, increased axillary branching and smaller leaf area, with their leaves sometimes curling to further decrease the exposed leaf area (reviewed by Caldwell *et al.*, 1998; Jansen *et al.*, 1998; Ballaré *et al.*, 2011). Also, increased UV-B exposure reduces yield, e.g. in maize, pea and bean (Mark *et al.*, 1996; Mepsted *et al.*, 1996; Saile-Mark and Tevini 1997). An important adaptation is the

production of UV-B-absorptive compounds such as flavonoids that protect the plant against UV-B damage (Li *et al.*, 1993). This is found across a wide range of species: in *Arabidopsis thaliana*, crops like tobacco and tomato, and in field-grown tropical and arctic species (Searles *et al.*, 1995; Ballaré *et al.*, 1995; Björn *et al.*, 1999; Demkura *et al.*, 2010; Demkura and Ballaré 2012). When growing in elevated UV-B for many generations, e.g. at high altitude, plants can successfully adapt to UV-B exposure to the extent that UV-B no longer affects their growth (Ziska *et al.*, 1992).

UV-B can enhance stress resistance

Physiological adaptations of plants to UV-B can also be advantageous. UV-B makes plant leaves less palatable, reducing herbivore (population) growth and resulting in less herbivore damage (Caldwell *et al.*, 2007). Moreover, UV-B activates part of the herbivore defence pathway (Demkura *et al.*, 2010) and induces herbivore defence gene expression (Mackerness *et al.*, 1999; Izaguirre *et al.*, 2003). Exposure to UV-B also improves abiotic stress tolerance, potentially by priming plant stress acclimations (Wargent and Jorden 2013).

UV-B signalling responses

As described above, perception of UV-B by the UVR8 photoreceptor dimer leads to quick monomerisation of this protein, activating UV-B signalling responses. Figure 1.4 gives a schematic overview of the UV-B signal transduction pathway (reviewed by Tilbrook *et al.*, 2013). First, UVR8 binds to the E3 ubiquitin ligase CONSTITUTIVELY PHOTOMORPHOGENIC (COP)1 in the nucleus (Favory *et al.*, 2009), relieving COP1 repression and activating the bZIP transcription factor LONG HYPOCOTYL IN FAR-RED (HY)5 (Brown *et al.*, 2005). HY5 then activates UV-B response genes (Ulm *et al.*, 2004; Oravec *et al.*, 2006). In addition to these positive regulators, the pathway has a “switch-off” mechanism that is essential for optimal plant growth and development. REPRESSOR OF UV-B PHOTOMORPHOGENESIS (RUP)1 and RUP2 regenerate UVR8 homodimers by disrupting the UVR8–COP1 interaction, which halts UV-B signalling (Heijde and Ulm 2013). Besides this UVR8-dependent pathway that needs only low UV-B fluence rates to be activated, higher UV-B fluence rates also activate UVR8-independent signalling pathways (Brown and Jenkins 2008). An example is the UV-B-damage activated MAPK pathway which is induced by DNA pyrimidine dimers (Gonzalez Besteiro *et al.*, 2011). While several physiological UV-B responses are mediated by UVR8, including growth responses and UV-B-enhanced pathogen resistance (Demkura and Ballaré 2012; Tilbrook *et al.*, 2013), for most responses, including the dynamics of phytohormones (Sävenstrand *et al.*, 2004; Hectors *et al.*, 2012) and production of secondary metabolites (Jansen *et al.*, 2008; Kusano *et al.*, 2011), it is yet unknown if they are controlled through the UVR8 pathway.

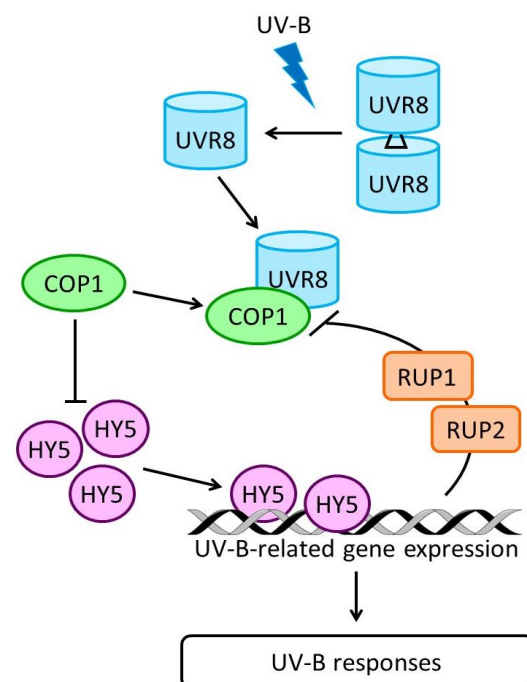


Figure 1.4 UV-B activates the UVR8 signalling pathway. UVR8 dimers monomerise upon reception of UV-B and bind to COP1. HY5 is released from COP1 repression, binds to DNA and activates UV-B response genes. RUP1 and RUP2 form a “switch-off” mechanism that regenerates UVR8 dimers. Abbreviations: UVR8, UV RESISTANCE LOCUS 8; COP1, CONSTITUTIVELY PHOTOMORPHOGENIC 1; HY5, LONG HYPOCOTYL IN FAR-RED 5; RUP, REPRESSOR OF UV-B PHOTOMORPHOGENESIS.

Not much is known about the role of hormones in UV-B signalling and responses. However, reduced expression levels of UV-B-inducible genes in BR-deficient mutants (Sävenstrand *et al.*, 2004) and increased UV-B sensitivity of auxin mutants (Hectors *et al.*, 2012) hint to involvement of at least BR and auxin in UV-B responses.

Plant-plant competition for light

Plants perceive their proximate neighbours through changes in light quantity and quality. Since green plant parts absorb B and R light for photosynthesis while reflecting FR and G light, the proximity of neighbours can be sensed by FR-enrichment leading to a drop in the R:FR ratio, while a decrease of PAR and B light levels indicates actual shading (Ballaré *et al.*, 1990; Casal 2013; Pierik and de Wit 2013). Because of horizontal FR reflection by vertical plant structures, a reduced R:FR ratio may be observed at relatively large inter-plant distances (Smith *et al.*, 1990). Reduced R:FR has therefore been described as the earliest cue in neighbour detection, but touching of leaf tips may precede this early signal in rosette-forming species (De Wit *et al.*, 2012). Plants respond to a drop in R:FR by expressing the shade avoidance syndrome (SAS, reviewed by Casal 2012). This phenotype includes (i) an upward movement of the leaves (hyponasty), created by elongation of the abaxial cells at the base of the petiole (Polko *et al.*, 2012), (ii) elongation of upward-growing plant parts like stems, petioles and hypocotyls and (iii) increased apical dominance. As a result, the plant reduces the degree of current or future shading by neighbours and increases its photosynthetic potential.

Low R:FR signalling responses

Figure 1.5 gives a schematic overview of the main players in the R:FR signal transduction network. As described above, R:FR ratios are detected by the phytochrome photosensors, with low R:FR leading to their inactivation. Since active phytochrome interacts with PHYTOCHROME INTERACTING FACTORS (PIFs) in the nucleus and targets them for degradation, low R:FR releases this repression and allows PIFs to be active and abundant. As a consequence, these basic-helix-loop-helix (bHLH) transcription factors bind to DNA, control transcription of target genes and activate shade avoidance responses within minutes (Lorrain *et al.*, 2008). PIF action is repressed by DELLA proteins, which bind PIF4 and thereby prevent it from binding DNA (De Lucas *et al.*, 2008). DELLAs thus inhibit SAS, and DELLA abundance is down-regulated by low R:FR (Djakovic-Petrovic *et al.*, 2007). DELLA stability is primarily controlled by gibberellic acid (GA), which induces DELLA degradation, but other hormonal routes to control these growth-repressing proteins might also exist (Achard *et al.*, 2003; Fu and Harberd 2003; Achard *et al.*, 2007; Pierik *et al.*, 2009). In addition to PIFs and

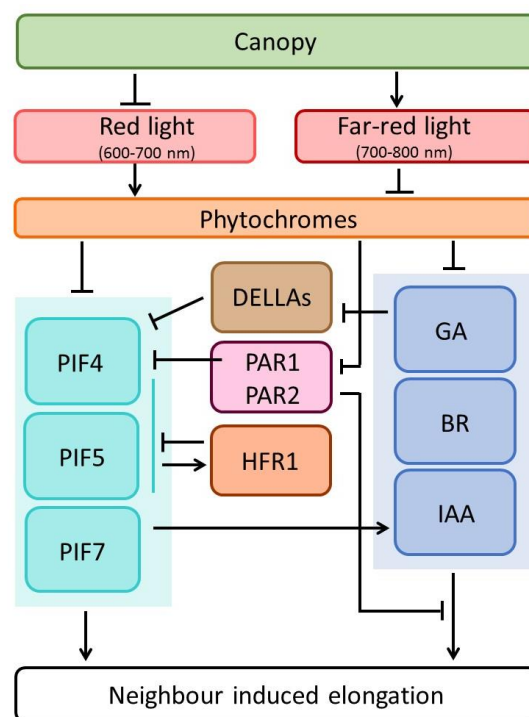


Figure 1.5 Main components of the R:FR signalling network. Phytochromes are inactivated by low R:FR ratios, releasing repression of PIFs and activating hormone-related responses that lead to neighbour induced elongation as part of the shade avoidance syndrome. PIF action is negatively affected by DELLA proteins, which are broken down by GA. PAR1, PAR2 and HFR1 negatively control signalling to prevent an excessive response to low R:FR. PAR1 and PAR2 also repress auxin responses. PIF7 mediates low R:FR-induced auxin biosynthesis. Abbreviations: PIF, PHYTOCHROME INTERACTING FACTOR; GA, gibberellic acid; BR, brassinosteroids; IAA, auxin; PAR, PHYTOCHROME RAPIDLY REGULATED; HFR1, LONG HYPOCOTYL IN FR 1.

DELLAs, other important R:FR signalling components are LONG HYPOCOTYL IN FR (HFR)1 and PHYTOCHROME RAPIDLY REGULATED (PAR)1 and PAR2. They are transcriptionally induced by low R:FR (Sessa *et al.*, 2005; Roig-Villanova *et al.*, 2007) and form negative feedback loops to prevent an excessive response to shade. HFR1, PAR1 and PAR2 are atypical bHLH proteins that lack a critical DNA binding motif and need homo or heterodimerisation for their biological activity (Galstyan *et al.*, 2011). HFR1 can form these heterodimers with PIF4 and PIF5 (Hornitschek *et al.*, 2009), while PAR1 can heterodimerise with PIF4 (Hao *et al.*, 2012). This heterodimerisation prevents PIFs from binding DNA and thus inhibits shade avoidance. PAR1 and PAR2 also suppress auxin-mediated shade avoidance responses, which potentially provides an additional mode of action of these proteins (Roig-Villanova *et al.*, 2007).

Shade avoidance responses require the action of several hormones, including auxin, brassinosteroids (BR) and gibberellic acid (GA). Auxin biosynthesis is rapidly induced by low R:FR and is essential for full induction of SAS (Stepanova *et al.*, 2008; Tao *et al.*, 2008; Keuskamp *et al.*, 2010). This increase in auxin biosynthesis is at least partly mediated by PIF7 (Li *et al.*, 2012). In addition, many auxin-related genes are up-regulated during shade avoidance (Devlin *et al.*, 2003; Roig-Villanova *et al.*, 2007; De Wit *et al.*, 2013), including the gene encoding auxin efflux carrier PIN3, whose cellular relocalisation leads to low R:FR-induced elongation (Keuskamp *et al.*, 2010). Auxin frequently interacts with growth promoting BR, which were recently also associated with shade avoidance. Low R:FR regulates many BR-related genes and BR-deficient mutants have reduced low R:FR-induced elongation responses (Kozuka *et al.*, 2010). Finally, shade avoidance is one of many growth processes for which GA is essential (Djakovic-Petrovic *et al.*, 2007). Low R:FR enhances GA biosynthesis and responsiveness and induces GA-related genes (Reed *et al.*, 1996; Hisamatsu *et al.*, 2005). As described above, one mode of action of GA in R:FR signalling is the degradation of DELLA proteins to induce shade avoidance responses.

Thesis outline

To investigate how UV-B affects emission of volatiles, we setup a system with flexible plant chambers and proton-transfer-reaction mass spectrometry (PTR-MS) as well as gas chromatography (GC) as analytic tools. This system and its performance are described in chapter 2. Its high sensitivity and temporal resolution allows us to investigate the temporal dynamics of VOC emission during experiments. This is in contrast to most VOC measuring methods used so far which involve longer-term trapping of VOCs and analysis afterwards. In chapter 3, we demonstrate the effect of UV-B on tomato volatile emissions and investigate what mechanisms may cause the observed emission patterns. In chapter 4, we show how UV-B affects volatile emissions of *Arabidopsis thaliana* and test the UVR8-dependency of the response. In chapter 5, we use *A. thaliana* to investigate the interaction between UV-B and low R:FR-induced shade avoidance responses on a physiological as well as signal transduction level. This thesis is concluded with a general discussion in chapter 6.

A plant chamber system with PTR-TOF-MS to study the effects of pollution on plant volatile emissions

P. Gankema¹, J. Timkovsky², R. Holzinger² and R. Pierik¹

1 Plant Ecophysiology, Institute of Environmental Biology, Utrecht University, the Netherlands

2 Institute for Marine and Atmospheric Research Utrecht, Utrecht University, the Netherlands

Part of this manuscript was published in modified form in:

Timkovsky J, Gankema P, Pierik R, Holzinger R (2014) A plant chamber system with downstream reaction chamber to study the effects of pollution on biogenic emissions. *Environmental Science: Processes and Impacts* 16: 2301-2312

Abstract: Biogenic volatile organic compounds (BVOCs) are important signalling molecules between organisms that also impact climate systems and human health. To investigate how BVOC emissions are affected by pollutants such as UV-B and ozone, we set up a system of two plant chambers and a downstream reaction chamber. The two plant chambers can be used to compare BVOC emissions from differently treated plants, while the reaction chamber can be used to study the chemistry of plant emissions under polluted conditions without exposing the plants to pollutants. The main analytical tool is a proton-transfer-reaction time-of-flight mass spectrometer (PTR-TOF-MS) which allows online monitoring of biogenic emissions and chemical degradation products. The identification of BVOCs is aided by cryogenic trapping and subsequent in situ gas chromatographic analysis. Here, we demonstrate the performance of this system as a valuable new tool in BVOC research.

Introduction

Volatile organic compounds (VOCs) are reactive substances with a strong impact on atmospheric chemistry (Fehsenfeld *et al.*, 1992; Riipinen *et al.*, 2011; Sahu 2012). Biogenic sources emit $\pm 90\%$ of global VOC emissions, estimated to be $\sim 1150 \text{ Tg C year}^{-1}$ (Guenter *et al.*, 2006). Oxidation of these Biogenic VOCs (BVOCs) in the atmosphere in the presence of NO_x leads to the formation of ozone, a strong oxidant (Summerfelt and Hochheimer 1997; Denman *et al.*, 2007). Oxidation products of BVOCs also contribute to secondary organic aerosol (SOA) formation through condensation on existing particles or the formation of new particles (Kulmala 2003; Goldstein and Galbally 2007). Aerosols and ozone negatively affect human health on both short and long term (Harrison and Yin, 2000). Furthermore, aerosols and ozone affect the Earth's climate: ozone is a strong greenhouse gas and aerosols scatter and/or absorb solar radiation. Aerosols also influence the climate indirectly by serving as cloud-condensation nuclei (Andreae and Crutzen 1997). Through atmospheric interactions BVOCs thus have significant impact on our health and climate.

Plants produce BVOCs both constitutively as well as in an inducible fashion (Scutareanu *et al.*, 2003; Arimura *et al.*, 2005). BVOC blends mainly consist of green leaf volatiles (GLVs) and terpenes. GLVs are six-carbon aldehydes and alcohols that are typically released when plant tissue is ruptured. Terpenes are categorised into mono-, sesqui-, di- or homoterpenes based on the number of carbon molecules in their backbone (10, 15, 20 or >20, resp.). In many biological systems, BVOCs function as signals between plants and higher trophic levels: plant VOCs can attract or repel herbivores (Heil 2008; Unsicker *et al.*, 2009) and pollinators (Raguso 2008) as well as their predators and parasitoids (Dicke and Baldwin 2010). BVOCs also play a role in plant-plant signalling, at least on a small spatial scale (Heil and Karban, 2009).

Plant VOC emissions are affected by many environmental factors, including abiotic factors like temperature and light as well as biotic factors such as herbivores, pathogens and neighboring plants (Arimura *et al.*, 2005; Leitner *et al.*, 2008; Loreto and Schnitzler 2010; Kegge and Pierik 2010; Kegge *et al.*, 2013). However, much remains unknown about how atmospheric pollutants affect plant VOC emissions. Increased UV-B and ozone levels may increase or decrease BVOC emissions, depending on plant species and environmental conditions (Loreto and Schnitzler 2010; Llusà *et al.*, 2012; Hartikainen *et al.*, 2012). If changes in the level of UV-B or ozone alter the emitted plant VOC blend, this might affect interactions between plants or between plants and higher trophic levels. When studying the effects of atmospheric pollutants on plant emissions, it is important to be able to distinguish between effects on plant emissions and effects on the emitted compounds. The setup presented here allows such discrimination.

We present a novel setup of plant chambers and a reaction chamber to study interactions between BVOC emissions and pollutants like ozone and UV-B. BVOC analysis is based on proton-transfer-reaction time-of-flight mass spectrometry (PTR-TOF-MS) which allows precise online measurements with high mass and temporal resolution (Jordan *et al.*, 2009; Graus *et al.*, 2010). An extension is included with a gas chromatograph (GC) for identification of isomers (e.g. different monoterpenes). Ozone and reaction chamber experiments, investigating the fate of BVOCs once emitted, are described more elaborately in Tsimkovsky *et al.* (2014). Experiments with birch (*Betula pendula*), tomato (*Solanum lycopersicum*) and *Arabidopsis thaliana* demonstrate the performance of the system. These data show that the presented setup is a flexible and efficient tool to investigate the effects of a changing environment on plant VOC emissions.

Description of the setup

Figure 2.1 gives a schematic overview of the setup. Panels A and B represent two optional chamber setups and panel C shows the functioning of the GC and PTR-TOF-MS. Elements of the setup drawn in dashed lines are optional: different levels of ozone and UV-B can be introduced depending on the experiment.

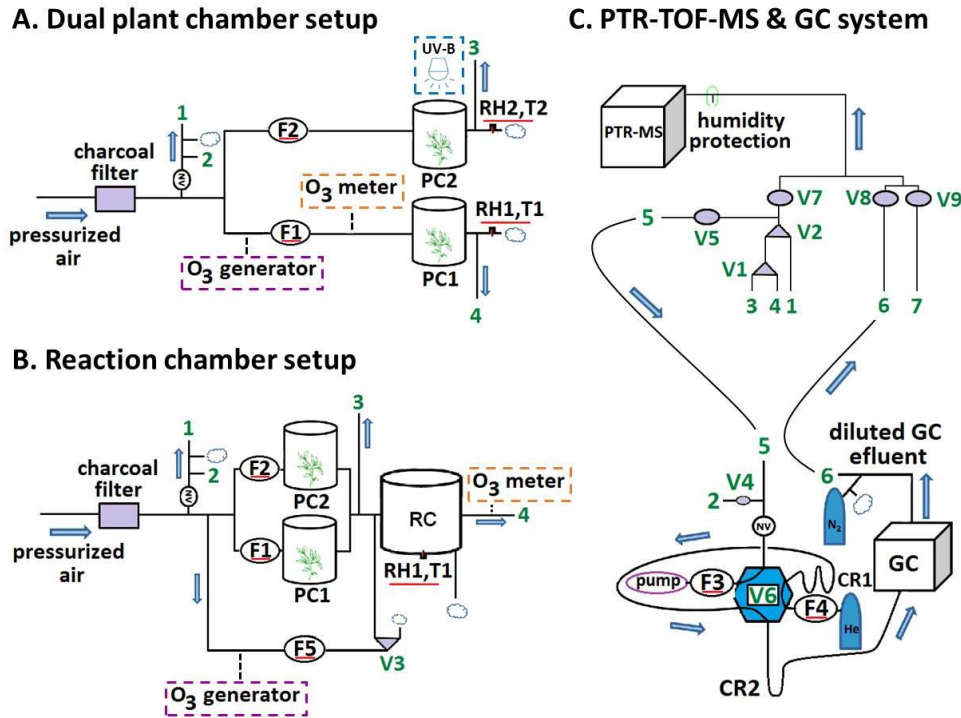


Figure 2.1 Schematic overview of the setup with two optional chamber configurations (A and B), and the PTR-TOF-MS and GC sampling system (C). Port 1, 2, 3 and 4 connect (A) and (B) to (C). The parts of the system inside dashed line boxes are optional. Lab air is analysed through port 7. Port 2 connects the GC system to purified air for cleaning. Abbreviations: NV, needle valve; PC, plant chamber; RC, reaction chamber; PTR-MS, proton-transfer-reaction mass spectrometer; GC, gas chromatograph; V, valve, with circles depicting two-way and triangles three-way valves, V6 is a 6-port Valco valve; F, flow controller; RH, relative humidity sensor; T, temperature sensor; CR1, sampling cryotrap; CR2, focusing cryotrap; N₂, nitrogen cylinder; He, helium cylinder. Arrows indicated direction of air flow, small clouds depict overflow outlets. Parameters that are underlined in red are recorded during measurements.

The plant and reaction chambers

Two types of plant chambers are available. Their internal volumes are 25 L and 785 mL, and we refer to them as large and small plant chambers, respectively. As large plant chambers we use two glass desiccators, each consisting of three parts: the cap, the desiccator body and the hose, which is located in the cap. The hose has a long outlet ($l = 25$ cm, ID = 9 mm), which is directed towards the bottom of the desiccator and allows sampling from the centre of the plant chamber. The inlet to the chamber is located at the top of the hose. The small plant chambers, one of which is shown in figure 2.2, are custom built and consist of a glass cylinder (inner diameter 100 mm, height 100 mm), a glass lid and a dividable Teflon (PFTE) bottom plate sealed with spring clamps and Teflon coated O-rings. For UV-B treatment, we use a lid with 2 mm thick quartz glass and a broad spectrum UV-B lamp (UV21, 9 W, Waldmann, Tiel, the Netherlands) at adjustable height above the plant chamber. The bottom plate has a 2 mm hole in the middle that fits around the hypocotyl of an individual plant, allowing measuring of shoot emissions only. Inlet and outlet (inner diameter 18 mm) are positioned



Figure 2.2 A four-week old *Arabidopsis thaliana* Col-0 plant in the small plant chamber with the lid with quartz glass. The pot in the middle contains plant roots and soil, pots on either side are for support.

Chapter 2

opposite each other 40 mm above the bottom of the chamber. Nine 36 W 840 TL-D lamps (Philips, Eindhoven, the Netherlands) above the plant chambers produce light levels of 130-150 $\mu\text{mol m}^{-2} \text{s}^{-1}$ photosynthetically active radiation (PAR: $\lambda = 400\text{-}700 \text{ nm}$) at leaf level inside the plant chamber when the lid is closed.

The custom-made reaction chamber is made from perfluoroalkoxy film (PFA, thickness 0.05 mm, HP Products, Raamsdonksveer, the Netherlands) and has a cylindrical shape. Walls were sealed by welding the PFA film with a heat gun (Steinel, Herzebrock-Clarholz, Germany). The reaction chamber is 45 cm in diameter with a height of 50 cm and a volume of 80 L. The bottom of the chamber is fixed to a ground plate covered with a PFA film. The axle of a polytetrafluoroethylene ventilator (PTFE, OD = 10 mm, Bola, Grünsfeld, Germany) is lead through the centre of the ground plate, positioning the ventilator in the centre of the chamber. Operating the ventilator at 2 Hz keeps the chamber air well mixed during experiments. All mounting parts in contact with the air inside the reaction chamber are made of Teflon (PTFE). The tightness of the reaction chamber was tested by filling the chamber with acetone at levels of $\sim 350 \text{ nmol mol}^{-1}$ and monitoring the mixing ratio without gas flow through the chamber. No significant leaks were detected.

The air flow through the large plant chambers is controlled by thermal mass-flow controllers (MKS Instruments, München, Germany) in the range 0-20 and 0-5 standard L min^{-1} for chamber 1 and 2, respectively (standard refers to standard conditions: 1013.25 hPa, 273.15 K). The flow through the small plant chambers is controlled by mass-flow controllers in the range 0-2 standard L min^{-1} . We use pressurised (5 bars) ambient air purified by a custom made charcoal filter. The charcoal is cleaned once a week by placing it overnight in an oven at 160 °C. Purified air is monitored throughout each experiment. Teflon (PFA) tubing is used for all connections (length between plant and reaction chamber = 145 cm, ID = 9 mm). Relative humidity and temperature sensors (HMP 60, Vaisala, Helsinki, Finland) are located at the outlets of the chambers to monitor humidity and temperature. Defined amounts of ozone can be added to the air flow to the plant chamber (Fig 2.1A) or to the air flow to the reaction chamber (Fig 2.1B) with an ozone generator (Model 49i-PS, Thermo Scientific, Waltham, U.S.A.). Ozone addition is controlled with a thermal mass-flow controller (MKS Instruments, München, Germany) in the range 0-2 L min^{-1} and monitored with an ozone meter (O_3 analyzer model 49 W003, Thermo Environmental Instruments Inc., Franklin, U.S.A.). Before ozone experiments, the empty reaction chamber was pre-cleaned overnight by flushing with purified air containing ozone mixing ratios of $\pm 430 \text{ nmol mol}^{-1}$.

To test the mixing of air in the large plant chambers, synthetic limonene (Sigma Aldrich, Zwijndrecht, the Netherlands) was added to empty plant chambers at a concentration of 45 nmol mol^{-1} in purified air with a flow of 2.5 L min^{-1} . Mixing ratios were measured in the middle and at the bottom corner of the plant chamber with the PTR-TOF-MS and found to be equal to the incoming limonene mixing ratio after ± 30 min. This indicates that the mixing in the large plant chambers is sufficient for the experiments presented here.

PTR-TOF-MS

Figure 2.1C shows how the PTR-TOF-MS can be switched between the sampling ports of the chamber system, the effluent of the GC column (the PTR-TOF-MS is also used as detector for the GC system) and purified and laboratory air, which are monitored routinely. This valve system is implemented with 1/8" PFA tubing, four 2-way and two 3-way Teflon (PFA) solenoid valves (TEQCOM, port size 1/8", orifice 0.125). We use a commercial PTR-TOF 8000 instrument (Ionicon Analytik GmbH, Innsbruck, Austria, described by Jordan *et al.*, 2009) with the following parameters: drift tube temperature 60 °C; inlet tube temperature 60 °C; drift tube pressure 2.15 hPa; ion source voltages $U_s = 140$ and $U_{so} = 92 \text{ V}$; ratio of drift tube voltage and number of molecules in the drift tube (E/N) 134 Td; extraction voltage at the end of the drift tube $U_{dx} = 35 \text{ V}$. The ion source current is kept between 5 and 7 mA, water flow to the ion source is 4

mL min⁻¹. At normal operational conditions the intensity of the primary signal H₃O⁺ (detected at *m/z* 21.023 as H₃¹⁸O⁺) is around 2.5 x 10⁵ to 1 x 10⁶ cps. The settings of the TOF are such that every 60 microseconds a pulse of ions is injected into the mass spectrometer, which corresponds to a mass range of 0-1157 Th. These initial mass spectra are averaged every 16667 measurements, giving a time resolution of one second. The mass resolution ($m \Delta m^{-1}$, where Δm is the full width at half maximum) is in the range of 3500-5000. Data processing is done with Interactive Data Language software (IDL, version 7.0.0, ITT Visual Information Solutions B.V., Apeldoorn, the Netherlands) using custom-made routines described by Holzinger *et al.* (2010a). Mixing ratios of most compounds are calculated according to the method described in Holzinger *et al.* (2010b), which involves the use of default reaction rate constants (3×10⁻⁹ cm³ s⁻¹ molecule⁻¹), default transmission efficiencies and calculated reaction times. The mixing ratios of monoterpenes can be calculated as the sum of the signals detected at *m/z* 81.069 and *m/z* 137.133 for experiments with pure compounds. However, pilot experiments with biogenic emissions also showed six-carbon alcohols and aldehydes at *m/z* 81.069. By calibration with a gas standard containing α -pinene, we determined that 32 % of the total amount of the monoterpene is found at *m/z* 137.133. Monoterpene mixing ratios of biogenic sources are therefore calculated by multiplying the signal detected at *m/z* 137.133 by a calibration factor of 3.13.

GC system with cryogenic trapping

The GC system features a two-cryotrap system with a sampling and focusing trap. The focusing trap focuses the sample in a smaller volume, allowing for quicker transfer onto the column. This also prolongs the lifetime of the GC column by reducing the amount of water in the sample. The amount of water is reduced by \pm 90 % via condensation on the line downstream of the sampling cryotrap. This water is removed from the system during the consecutive sampling step. The two cryotraps are electrically heated with resistance wire and submerged into liquid nitrogen by pneumatic lifters. The GC sampling line (1/8" PFA, port 5 in Fig 2.1C) is connected downstream of the valves that connect the PTR-TOF-MS to the chamber system to ensure GC sampling and online measurements are from the same source and time period. The sampling trap is a W-shaped 1/8" stainless steel tube with sulfinert coating (ID = 1.5 mm, Restek Inc., Bellefonte, U.S.A.) which is connected with 1/16" PEEK tubing to a 6-port stainless steel Valco valve (sulfinert coating). A needle valve before the trap regulates the sampling flow and ensures that sampling is done at low pressure (~200 hPa) to prevent oxygen condensation. Recovery tests with pure compounds showed that the collection efficiency for α -pinene, methanol and toluene is close to 100 % for sampling flows up to 35 mL min⁻¹. Traps are pre-cooled for 5 minutes before sampling. Sampling flow is 30 mL min⁻¹, measured with a thermal mass-flow meter (MKS Instruments, München, Germany) and maintained by a membrane pump downstream of the sampling trap (Vacuubrand GmbH, Wertheim, Germany). The focusing trap is a U-shape 1/8" stainless steel tube with a glass capillary through it (ID = 320 μ m, SGE Analytical Science, Melbourne, Australia). To transfer the sample to the focusing trap, the 6-port valve is switched and the sample released by heating the sampling trap to 100 °C within 2 minutes. A 2 mL min⁻¹ helium flow (ultrapure He, Air products, Utrecht, the Netherlands) transfers the sample to the focusing trap. Typically, a period of 10 minutes is allowed to complete the transfer, which corresponds to a gas volume 5 times the internal volume of the sampling trap, the focusing trap and the transfer lines. Immediately thereafter the 6-port valve is switched back and the sample is injected into the GC column by heating the focusing trap to 200 °C within 75 seconds, while the GC effluent is monitored with the PTR-TOF-MS.

For gas chromatography we use a 30 m DB-5ms column (ID = 0.25 mm, film thickness = 0.25 μ m) with He as a carrier gas (2 mL min⁻¹, controlled by a 20 mL min⁻¹ thermal mass-flow controller, MKS Instruments, München, Germany). After injection the column is kept at 40 °C for one minute, heated to 150 °C at 5 °C min⁻¹ and then to 250 °C at 20 °C min⁻¹. For analysis by PTR-TOF-MS the effluent of the GC column is diluted with 38 mL min⁻¹ of nitrogen (ultrapure nitrogen, 5.7 purity, Air products, Utrecht, the Netherlands) by providing excess nitrogen and setting the flow into the PTR-TOF-MS to 40 mL min⁻¹.

Chapter 2

The mixture of effluent and nitrogen is transferred through 1/8'' PFA line to port 6 (see also Fig 2.1C). Individual compounds are identified based on the presence of other ions with the same retention times in combination with a retention time database (Goodner 2008), performed calibration measurements and previous studies (König *et al.*, 1995).

Automation and control system

Valve positions, flows, cryotrap positions and temperatures, and settings of the ozone generator, pump and GC are automatically operated with a controlling set (NI cDAQ-9178, National Instruments, Woerden, the Netherlands) programmed in the LabVIEW interface (LabVIEW 2011, National Instruments, Woerden, the Netherlands). Control sequences are created as simple text documents containing the commands and duration of each step in a measurement cycle. The values of the elements which are underlined in red in figure 2.1 are saved to an engineering log together with parameters such as time and the actual temperatures of the cryotrap and GC. These data are recorded every second to fit the time resolution of the PTR-TOF-MS.

Data handling and statistics

For all analyses performed we consider ions above m/z 40, and ions detected at m/z 31.018 (CH_3O^+) and m/z 33.033 (CH_5O^+). Means are compared statistically using a Student's t-test in Microsoft Excel.

Recovery factors (RF) are defined as (equation 1) the ratio between the amount of substance measured with the GC setup ($n(\text{VOC})_{\text{GC}}$) and the amount of substance sampled online ($n(\text{VOC})_{\text{sampled}}$). The former is calculated by integrating the GC peak(s) at a particular mass, using the first 15 minutes of a GC chromatogram. The latter is calculated from online measured mixing ratios at the same mass during the time of sampling, and the sampled volume.

$$\text{RF} = \frac{n(\text{VOC})_{\text{GC}}}{n(\text{VOC})_{\text{sampled}}} \quad (1)$$

Plant emission rates (ER) are calculated according to equation 2:

$$\text{ER} = \frac{[\text{VOC}]F_{\text{cham}}}{\text{DW}} \quad (2)$$

where [VOC] is the mixing ratio with subtracted background (in nmol mol^{-1}), F_{cham} is plant chamber air flow in mol h^{-1} , and DW is leaf dry weight in g. The resulting emission rate has the unit of $\text{nmol g}_{(\text{DW})}^{-1} \text{h}^{-1}$. To allow stabilisation of the signal, the first minute of a sampling period was discarded. Mixing ratios in purified air were used as background.

Plant growth and treatment conditions

Birch (*Betula pendula*) is a tree species known to emit a wide variety of VOCs (König *et al.*, 1995). Seedlings were collected with their surrounding sandy soil from a forest close to Utrecht Science Park 1-2 days before the experiments (in August 2012), and placed in 250 mL pots. The seedlings were 1-2 years old. In the lab, seedlings were placed next to the large plant chambers, where the TL-D lamps produced light levels of 130-150 $\mu\text{mol m}^{-2} \text{s}^{-1}$ PAR with a light period from 7 am till 11 pm (16 h light, 8 h dark). Before the start of the experiment, three plants were put in each large plant chamber, resulting in a total leaf dry weight of 4.1-5.3 g and a total leaf area of 1296-1413 cm^2 per chamber. Day and night temperatures in chamber 1 and 2 were stable at 25.7 ± 0.1 and 22.0 ± 0.1 °C, respectively. Relative humidity (RH) was 40-60 %. After the lids were closed, an air flow of 2.5 L min^{-1} was maintained and plant emissions were allowed to stabilise for 30 minutes before the start of the experiment to allow.

Tomato (*Solanum lycopersicum*) is an important crop species and a strong VOC emitter that is often used in VOC studies (Kant *et al.*, 2004; Bleeker *et al.*, 2011). Plants of the Moneymaker cultivar were grown on moist Primasta soil (mix Z2254, Primasta B.V., Asten, the Netherlands) under a long-day light regime (16

A plant chamber system to study plant volatile emissions

h light, 8h dark) in climate chambers at 20 °C, 160-180 $\mu\text{mol m}^{-2} \text{s}^{-1}$ PAR and 70 % RH. After 10 days seedlings were transplanted to individual pots. Four-week old plants were transferred to the plant chamber setup, their pots covered with Teflon film, and left to acclimatise overnight. The UV-B lamp was turned on above the treatment group from the start of the light period to create UV-B radiation levels of 1 W m^{-2} for eight hours, resulting in a total daily UV-B dose of 28.8 $\text{kJ m}^{-2} \text{day}^{-1}$. Afterwards, UV-B-treated and control plants were put into the large plant chambers, lids were closed and an air flow of 2.5 L min^{-1} was maintained. Three plants were used per chamber.

Arabidopsis thaliana is an important genetic model species in plant research. Seeds from the accession Col-0 were stratified in the dark for three days before transfer to climate chambers, where they were grown on Primasta soil (mix Z2254, Primasta B.V., Asten, the Netherlands) under a short-day light regime (8 h light, 16 h dark) at 20 °C, 160-180 $\mu\text{mol m}^{-2} \text{s}^{-1}$ PAR and 70 % RH. After 10 days, seedlings were transplanted to individual 70 mL pots. Four-week old plants were transferred to the plant chamber setup, placed into the small plant chambers with an air flow of 0.1 L min^{-1} and left to acclimatise overnight. The UV-B lamp was turned on from 10 a.m. till 2 p.m. at an intensity of 1 W m^{-2} , so that the plant in small plant chamber 2 (with quartz lid) was exposed to UV-B light for four hours, while the plant in chamber 1 (with glass lid) was not. This UV-B treatment resulted in a total daily UV-B dose of 14.4 $\text{kJ m}^{-2} \text{day}^{-1}$.

After each experiment plant leaves were harvested, fresh weight measured and leaf area determined with a Li-3100 Area Meter (LI-COR, Lincoln, Nebraska U.S.A.). Dry weight was measured after placing the leaves in an oven at 70 °C for at least 48 hours. VOCs were measured according to the measurement cycle described below in ‘Online measurements’ (see also Fig 2.3).

System performance

We demonstrate the functionality and performance of the system with the results of three independent experiments. Results of ozonolysis experiments with pure compounds and birch VOC emissions, that demonstrate the performance of the reaction chamber, but whose scope lays outside the scope of this thesis, are described in Timkovsky *et al.* (2014).

Online measurements

Figure 2.3 demonstrates the operation of the system by showing online measurements during a typical measurement cycle. The figure displays the course of the mixing ratios detected at m/z 81.069 (C_6H_9^+ fragment) for one cycle of an experiment with birch plants in the reaction chamber setup (Fig 2.3A) and one cycle of an experiment with tomato plants in the dual plant chamber setup (Fig 2.3B). In the first experiment, the PTR-TOF-MS was switched between the different ports as follows: 10 min reaction chamber, 5 min purified air, 10 min plant chambers, 25.5 min GC effluent, 10 min plant chambers, 36 min reaction chamber (ozone addition happens during this period), 25.5 min GC effluent, 5 min lab air. In the second experiment, the PTR-TOF-MS was switched similarly, with a six-minute sampling period for each plant chamber and a four-minute sampling period of clean air. GC sampling was performed during the online measurements of the respective chamber, as indicated by brackets in figure 2.3. During the experiment with *A. thaliana* plants in the dual plant chamber setup with small plant chambers, we took only online measurements and the PTR-TOF-MS was switched as follows: 6 min plant chamber 1, 6 min plant chamber 2, 5 min purified air, 5 min lab air (online data not shown). After each cycle, a new cycle started automatically.

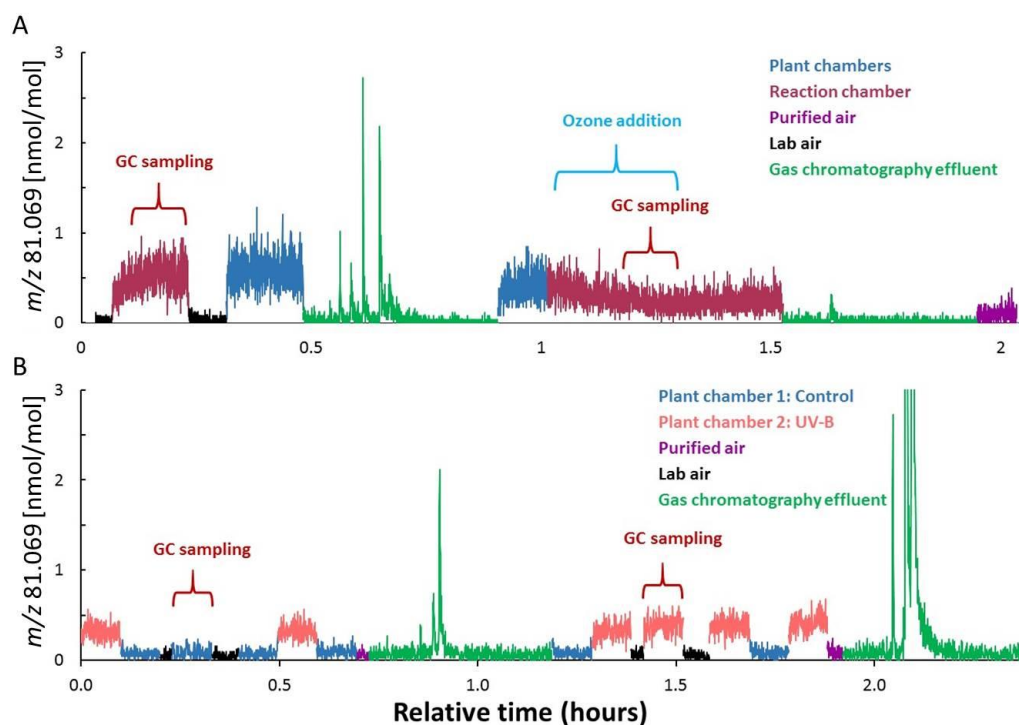


Figure 2.3 Online measurements during one cycle of measurements of (A) an experiment with birch in the reaction chamber setup and (B) an experiment with tomato in the dual plant chamber setup, both using large plant chambers. The signal observed at m/z 81.069 is shown as an example, colours indicates the emission source (see legend). Brackets indicate GC sampling and ozone addition periods.

GC performance

For a good performance of the system, it is crucial that our GC and online measurements are quantitatively similar. In table 2.1 we present recovery factors of several compounds based on three individual experiments with birch seedlings. Note that no background was subtracted from the measured signal for these calculations. The obtained recovery factors are in the range 0.71 - 1.38, indicating a reasonable agreement between online and GC measurements. The variation is most likely due to different levels of instrumental background during the online and GC effluent measurements. Also, there might be an overestimation of compound mixing ratios in nitrogen-based GC effluent versus air-based online measurements. To demonstrate the identification of different isomers, figure 2.4 displays a chromatogram at m/z 81.069 obtained from birch. The five labelled peaks are attributed to a six-carbon leaf alcohol or aldehyde, 2-hexenal, α -pinene, d-limonene and β -phellandrene. The two small peaks observed after α -pinene and d-limonene are not identified.

Table 2.1 Recovery factors (RF) for several compounds, calculated from all chromatograms without ozone addition sampled during the experiments with birch ($n=40$). Averages \pm SE are shown.

m/z	Formula \cdot H ⁺	RF
33.033	CH ₄ OH ⁺	0.75 \pm 0.016
43.018	C ₂ H ₃ O ⁺	0.82 \pm 0.011
59.049	C ₃ H ₇ O ⁺	0.71 \pm 0.013
61.029	C ₂ H ₅ O ₂ ⁺	1.38 \pm 0.041
69.07	C ₅ H ₉ ⁺	1.09 \pm 0.044
87.045	C ₄ H ₇ O ₂ ⁺	1.10 \pm 0.025
87.081	C ₅ H ₁₁ O ⁺	1.20 \pm 0.040
137.13	C ₁₀ H ₁₇ ⁺	1.23 \pm 0.049

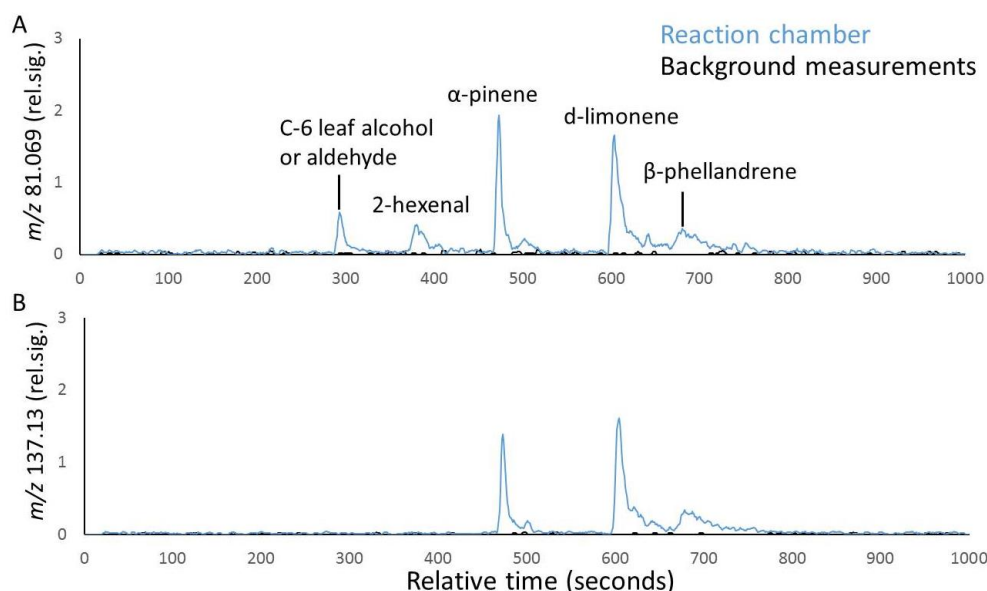


Figure 2.4 Gas chromatograms from birch. For every profile a running mean over five points is used. The blue lines are sampled from the non-ozonated reaction chamber, black lines are background measurements (purified air). (A) m/z 81.069 corresponds to monoterpenes, alcohols and aldehydes; (B) m/z 137.133 corresponds to monoterpenes only.

UV-B alters VOC emissions in *A. thaliana*

We were able to observe that UV-B altered the emission of several volatile organic compounds in *A. thaliana*. Figure 2.5 shows the average emission of m/z 61.029 during the four-hour UV-B exposure period as an example. This demonstrates that changes in BVOC emissions upon UV-B exposure can be detected in our setup for the genetic model plant species *A. thaliana*.

Conclusions

We present a setup with plant and reaction chambers (Fig 2.1) to measure the impact of pollution on plant emissions and demonstrate its performance with the results of three experiments. First of all, recovery factors are within the range of 0.71 - 1.38 (Table 2.1), indicating that cryogenic sampling and transfer through the GC system is adequate. Online measurements of birch and tomato (Fig 2.3) in the two optional chamber setups of the system illustrate that our measurements have a high temporal resolution, and that differences between plant emissions and purified air are easily detectable. These data also give an idea of the flexibility and broad possibilities of the setup. The addition of a GC system to the setup allowed us to distinguish three specific monoterpenes emitted by birch (Fig 2.4). Ideally, a database of known VOCs and their specific retention times in our setup would be added to the system and used for a more robust identification. However, since the general emission profiles of the plant species we use are well known and consistent with the chromatograms we observe in our system, we are confident that we can correctly identify most individual components using the current method. Finally, results from an experiment with *A. thaliana* plants using the small plant chambers and UV-B lamp show that our setup can also be used to study volatile emission responses during treatment, even in small plants that are weak VOC emitters (Fig 2.5). Moreover, the use of the genetic model species *A. thaliana* opens up the possibility to

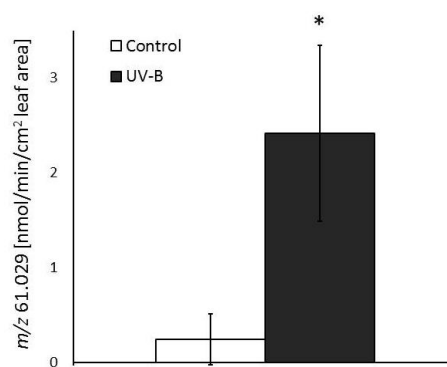


Figure 2.5 *Arabidopsis thaliana* emissions of m/z 61.029 increase significantly during the four-hour UV-B exposure period. Averages \pm SE are shown, asterisk indicates significant difference ($p \leq 0.05$, $n=3$).

Chapter 2

investigate the regulation of VOC emissions in e.g. signal transduction mutants, potentially providing new clues to elucidating the signalling networks controlling VOC emissions

In summary, experiments using three different species (a tree, a crop and model species *A. thaliana*) with different treatments (ozone gas and UV-B radiation) and of different sizes show the flexibility of the described setup. Automation and control via a user-friendly interface make operation of the system efficient and easy to adjust to any kind of desired setup. This system thus allows for a broad spectrum of experiments, where both short term stress dynamics as well as long-term responses on the level of volatiles can be studied. This makes our setup a valuable tool to study the dynamics of plant volatile responses to changing environmental conditions.

Interestingly, UV-B significantly increased emissions in *A. thaliana* (Fig 2.5), while a similar increase was observed after UV-B pre-treatment in tomato plants (Fig 2.3B). We will use the setup described here to further investigate the effect of UV-B on VOC emissions in the next two chapters.

Acknowledgements

The TD-PTR-MS has been funded by the Netherlands Organization for Scientific Research (NWO) under the ALW-Middelgroot program (Grant 834.08.002). This project is funded by a strategic funding scheme (Focus and Mass) of Utrecht University. We would like to thank Carina van der Veen, Henk Snellen, Michel Bolder and Marcel Portanger of Utrecht University, the Netherlands for excellent technical support and L.A.C.J. Voeselek and Thomas Röckmann for scientific discussion.

A plant chamber system to study plant volatile emissions

Ultraviolet-B radiation alters tomato volatile emissions

P. Gankema¹, J. Timkovsky², R. Holzinger² and R. Pierik¹

1 Plant Ecophysiology, Institute of Environmental Biology, Utrecht University, the Netherlands

2 Institute for Marine and Atmospheric Research Utrecht, Utrecht University, the Netherlands

Abstract: Plant volatile emissions are altered by environmental factors such as light, temperature and interactions with herbivores or pathogens. The composition of the emitted volatile blend is both flexible and specific, depending on plant species and environmental interactions. Volatiles can function as signals, as has been shown within and between plants as well as in interactions between plants and higher trophic levels. UV-B radiation negatively affects plant growth but can also alter plant-herbivore relations, although the mechanism underpinning this remains unclear. Using the setup from chapter 2, we show here that UV-B induces volatile emissions in tomato plants with differential timing. Damage-related compounds are emitted during UV-B exposure, whereas other compounds are induced after UV-B exposure stopped. This group includes monoterpenes, known to function as signals in plant-herbivore interactions. Although no such correlation was observed for other terpenes, we found that transcriptional up-regulation of the terpene synthesis gene *TPS4* correlates with the UV-B-induced emission of its product, β -phellandrene.

Introduction

Volatile organic compounds (VOCs) are secondary metabolites involved in plant stress responses and ecological interactions. Volatile emissions increase with increasing light intensity (Arimura *et al.*, 2008), temperature (Staudt and Bertin 1998) and drought (Takabayashi *et al.*, 1994a). Increased levels of carbon dioxide (CO₂) and ozone (O₃) can also alter emissions (Loreto and Schnitzler 2010). In addition, herbivore and pathogen attack can induce volatiles very specifically depending on the species (Arimura *et al.*, 2005; Leitner *et al.*, 2008; Heil 2008). Plant VOC blends consist mainly of green leaf volatiles (GLVs) and terpenes, in addition to other compounds including the volatile hormones ethylene and methyl salicylate (MeSA). GLVs are relatively small (C5) alcohols and aldehydes, often emitted from storage directly after plant tissue is ruptured. Terpenes are categorised based on their carbon backbone into mono- (C10), sesqui- (C15), di- (C20) and homoterpenes (>C20), and are often emitted from specialised structures like trichomes. Terpenes are emitted either from storage or upon *de novo* synthesis. Emission of these compounds is typically inducible, with individual compounds affected differentially (Frag and Pare 2002; Leitner *et al.*, 2005; Blande *et al.*, 2010). The exact composition of the emitted blend thus depends on environmental factors, but also on plant species, developmental stage and the plant part affected. Even cultivars and accessions of the same species emit different blends (Takabayashi *et al.*, 1991; Snoeren *et al.*, 2010), and herbivore-induced blends depend on the exact herbivore attacking (Dicke *et al.*, 1999). A plant's volatile blend thus contains intricate putative information about plant identity and environmental conditions.

Several VOCs and VOC combinations are indeed known to act as signalling compounds. Within a plant, volatiles can function as signals between branches (Rodriguez-Saona *et al.*, 2009). VOCs can also transfer information between plants. VOCs emitted by herbivore-attacked plants have for example been shown to prime neighbouring plants for subsequent herbivore attack (Ton *et al.*, 2006). VOCs can also reduce the performance of neighbouring plants, for example by suppressing germination (Karban *et al.*, 2007). At higher trophic levels, plant volatiles attract pollinators (Raguso *et al.*, 2008) and repel herbivores (Dicke and Dijkman 1992). Moreover, herbivore-induced plant volatiles attract predators and parasitoids, recruiting them as the plant's "bodyguards" to reduce herbivore damage (Dicke and Sabelis 1988; Van Poecke *et al.*, 2001). VOCs can also alter oviposition behaviour (De Moraes *et al.*, 2001), thereby affecting future herbivore damage.

The effect of ultraviolet (UV)-B (280–315 nm) stress on plants has been studied intensively after the discovery of the hole in the ozone layer in 1985 (Solomon 1990). UV-B generally reduces growth, damages DNA, impairs photosynthesis and can lead to increased production of protective compounds and a more branched plant stature (reviewed in Caldwell *et al.*, 1998; Ballare *et al.*, 2011). UV-B exposure at the Earth's surface is expected to increase in areas where prolonged and more severe drought periods will result in less cloud coverage, like the Mediterranean, South-West U.S.A. and Australia (IPCC 2007). Higher doses of UV-B in these areas will likely affect agricultural yields. In addition, elevated UV-B might affect ecological interactions. Field studies indicate that UV-B enhances herbivore resistance (Caldwell *et al.*, 2007), potentially since both stresses elicit overlapping transcriptional responses (Izaguirre *et al.*, 2003) and part of the herbivore defence signalling pathway is activated by UV-B (Demkura *et al.*, 2010). It remains unknown, however, if herbivore-induced volatile emissions are also influenced by UV-B.

Tomato is a widely-cultivated crop plant known to emit large amounts of volatile organic compounds and is therefore often used as a model species to study VOC emissions (Frag and Pare 2002; Kant *et al.*, 2004; Bleeker *et al.*, 2011). In addition, its genome is substantially determined and tomato VOC synthesis genes have recently been described (Falara *et al.*, 2011).

Here, we describe that UV-B radiation affects tomato VOC emissions. We show that different compounds have different emission patterns under UV-B and investigate what causes these emission patterns.

Methods

Plant growth conditions

Tomato (*Solanum lycopersicum*) cv. Moneymaker were grown on moist Primasta soil (mix Z2254, Primasta B.V., Asten, the Netherlands) under a long-day light regime (16h light, 8h dark) in climate chambers at 20 °C, 160-180 $\mu\text{mol m}^{-2} \text{s}^{-1}$ photosynthetically active radiation (PAR) and 70% relative humidity. Seeds were sown on moist soil. After 1 week, equally large seedlings were transferred to individual pots.

Plant treatments

Experiments were performed when plants were 2.5 weeks old, with their third leaf emerging. For volatile measurements plants were transferred to the setup, placed into the small plant chambers (see chapter 2) with an air flow of 0.1 L min^{-1} and left to acclimatise overnight. We used one small plant chamber with a lid with 2 mm thick quartz glass that allows UV-B penetration and a second small plant chamber with a standard glass lid that blocks UV-B. For growth and physiological measurements and sampling for gene expression, control and treatment groups were treated in separate light boxes in the climate chamber. Broad-spectrum UV-B lamps (UV21, 9 W, Waldmann, Tiel, the Netherlands; see Fig S3.1) were placed above the plants to create UV-B radiation levels of 1 W m^{-2} at leaf level (measured with a handheld UV meter from Waldmann, Tiel, the Netherlands). Four, eight or twelve hours of UV-B exposure thus resulted in a total daily UV-B dose of 14.4, 28.8 or 43.2 kJ $\text{m}^{-2} \text{day}^{-1}$, respectively. UV-B treatments started with the start of the light period at 7 a.m.

Growth and physiological measurements

Stem length was measured from photographs taken at the start and after three days of treatment using the open-source software package ImageJ (Abràmoff *et al.*, 2004). Shoots were harvested and leaf area was determined with a Li-3100 Area Meter (LI-COR, Lincoln, Nebraska U.S.A.). Dry weight of leaves and shoot were measured after drying the plant material in an oven at 70 °C for at least 48 hours.

For UV-B absorptive compound measurements, 0.7 cm^2 leaf discs were sampled from the main leaflet of the second leaf, stored in 1.5 mL Eppendorf tubes and kept on ice or at -20 °C until analysis. For analysis, 700 μL methanol : HCl (99 : 1) was added to each leaf disc and kept at -20 °C for 48 hours to extract, before measuring absorbance at 310 nm using a BioTek Synergy HT Multi-Mode Microplate reader (Beun-De Ronde, Abcoude, the Netherlands).

Chlorophyll content was measured using a second 0.7 cm^2 leaf disc sampled from the same leaflet. For this analysis, 1.5 mL dimethyl sulfoxide (DMSO) was added to each tube, mixed well and allowed to extract for 30 min in a 65 °C shaking water bath. Samples were cooled on ice for 1 min and subsequently kept at room temperature in the dark for 30 min. Absorbance at 664, 647 and 750 nm was measured using a BioTek Synergy HT Multi-Mode Microplate reader (Beun-De Ronde, Abcoude, the Netherlands). Chlorophyll A content (in mg L^{-1}) was calculated as $12.25 \cdot (A_{664} - A_{750}) - 2.55 \cdot (A_{647} - A_{750})$, and chlorophyll B content as $20.31 \cdot (A_{647} - A_{750}) - 4.91 \cdot (A_{664} - A_{750})$ (Porra *et al.*, 1989).

Stomatal aperture measurements were performed in a separate experiment. Leaf epidermal imprints were obtained from the abaxial surface of the main leaflet of the second leaf at six time points during the first day of treatment, according to the method described by Polko *et al.* (2012). Using an optical microscope,

Chapter 3

images of stomata were recorded and the height and width of at least 60 individual stomata per sample were measured.

Volatile measurements

Volatile organic compound emissions were measured in the custom-made setup described in chapter 2 (see also Timkovsky *et al.* 2014). We used the small plant chambers with dividable bottom plates that fit around the stem in order to measure shoot emissions only. Online plant emissions were averaged over a six-minute period and calculated as described in chapter 2. For gas chromatographic (GC) measurements, we sampled onto the cryotrap for seven minutes. Individual compounds were identified based on the presence of other ions with the same retention time in combination with a retention time database (Goodner 2008), performed calibration experiments and previous studies (Buttery *et al.* 1987, Maes *et al.* 2001).

QRT-PCR

For gene expression analysis, plants were sampled at six time points during the first day of treatment in a separate experiment. Trichomes were collected by snap freezing the first internode and the petiole of the second leaf in liquid nitrogen in an Eppendorf tube, shaking the tube on a vortex to separate trichomes from stems and petioles, and subsequently removing the bald stems and petioles from the sample. For leaf samples, the second leaf was harvested and frozen in liquid nitrogen. RNA extraction and DNase treatment were done with the RNeasy Mini Kit and RNase-Free DNase Set (Qiagen Benelux B.V., Venlo, the Netherlands). cDNA was synthesised with random hexamer primers and SuperScript III Reverse Transcriptase from Invitrogen (Bleiswijk, the Netherlands) and dNTP's and Ribolock RNase Inhibitor from ThermoScientific (Landsmeer, the Netherlands). Quantitative RT-PCR was performed in a ViiA™ 7 Real-Time PCR System (Life Technologies Europe B.V., Bleiswijk, the Netherlands) using iTaq universal SYBR Green Supermix (Bio-Rad, Veenendaal, the Netherlands) with gene specific primers (listed in Supplemental table S3.1) based on sequences as published by Falara *et al.* (2011).

Statistics

Growth and physiological data were analysed with a Student's t-test. Volatile measurements were analysed with a repeated-measures ANOVA with post-hoc LSD for pairwise comparisons at each time point. Stomatal aperture and gene expression data were analysed with a two-way ANOVA with post-hoc LSD. ANOVAs were done using SPSS Statistics version 22 (IBM, Amsterdam, the Netherlands), t-tests were done in Microsoft Excel.

Results

UV-B affects the tomato vegetative phenotype

Figure 3.1A shows that UV-B induces the typical stunted UV-B phenotype in 2.5-week old tomato plants. Figure 3.1B to E show that UV-B reduces growth: stem length, dry weight, leaf area and specific leaf area are significantly smaller in UV-B treated plants compared to control plants. In addition, reduced chlorophyll levels in the leaves of UV-B treated plants (Fig 3.1F) point at reduced photosynthetic capacity, while higher levels of UV-B absorptive compounds (Fig 3.1G) indicate activation of UV-B defence mechanisms in UV-B treated plants. Thus, as expected, we found a negative effect of UV-B on plant performance and an activated UV-B stress response.

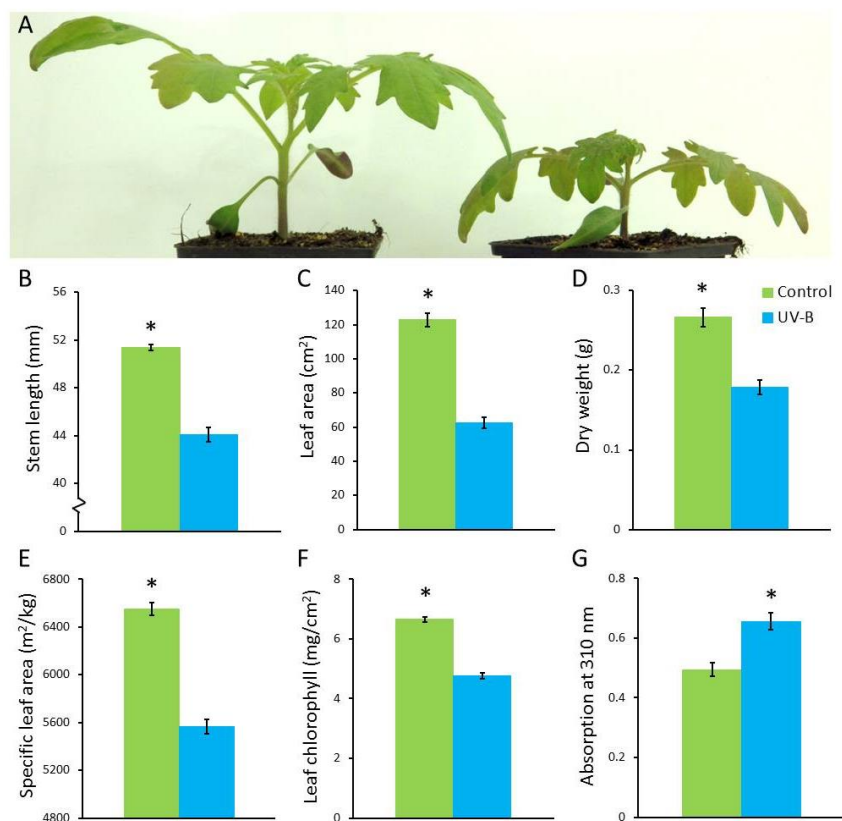


Figure 3.1 UV-B reduces growth and activates a UV-B response in tomato plants. 2.5-week old plants were exposed to UV-B for eight hours per day, resulting in a total daily UV-B dose of $28.8 \text{ kJ m}^{-2} \text{ day}^{-1}$. Photographs (A) and measurements were taken after three days of treatment. (A) Appearance of control (left) and UV-B (right) treated plants. Stem length (B), leaf area (C), shoot dry weight (D), specific leaf area (E) and total leaf chlorophyll (F) are reduced, while UV-B absorptive compounds in leaves (G) increased. Data shown are averages \pm SE (n=9), asterisks indicate significant differences ($p \leq 0.05$).

UV-B induces VOC emission differentially

UV-B exposure affects the emission of volatile organic compounds (VOCs) by tomato plants. Interestingly, the timing of the response differs between different VOC types. The induced compounds can be divided into three classes: (i) those that respond immediately at the start of the UV-B treatment, (ii) those with a delayed response of about one hour, and (iii) those whose emission increases only *after* UV-B exposure ended. Figure 3.2 shows the emission patterns of masses corresponding to acetone (A), methanol (B) and monoterpenes (C) as examples of each class. We find the emission pattern of the third class especially interesting, since this pattern suggests that the emissions are not caused by direct damage and because this class contains masses corresponding to compounds known to function as signalling molecules in ecological interactions: monoterpenes and MeSA. We, therefore, further investigated the emission pattern of this class of compounds, and show monoterpene emissions as an example.

Monoterpene emissions increase after UV-B exposure

Figure 3.3 displays tomato monoterpene emission patterns after four, eight and twelve hours of UV-B exposure. The lack of change after four hours (Fig 3.3A) suggests there is a threshold for the induction of these emissions. In contrast, methanol and acetone have similar emission patterns independent of the duration of UV-B exposure (data not shown). The significant increase of monoterpene emissions after eight and twelve hours of exposure (Fig 3.3B and 3.3C) demonstrates that tomato plants start emitting monoterpenes when the duration threshold is reached, but only after UV-B exposure stops.

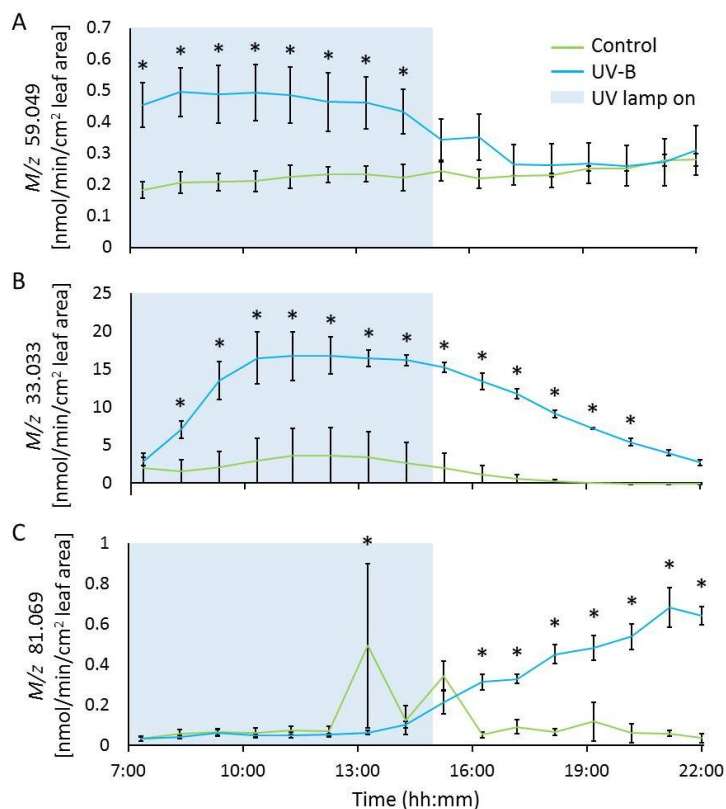


Figure 3.2 UV-B induces three classes of volatile compounds with differential timing: (A) immediately after start of treatment, (B) delayed by about one hour, (C) after the treatment stopped. 2.5-week old tomato plants were exposed to UV-B for eight hours, resulting in a total daily UV-B dose of $28.8 \text{ kJ m}^{-2} \text{ day}^{-1}$. (A) m/z 59.049, corresponding to acetone, is shown as example of the first class. Also in this class are m/z 45.033, 63.043, 71.049, 71.084 and 83.049. (B) m/z 33.033, corresponding to methanol, is shown as an example of the second class. Also in this class are m/z 51.044, 75.027 and 75.043. (C) m/z 81.069, corresponding to monoterpenes, aldehydes and alcohols, is shown as an example of the third class. Also in this class are m/z 69.069, 79.054, 82.073, 85.101, 93.069, 95.085, 107.084, 109.1, 121.1 and 137.13. Averages \pm SE are shown, asterisks show significant differences at that time point ($p \leq 0.05$, $n=3$).

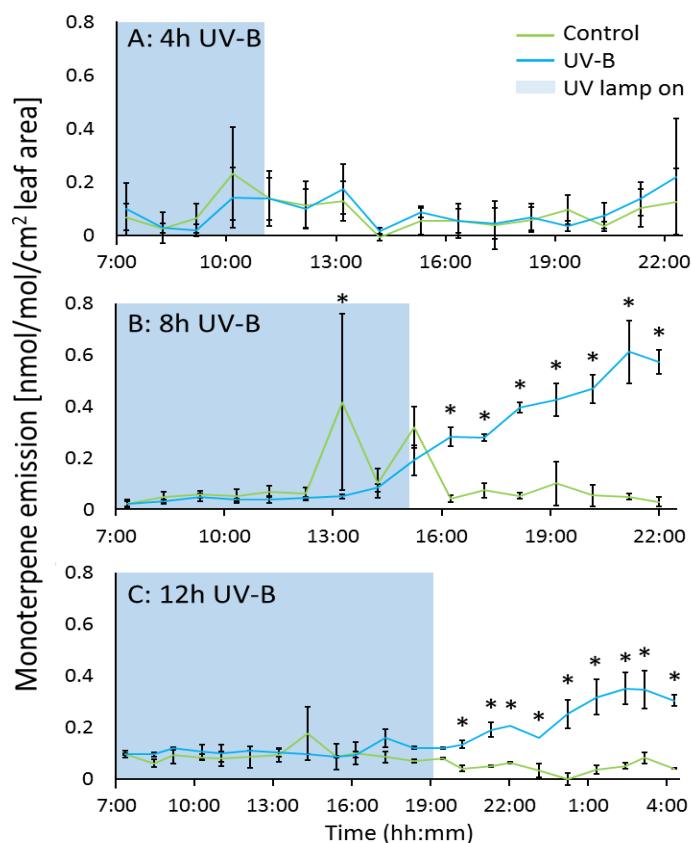


Figure 3.3 Monoterpene emission of tomato plants after (A) four, (B) eight and (C) twelve hours of UV-B treatment. Monoterpene emission was calculated as m/z 137.13 multiplied by a factor of 3.13. Data shown in (B) are from the same experiment as in figure 3.2. Averages \pm SE are shown, asterisks show significant differences at that time point ($p \leq 0.05$, (A) $n=5$, (B) $n=3$, (C) $n=2$).

To confirm that the observed monoterpene emission pattern was caused by induction after exposure rather than induction and closing of the stomata during treatment, we measured stomatal aperture during and after exposure. Figure 3.4 shows that stomatal aperture decreases significantly upon UV-B exposure, and that this effect lasts for several hours after the exposure. However, stomata do not close completely upon UV-B. In fact, only a few fully closed stomata were observed in all samples. This does not parallel the observed increase in monoterpene emissions after UV-B exposure (Fig 3.3) and confirms a regulated increase of monoterpene emissions induced by UV-B.

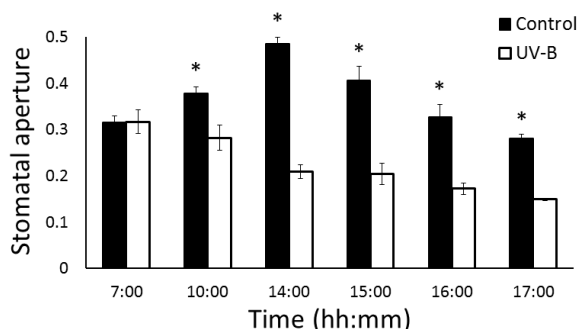


Figure 3.4 Stomatal aperture decreased during and after UV-B exposure. Tomato plants were exposed to UV-B for eight hours, from 7 a.m. till 3 p.m., resulting in a total daily UV-B dose of $28.8 \text{ kJ m}^{-2} \text{ day}^{-1}$. Averages \pm SE are shown, asterisks show significant differences at that time point ($p < 0.05$, $n \geq 60$).

UV-B induces emission of several monoterpenes

We identified the individual monoterpenes induced by UV-B using gas chromatography. This revealed that two monoterpenes are emitted constitutively and increasingly upon UV-B exposure. Based on their retention times, these are most likely limonene and β -phellandrene. These monoterpenes have also been described by e.g. Kant *et al.* (2004) to be the major monoterpenes emitted by this tomato cultivar. Figure 3.5 shows these two compounds as the largest peaks in example chromatograms obtained from control and UV-B-treated plants. Figure 3.5B shows four additional monoterpenes emitted upon UV-B exposure. Their relative retention times as well as previously described tomato headspace profiles suggest that these compounds are α -pinene, β -myrcene, α -phellandrene and α -terpinene.

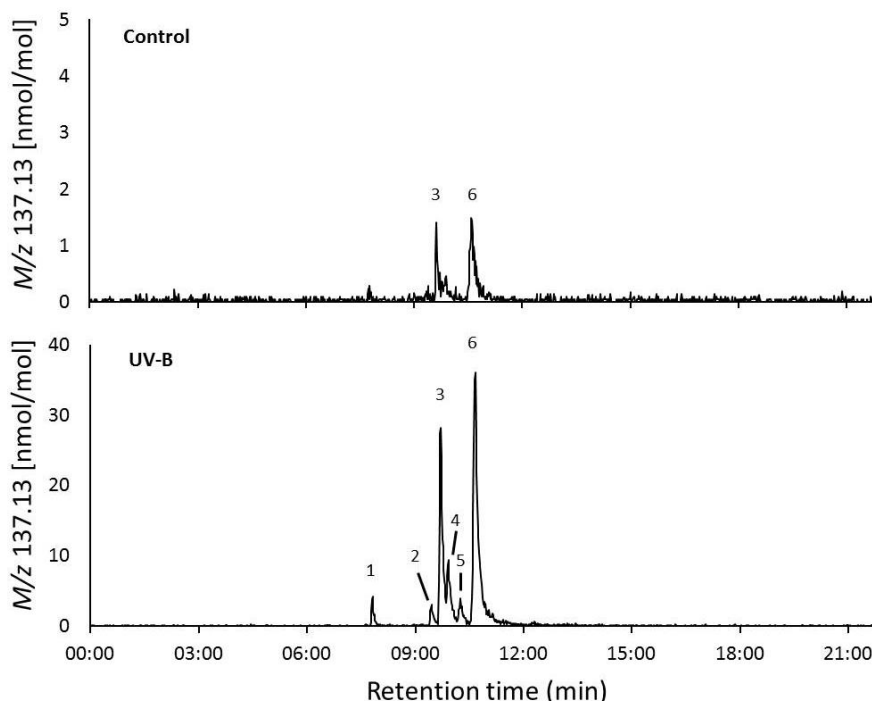


Figure 3.5 Chromatograms of (A) control and (B) UV-B treated tomato plants. M/z 137.13 corresponds to monoterpenes. Chromatograms shown were obtained around 10 p.m. during the same experiment as shown in figure 3.2. Individual compounds are identified as (1) α -pinene, (2) β -myrcene, (3) limonene, (4) α -phellandrene, (5) α -terpinene and (6) β -phellandrene.

UV-B inhibits expression of most *TPS* genes in trichomes

Terpene emissions are often controlled at the transcriptional level (Dudareva *et al.*, 2013). In tomato, many *TERPENE SYNTHASE* (*TPS*) genes are expressed and specifically induced in trichomes (Falara *et al.*, 2011, Van Schie *et al.*, 2007). We therefore investigate *TPS* gene expression in tomato trichomes under UV-B-enriched and control light conditions. From the 29 genes in the tomato *TPS* gene family (Falara *et al.*, 2011), we selected the ones expressed in aboveground vegetative tissue. Figure 3.6 shows a heatmap of their expression levels relative to start of treatment. Values are shown at time points where UV-B significantly altered expression compared to control. Expression data of each individual gene are shown in Supplemental figure S3.2. Surprisingly and in contrast to the emission pattern displayed in figure 3.2C, most monoterpene synthesis genes are down-regulated in trichomes upon UV-B. *TPS3*, encoding a camphene or tricylene synthase, *TPS4* (*MTS2*), encoding a β -phellandrene synthase, *TPS5* (*MTS1*), encoding a linalool synthase, *TPS19*, *TPS20* (*PHS1*), also encoding a β -phellandrene synthase, *TPS21*, and *TPS37*, encoding a linalool or nerolidol synthase, are all slightly but significantly down-regulated. The only monoterpene synthesis genes found to be up-regulated by UV-B in tomato trichomes are *TPS8* and *TPS39*, encoding a 1.8-cineole synthase and a linalool or nerolidol synthase, respectively. Their expression patterns match the monoterpene emission pattern, but we did not observe these oxygenated monoterpenoids in the chromatograms obtained from UV-B treated tomato plants (Fig 3.5), nor did we observe the emission of masses corresponding specifically to oxygenated monoterpenes. Expression of *TPS7*, encoding a β -myrcene or limonene synthase, is not affected by UV-B in tomato trichomes.

The other *TPS* genes investigated encode diterpene and sesquiterpene synthesis genes. We find up-regulation of the *DITERPENE SYNTHASE* *TPS24* (*KS*), encoding an ent-kaurene synthase, down-regulation of *TPS40*, involved in gibberellin biosynthesis, and no regulation of *TPS41*, a gene closely related to *TPS40* with unknown function. Also up-regulated is a group of closely related *SESQUITERPENE SYNTHASES*: *TPS31*, *TPS32* and *TPS33*. *TPS31* and *TPS32* are viridiflorene synthesis genes expressed specifically in trichomes (Bleeker *et al.*, 2011, Falara *et al.*, 2011). In contrast, *SESQUITERPENE SYNTHASES* *TPS9*, *TPS10*, *TPS12*, *TPS16* and *TPS17* are down-regulated by UV-B. *TPS9* (*SST1*) encodes a germacrene synthase, *TPS12* (*CAHS*) encodes a β -caryophyllene or α -humulene synthase, *TPS17* encodes a valencene synthase, the function of *TPS10* and *TPS16* is unknown. Incidentally, we observed the mass corresponding to sesquiterpenes (m/z 205.2) in our volatile samples, but we were not able to quantify this mass due to limitations of the system. Therefore, we cannot draw any conclusions concerning sesquiterpene emissions.

UV-B induces a *B-PHELLANDRENE SYNTHASE* in leaves

Although monoterpene emissions were induced (Fig 3.2), and their production is often regulated at the transcriptional level (Dudareva *et al.*, 2013), most terpene synthesis genes were down-regulated by UV-B in trichomes (Fig 3.6). Possibly, trichomes are not the right tissue to look for these responses. Therefore, we also investigated gene expression in leaf tissue, looking at three *TPS* genes known to produce the identified UV-B-inducible monoterpenes (Fig 3.5B). Figure 3.7 shows that *TPS7* and *TPS20* are down-regulated, while *TPS4* is up-regulated. Thus, UV-B-induced β -phellandrene emission is paralleled by transcriptional up-regulation of the *B-PHELLANDRENE SYNTHASE* *TPS4* in leaves. Apparently, the UV-B-induced emission of the other five monoterpenes is not regulated by UV-B at the *TPS* transcriptional level.

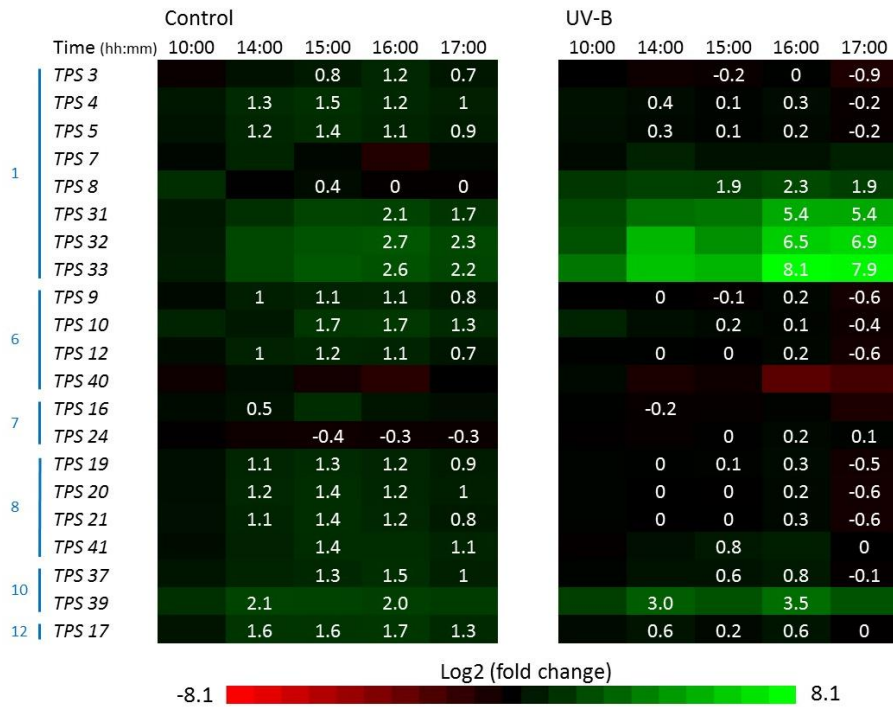


Figure 3.6 Regulation of *TERPENE SYNTHASE (TPS)* genes by UV-B in tomato trichomes. Shown are average log₂ fold changes (relative to start of treatment at 7 a.m.) of six plants. Plants were exposed to UV-B for eight hours, from 7 a.m. till 3 p.m., resulting in a total UV-B dose of 28.8 kJ m⁻² day⁻¹. Note that numbers are shown at time points where control and UV-B differed significantly from each other (p ≤ 0.05).

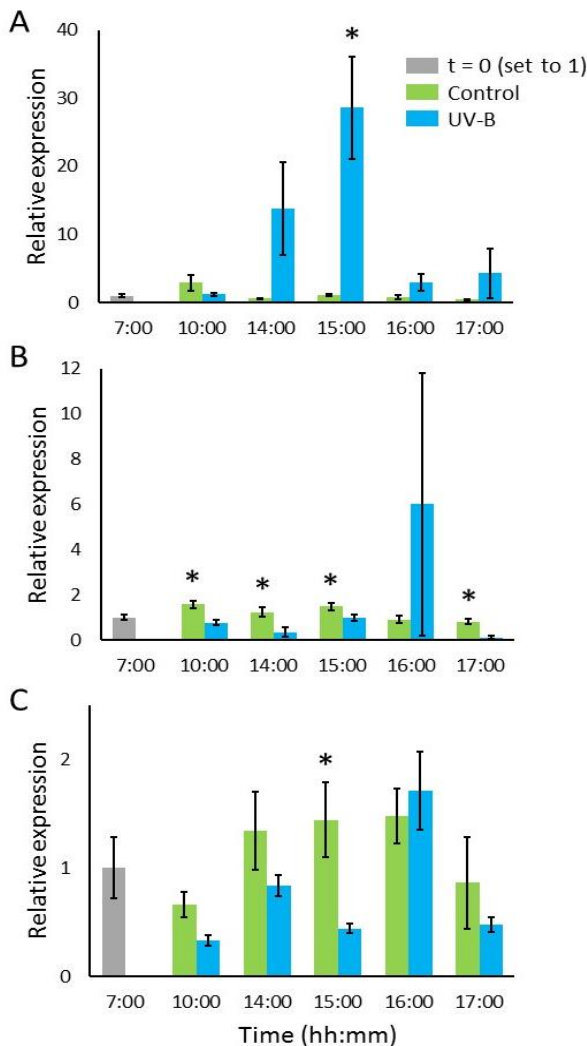


Figure 3.7 Effect of UV-B on gene expression levels in tomato leaves. (A) *TPS4/MTS2*, encoding a β -phellandrene synthase, is induced by UV-B. (B) *TPS7*, encoding a β -myrcene or limonene synthase, and (C) *TPS20/PHS1*, encoding a second β -phellandrene synthase, are down-regulated by UV-B. Plants were exposed to UV-B for eight hours per day, from 7 a.m. till 3 p.m., resulting in a total daily UV-B dose of 28.8 kJ m⁻² day⁻¹. Data shown are averages \pm SE, asterisks indicate significant differences (p ≤ 0.05) between control and UV-B treated plants at that time point (n=6).

Discussion

We investigated the effect of UV-B on the emission of volatile organic compounds in tomato plants. We found that UV-B increases the emission of VOCs with differential timing. A group of six masses increased immediately, the increase of four masses was delayed by about one hour and a third group of eleven masses only increased after UV-B exposure stopped (Fig 3.2). By looking at emission patterns after different exposure periods and by measuring stomatal aperture during and after exposure, we confirmed that the third group was indeed only induced after UV-B exposure stopped (Fig 3.3 and 3.4). Masses in the first two classes, corresponding to e.g. methanol and acetone, are likely the result of damage to cell walls, membranes and other plant parts (Von Dahl *et al.*, 2006). This damage could be caused directly by UV-B or indirectly through reactions with radical oxygen species. Masses in the third class of UV-B-induced VOCs, specifically m/z 137.13, 81.069, 95.085, 69.069, 82.073, 85.101 and 107.084, are associated with monoterpenes. Monoterpenes are known to have a signalling function when induced by herbivory (Heil 2008). In addition, we found m/z 121.1 and 93.069 in this class, corresponding to MeSA, which is also a known signalling molecule in plant-herbivore interactions (Blande *et al.*, 2010). Apparently the UV-B response overlaps with herbivore defence responses in terms of volatile emissions. This is consistent with the induction of direct herbivore defences by UV-B reported by Demkura *et al.* (2010).

Besides signalling, another function of monoterpenes in plant UV-B defence could be the quenching of radicals created by UV-B *in planta*. In *Quercus ilex*, monoterpenes were induced by ozone and protected leaves from ozone damage to the photosynthetic apparatus (Loreto *et al.*, 2004). If this mode of action would exist in tomato during UV-B exposure, the monoterpenes would have reacted away with radicals inside the plant. We would then expect to find monoterpene oxidation products during UV-B exposure (Calogirou *et al.*, 1999). However, we did not observe emission of these compounds during UV-B exposure. In addition, if monoterpene production was induced by UV-B to quench oxygen radicals *in planta* we would expect a steep increase right after UV-B exposure stopped (due to overproduction), followed by a drop in emissions, since stopping the UV-B exposure would halt the production of these quenchers. This does not match the observed emission pattern (Fig 3.3). We therefore hypothesise that UV-B-induced emissions of monoterpenes and MeSA have a signalling function and may be another readout of defence induction.

Six monoterpenes are emitted increasingly after UV-B exposure. These most likely are α -pinene, β -myrcene, limonene, α -phellandrene, α -terpinene and β -phellandrene (Fig 3.5). Surprisingly, their corresponding *TERPENE SYNTHASE* (*TPS*) genes - *TPS4*, *TPS7* and *TPS20* - were down rather than up-regulated in trichomes (Fig 3.6). Trichomes are where most *MONOTERPENE SYNTHASES* are expressed (Falara *et al.*, 2011) and increased terpene emissions usually correlate with induction of *TERPENE SYNTHASE* transcripts (Van Schie *et al.*, 2007). When we further investigated their expression in leaf tissue, we found that only a *B-PHELLANDRENE SYNTHASE* (*TPS4*, Fig 3.7) was up-regulated by UV-B in leaves (Fig 3.7). In trichomes, we investigated all 21 tomato *TPS* genes reported to be expressed in vegetative aboveground tissue (Falara *et al.*, 2011). Most of these genes were inhibited by UV-B (Fig 3.6 and S3.2). The only *TPS* genes induced by UV-B encode synthesis genes producing oxygenated monoterpenes (1.8-cineole and linalool or nerolidol) and sesquiterpenes (viridiflorene). Unfortunately, our detection system did not allow us to draw conclusions about sesquiterpene emissions. By contrast, the detection worked for masses corresponding specifically to oxygenated monoterpenes, but we did not observe any emission of these compounds. Thus, for monoterpenes, we can conclude that (i) the up-regulation of the *B-PHELLANDRENE SYNTHASE* gene *TPS4* in leaf tissue correlates with UV-B-induced β -phellandrene emission and (ii) no correlation was found between transcriptional regulation of *TPS* genes in trichomes and UV-B-mediated emission of their volatile terpenoid products.

Interestingly, we found transcriptional regulation by UV-B to be similar for genes that are closely related (Fig 3.6 and S3.2, see Falara *et al.*, 2011 for a phylogenetic tree). Since related genes will likely have homologous promotor sequences (Fernie and Tohge 2014), this suggests that a specific promotor pattern might be responsible for UV-B-regulated expression. Unravelling the regulation of tomato terpenes might help to improve this important crop species to fend off biological pests more effectively, which would reduce pesticide use and increase yields. Future research focusing on promotor regions of UV-B-regulated genes may be an important step in this direction.

Besides looking at promotor sequences, an important step to unravel how UV-B regulates terpene synthesis would be investigating the role of the UV-B receptor UVR8 that was recently discovered in *Arabidopsis thaliana* (Rizinni *et al.*, 2011). This would require measurements of volatile emissions upon UV-B exposure in this important model species as well as in its *uvr8* mutant.

Acknowledgements

The TD-PTR-MS has been funded by the Netherlands Organization for Scientific Research (NWO) under the ALW-Middelgroot program (Grant 834.08.002). This project is funded by a strategic funding scheme (Focus and Mass) of Utrecht University. We thank Carina van der Veen, Henk Snellen, Michel Bolder and Marcel Portanger for technical support with the VOC measurements, Graeme Dean and Ankie Ammerlaan for help with the stomatal aperture measurements and Jesse Küpers and Emilie Reinen for help with the qRT-PCR.

Supplemental figures

Table S3.1 Gene specific primers used for qRT-PCR

Primer target	Direction	Sequence (5' to 3')
<i>TPS3</i>	Forward	CACTCATGCTATTCAAAGAATGGAGAT
	Reverse	ATCTGCCCATGATTTTGTAAAGGTACG
<i>TPS4</i>	Forward	CTGTTCAAAGATGGGATACAAAAGCAATG
	Reverse	GTCCATGATTTTCGTAAGGTAGGGTA
<i>TPS5</i>	Forward	CACTCTTGCTATTCAAAGATGGGATAC
	Reverse	CTGCCCATGATTTTGTAAAGGTAGGGT
<i>TPS7</i>	Forward	CACTCATGCTGTTGAAAGATGGGA
	Reverse	GCATAAATCTGTCCATTGTTTTGTGAGG
<i>TPS8</i>	Forward	TTCACAAGAAACTTTTGGTGGTT
	Reverse	TTCTTGCCAACCTCCAATTCCTTT
<i>TPS9</i>	Forward	GATGCAATCCAGAGATGGGATGCT
	Reverse	CACCAACTTTTTTCATCTCATTTTTTGCATAG
<i>TPS10</i>	Forward	GCAATCCAGAGATGGGATGCTAG
	Reverse	CACAATCTTTTTTATCTCATGTTTTCCATAG
<i>TPS12</i>	Forward	CAACAATGCAATCCAGAGATGGGAT
	Reverse	CACCAACTTTTTTCATCTCATATTTTGCATAG
<i>TPS16</i>	Forward	GGCAATTGAAAGGTGGAATATTGATGC
	Reverse	CACCATCTTTTTTCATCTCTATTATGGAATAG
<i>TPS17</i>	Forward	CAGGCAATTGAAAGGTGGAATATTGATGC
	Reverse	CCTTACGACCTTTTTTCATCTCATTATGG
<i>TPS19</i>	Forward	GTGGTTTGAAGATTATAGATTGGACCAAC
	Reverse	GAGCATGGCGTATTTTCGCGTTCA
<i>TPS20</i>	Forward	CCCATTGTGCTATGGCTTTTCGAC
	Reverse	TTGTGGAGTTCAAGAATTTCAACATGAC
<i>TPS21</i>	Forward	GTCAAAGAAGGAGGTGGAACCTGC
	Reverse	TGTTGGGTGACCTATAAGCTGCTT
<i>TPS24</i>	Forward	TGACGAGGACCAATATTCTCAA
	Reverse	CTGTCATACGGCCTTGTGAG
<i>TPS31</i>	Forward	CCATACAGAGGTGGGATGTCAG
	Reverse	CAGCTCTGTTTCATAGTCGTTGT
<i>TPS32</i>	Forward	CCATACAGAGGTGGGATATTAGCCA
	Reverse	CAATCTCCTTCATTCTTTCTTTTGGCTACT
<i>TPS33</i>	Forward	CGATGCCATACAGAGGTGGGATA
	Reverse	CACAATTTCTTTTCATTCTTTCTTTAGCGTAGT
<i>TPS37</i>	Forward	GCTGTTCATAGGTGGGAATTGAGC
	Reverse	TGCCACGTATTTTGTAGATTTTGTAGTG
<i>TPS39</i>	Forward	GCTGTTAATAGGTGGGAATTATGTGTC
	Reverse	CCACGCATTCCGCAAATTTTGTAGTG
<i>TPS40</i>	Forward	CTGAATTCGAGGTACAACACAGAAG
	Reverse	GCCAATTTTCCCAAGCATGACGCA
<i>TPS41</i>	Forward	CCAACACACAATGTTTGGGAAGAGTG
	Reverse	GGAATTACAAATCTGATCATTTTGGAAGTC
<i>ACTIN</i>	Forward	GGAACTTGAAACCGCTAGGAGCA
	Reverse	GAGTTGTATGTAGTCTCATGGATACC

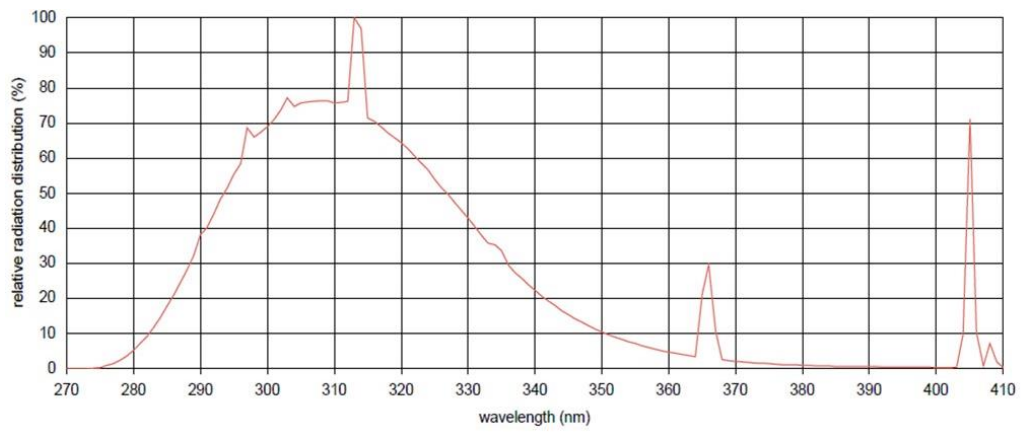


Figure S3.1 Spectral radiation distribution of the broad-spectrum UV-B lamp used in our experiments, according to the manufacturer (UV21, Waldmann, Tiel, the Netherlands).

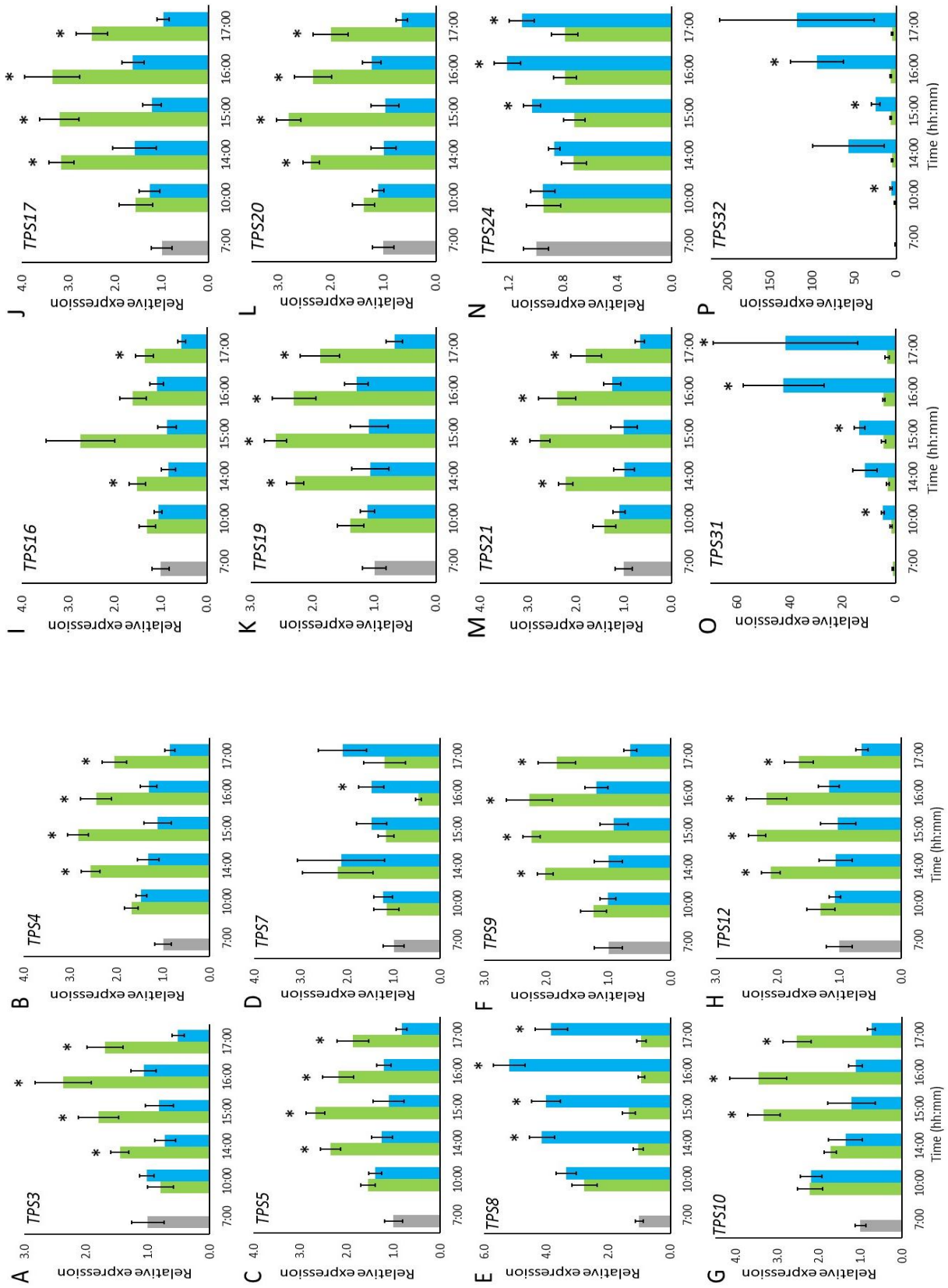
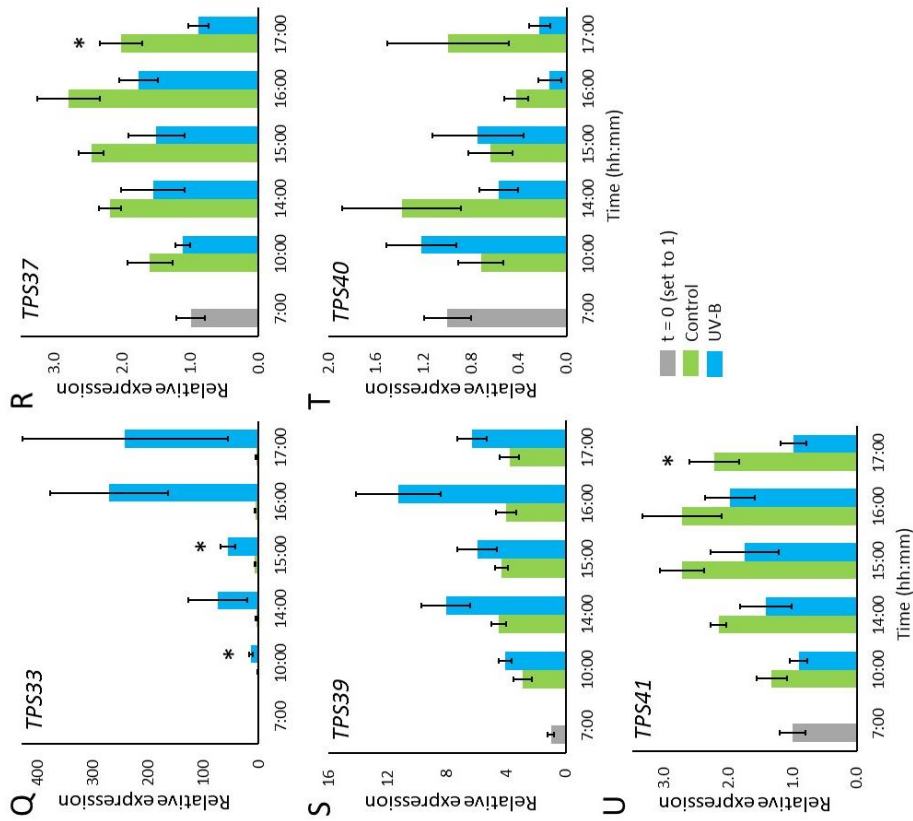


Figure S3.2 Effect of UV-B on expression levels of *TERPENE SYNTHASE (TPS)* genes in tomato trichomes. Plants were exposed to UV-B for eight hours per day, from 7 a.m. till 3 p.m., resulting in a total daily UV-B dose of 28.8 kJ m⁻² day⁻¹. (A) *TPS3* encodes a camphene or tricylene synthase; (B) *TPS4* (*MTS2*) encodes a β -phellandrene synthase; (C) *TPS5* (*MTS1*) encodes a linalool synthase; (D) *TPS7* encodes a β -myrcene or limonene synthase; (E) *TPS8* encodes a 1,8-cineole synthase; (F) *TPS9* (*SST1*) encodes a germacrene synthase; (G) *TPS10* encodes an unknown protein closely related to *TPS12*; (H) *TPS12* (*CAHS*) encodes a β -caryophyllene or α -humulene synthase; (I) *TPS16* encodes an unknown protein closely related to *TPS17*; (J) *TPS17* encodes a valencene synthase; (K) *TPS19* encodes an unknown protein closely related to *TPS20*; (L) *TPS20* (*PHS1*) encodes a β -phellandrene synthase; (M) *TPS21* encodes an unknown protein closely related to *TPS20*; (N) *TPS24* (*KS*) encodes an ent-kaurene synthase; (O) *TPS31* and (P) *TPS32* encode viridiflorene synthases; (Q) *TPS33* encodes an unknown protein closely related to *TPS31* and *TPS32*; (R) *TPS37* encodes a linalool or nerolidol synthase; (S) *TPS39* encodes a linalool or nerolidol synthase; (T) *TPS40* encodes a protein involved in gibberellic acid biosynthesis, and (U) *TPS41* encodes an unknown protein closely related to *TPS40*. Data shown are averages \pm SE and asterisks indicate significant differences ($p \leq 0.05$) between control and UV-B-treated plants at that time point (n = 6).



UV-B regulates volatile emission in *Arabidopsis thaliana* independent from the UV-B photoreceptor UVR8

P. Gankema¹, J. Timkovsky², R. Holzinger² and R. Pierik¹

1 Plant Ecophysiology, Institute of Environmental Biology, Utrecht University, the Netherlands

2 Institute for Marine and Atmospheric Research Utrecht, Utrecht University, the Netherlands

Abstract: Plant volatile organic compound (VOC) emissions are affected by biotic as well as abiotic factors, resulting in a specific blend that contains intrinsic putative information about plant identity and condition. In chapter 3, we demonstrated that UV-B induces volatile organic compounds in tomato plants with differential timing. Here, we study the effect of UV-B on VOC emissions of wild type and *uvr8* mutant *Arabidopsis thaliana* plants. As expected, UV-B negatively affects the growth of these plants. We demonstrate that the kinetics of UV-B-induced volatile emissions in *A. thaliana* are different from those in tomato. We further show that UV-B-induced VOC emissions in *A. thaliana* are independent of the UV-B receptor UVR8, implying an alternative, yet unknown, mode of regulation towards UV-B-induced VOC emissions.

Introduction

Volatile organic compounds (VOC) are important in plant stress responses and ecological interactions (Loreto and Schnitzler 2010; Dicke and Baldwin 2010), where the emitted volatile blend can function as a signal to ‘warn’ distant plant parts or neighbouring plants, deter herbivores or attract the enemies of herbivores to serve as ‘bodyguards’ (Arimura *et al.*, 2005; Heil 2008). Specific wavebands of the solar light spectrum can also affect ecological interactions and plant defences. Far-red light enrichment typically inhibits defence responses against herbivores and pathogens (reviewed in Ballaré 2014), whereas UV-B radiation can boost herbivore defences (Demkura *et al.*, 2010), resulting in less herbivore damage (Caldwell *et al.*, 2007). Nevertheless, UV-B also negatively affects plants by reducing growth and damaging DNA (Caldwell *et al.*, 1998; Britt 2004; Ballaré *et al.*, 2011). Climate change projections predict that UV-B doses will increase in agriculturally important areas such as the Mediterranean, South-West U.S.A. and Australia, potentially affecting yield (IPCC 2007). We found that, in tomato, UV-B alters volatile emissions with differential timings for different types of VOCs (chapter 3). However, we did not uncover how UV-B leads to a change of VOC emissions. Although we studied whether monoterpene emissions were associated with *TERPENE SYNTHASE* gene expression, no conclusive evidence was obtained. Furthermore, it was impossible to investigate if the regulatory pathway included the UV-B photoreceptor UV RESISTANCE LOCUS 8 (UVR8) since in tomato no mutants for this receptor are available. We therefore look further into this UV-B response using the genetic model plant species *Arabidopsis thaliana*, that has served VOC studies previously (Van Poecke *et al.*, 2001; Aharoni *et al.*, 2003). Upon the recent identification of UVR8 as the UV-B receptor in *A. thaliana* (Rizinni *et al.*, 2011), several components in the UVR8 signalling pathway have been identified in this species (Tilbrook *et al.*, 2013). Therefore, *A. thaliana* and its *uvr8* mutant offer a great opportunity to investigate the regulation of UV-B-induced VOC emissions. In this study we investigate if UV-B-mediated changes in VOC emissions are regulated via UVR8, which could be a stepping stone for future studies to unravel how UV-B controls VOC emissions in plants.

Methods

Plant growth and treatment

We used four-week old *Arabidopsis thaliana* accession Wassilewskija (Ws) and its mutant *uvr8-7* (Favory *et al.*, 2009) for all experiments. Seeds were dark stratified for four days at 4 °C on moist Primasta soil (mix Z2254, Primasta B.V., Asten, the Netherlands). Germinated seedlings were transplanted into individual pots at the two-leaf stage. Plants were grown under a short-day light regime (8h light, 16h dark) in climate chambers at 20 °C, 160-180 $\mu\text{mol m}^{-2} \text{s}^{-1}$ photosynthetically active radiation (PAR) and 70% relative humidity.

For growth measurements, control and treatment groups were treated in separate light boxes in the climate chamber. For volatile measurements, plants were transferred to the setup described in chapter 2, placed into the small plant chambers with an air flow of 0.1 L min^{-1} and left to acclimatise overnight. We used one small plant chamber with a lid with 2 mm thick quartz glass that allows UV-B penetration and a second small plant chamber with a standard glass lid that blocks UV-B. Broad-spectrum UV-B lamps (UV21, 9 W, Waldmann, Tiel, the Netherlands) were placed above the plants to create UV-B radiation levels of 1 W m^{-2} at leaf level (measured with a handheld UV meter from Waldmann, Tiel, the Netherlands), so that eight hours of UV-B exposure resulted in a total daily dose of 28.8 kJ $\text{m}^{-2} \text{day}^{-1}$. UV-B treatments started with the start of the light period at 8 a.m. To observe the effect of UV-B on volatile emissions after UV-B treatment, the light period was extended until 11 p.m.

Growth measurements

Petiole lengths were measured at the start and end of the experiment using a digital caliper. Plants were harvested after two days of treatment. Leaf area was determined with a Li-3100 Area Meter (LI-COR, Lincoln, Nebraska U.S.A.). Shoot dry weight was measured after drying the plant material in an oven at 70 °C for at least 48 hours.

Volatile measurements

Volatile organic compound emissions were measured in the set-up described in chapter 2 (see also Timkovsky *et al.*, 2014). We used the small plant chambers with a dividable bottom plate that fits around the hypocotyl in order to measure shoot emissions only. Online plant emissions were averaged over a five-minute measuring period.

Statistics

Data were analysed with either a two-way or a repeated-measures ANOVA with post-hoc LSD for pairwise comparisons using SPSS Statistics version 22 (IBM, Amsterdam, the Netherlands).

Results and discussion

UV-B reduces growth in *A. thaliana*

Figure 4.1 shows that UV-B treated wild type and *uvr8* mutant plants are smaller (A), have reduced petiole elongation (B), smaller leaf area (C) and lower shoot dry weight (D). UV-B thus reduces growth in *A. thaliana* wild type as well as *uvr8* mutant plants. Previously, *uvr8-7* mutant plants were found to be more susceptible to damage by UV-B radiation (Favory *et al.*, 2009), but this could not be observed in the current experiment. However, at the seedling stage this genotype does show enhanced UV-B susceptibility, as is shown in chapter 5.

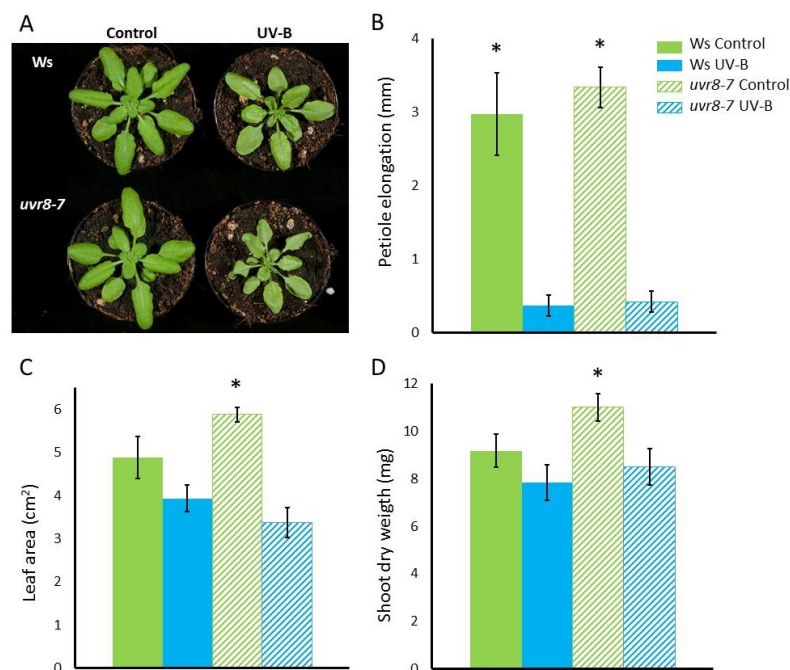


Figure 4.1 UV-B exposure reduces growth of wild type and mutant *Arabidopsis thaliana* plants. Four-week old plants were exposed to UV-B for eight hours, resulting in a total daily UV-B dose of 28.8 kJ m⁻² day⁻¹. Photographs (A) and measurements were taken 24 hours after start of treatment. Petiole elongation (B), leaf area (C) and shoot dry weight (D) are reduced in UV-B treated plants. Data shown are averages ± SE, asterisks indicate significant differences within genotype (p ≤ 0.05, n=6).

UV-B induces VOC emissions independent from UVR8

Figure 4.2 shows that UV-B induces VOC emissions in *A. thaliana* with differential timing: some compounds are induced immediately (A and C), others with a delay of about one hour (B). Figure 4.2 further shows that VOC emissions in the *uvr8* mutant (D to F) are induced by UV-B similarly as in the wild type (WT). We display the same masses as shown for tomato emissions in chapter 3 for comparison. These *A. thaliana* emissions are significantly altered by UV-B, but there is no genotype effect. Even when we averaged emissions over the eight-hour UV-B exposure period, we found no significant difference between WT and *uvr8* (Fig 4.3A to C). This is consistent for all UV-B-induced masses, of which figure 4.3D to L shows a selection. UV-B thus induces VOC emissions in *A. thaliana* independent from the UVR8 UV-B photoreceptor. This is surprising, since several physiological UV-B responses were found to be mediated by UVR8, including growth responses and UV-B-enhanced pathogen resistance (Demkura and Ballare 2012; Tilbrook *et al.*, 2013). However, a role for UVR8 in many other UV-B responses, including alterations in secondary metabolism, remains to be investigated (Jansen *et al.*, 2008; Kusano *et al.*, 2011). Our results indicate that UV-B induces VOC emissions through a UVR8-independent pathway. Although the existence of such pathways is not novel (Brown and Jenkins 2008; Gonzalez Besteiro *et al.*, 2011), our results underline the importance of unravelling the distinct pathways plants use to respond to UV-B and demonstrate the value of *uvr8* mutants in doing so.

In tomato, *TERPENE SYNTHASE (TPS)* gene expression correlated with terpenoid emission for one of the emitted monoterpenes (Fig 3.6). Therefore, we looked into existing *A. thaliana* micro array data for *TPS* gene expression levels under UV-B treatment. Killian *et al.* (2007) obtained their data from adult *A. thaliana* plants with treatment conditions similar to ours. However, no regulation of *TPS* gene expression by UV-B was reported at the 0.25, 1, 3, 6 or 24-hour time point. We thus found no evidence that UV-B-mediated volatile emission in *A. thaliana* correlates with regulation at the *TPS* transcriptional level.

Kinetics of UV-B-induced VOC emissions are species specific

Interestingly, the kinetics of UV-B-induced VOC emission in *A. thaliana* are different from those in tomato: we find immediate and delayed emissions in *A. thaliana*, but no “late” class. Masses induced “late” in tomato are masses that were emitted only after the UV-B exposure had ended. Late masses in tomato, but induced immediately in *A. thaliana* are those corresponding to monoterpenes (m/z 81.069, 95.085, 69.069, 82.073, 85.101 and 107.084). The kinetics of these UV-B-induced VOC emissions thus appear to be species specific. The other masses that were induced late in tomato were those corresponding to MeSA (m/z 121.1 and 93.069). These are not detectably induced by UV-B in *A. thaliana*, suggesting their induction by UV-B is species specific as well.

Conclusions

We investigated the effect of UV-B on VOC emissions in *Arabidopsis thaliana* and demonstrate that UV-B induces VOC emissions independent from the UV-B photoreceptor UVR8. Besides, comparing these results to those obtained with tomato plants in chapter 3, we found that the kinetics of UV-B-induced VOC emissions as well as UV-B-mediated induction of MeSA emissions are species specific.

Acknowledgements

The TD-PTR-MS has been funded by the Netherlands Organization for Scientific Research (NWO) under the ALW-Middelgroot program (Grant 834.08.002). This project is funded by a strategic funding scheme (Focus and Mass) of Utrecht University. We thank Carina van der Veen, Henk Snellen, Michel Bolder and Marcel Portanger for technical support and Roman Ulm for kindly providing seeds of the *uvr8* mutant.

UV-B regulates *A.thaliana* volatile emissions independent from UVR8

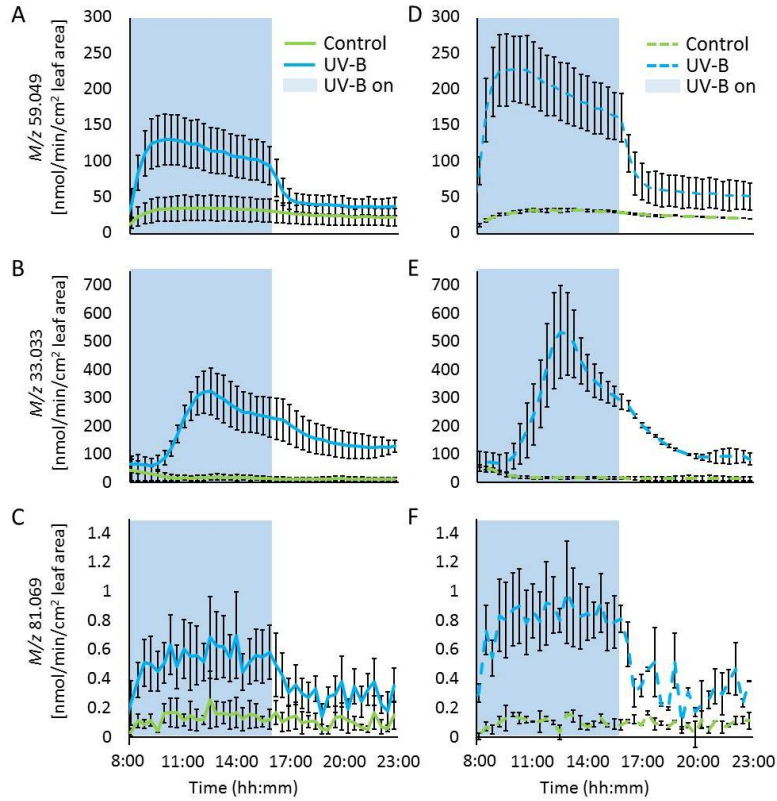


Figure 4.2 Effect of UV-B on VOC emissions of wild type (A-C) and *uvr8* mutant *Arabidopsis thaliana* plants (D-F). Four-week old plants were exposed to UV-B for eight hours, resulting in a total daily UV-B dose of 28.8 kJ m⁻² day⁻¹. UV-B significantly alters emissions of 59 masses, while genotype has no effect. Most masses are induced immediately upon UV-B exposure, like *m/z* 59.049 (A and D) and *m/z* 81.069 (C and F). Others are induced with about one hour delay, like *m/z* 33.033 (B and E). Data shown are averages ± SE (n=3).

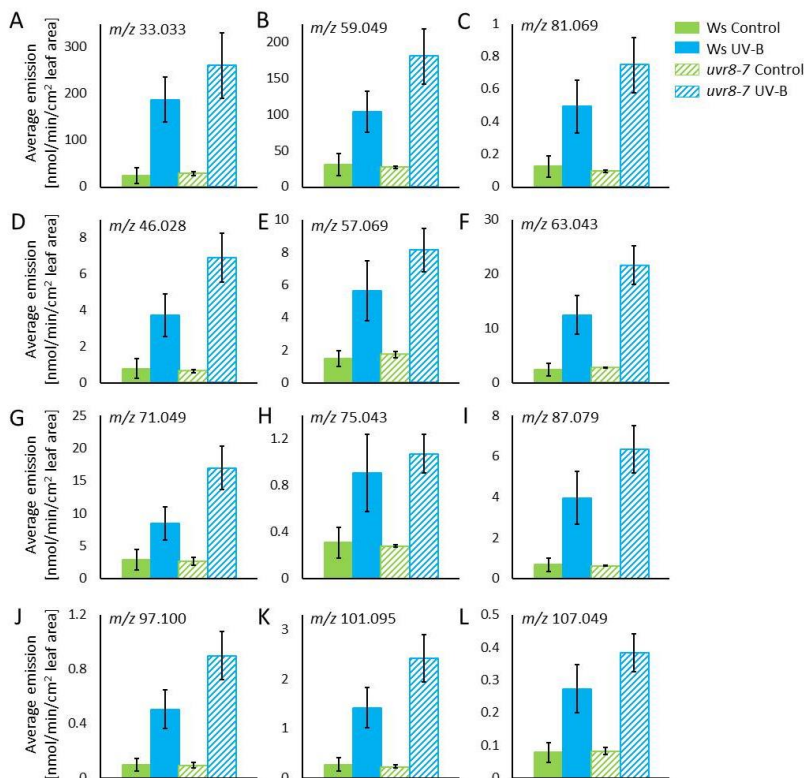


Figure 4.3 UV-B increases emissions of wild type and *uvr8* mutant *Arabidopsis thaliana* plants similarly. Twelve masses are shown to illustrate similar, UVR8-independent induction by UV-B for all induced masses. The data shown in figure 4.2 is from the same experiment. Data shown here are average emissions during the eight-hour UV-B exposure period ± SE (n=3).

Crosstalk between UV-B and R:FR signalling pathways regulates elongation in *Arabidopsis thaliana*

P. Gankema¹, E. Reinen¹, J.J. Küpers¹, H.J. Beumer¹, L.A.C.J. Voesenek¹ and R. Pierik¹

1 Plant Ecophysiology, Institute of Environmental Biology, Utrecht University, the Netherlands

Abstract: We investigated plant responses to changes in light quality. When growing in direct sunlight, plants are exposed to ultraviolet (UV)-B light, which reduces elongation and leads to a more compact plant stature. An opposite (elongated) phenotype is induced by a low red to far-red (R:FR) ratio, which is a signal for proximate neighbours in a closing plant canopy. By exposing plants to both light signals simultaneously, we demonstrate that the UV-B and R:FR signalling pathways interact. UV-B can repress low R:FR-induced responses, and does so via the UVR8 UV-B receptor. Also, several components of the early R:FR signalling pathway are suggested to play a role in the interaction. In addition, we found evidence that brassinosteroids are involved in this interaction, whereas no such evidence was found for auxin and gibberellic acid. These results provide novel insights into the entanglement of the distinct signal transduction pathways that plants use to adjust to a changing light environment.

Introduction

To optimise their fitness, plants are well-equipped to assess and respond to their light environment, acclimating to changes in light quantity and quality as they grow. Their phenotypic plasticity in response to light cues derived from light reflection and transmission by vegetation has been particularly well-studied (Franklin 2008). In agricultural as well as natural settings, most plants compete with neighbours for sunlight. Green plant parts absorb blue (B) and red (R) light for photosynthesis, while reflecting far-red (FR) and green (G) light. In a closing canopy, the R:FR ratio drops first because of horizontal FR reflection by vertical plant structures, followed by a reduction in the level of B and photosynthetically active radiation (PAR; Ballaré *et al.*, 1990; Casal 2013; Pierik and de Wit 2014). Plants sense a change in R:FR ratio with their phytochrome photoreceptors, detecting neighbouring plants before they are actually shaded. They typically respond by elongating their upward-growing plant parts (hypocotyls, stems and petioles) and moving their leaves in a more upright position (hyponasty) in an attempt to grow away from shaded canopy layers. The signalling network regulating this suite of responses, called the shade avoidance syndrome (SAS), has been studied elaborately in the past decades (reviewed by Casal 2012, see also Fig 1.5). Detection of shade signals by phytochromes (Phy) leads to their inactivation, thus relieving Phy-mediated degradation of PHYTOCHROME-INTERACTING FACTOR (PIF) proteins. At the same time, DELLA proteins are degraded, which also relieves their inhibitory interaction with PIFs. As a consequence, PIFs bind to DNA and activate shade avoidance responses. Partly through PIF action, low R:FR increases the expression of genes associated with auxin, gibberellic acid and brassinosteroids; hormones that control growth and whose coordinated activity results in the typical elongated shade avoidance phenotype. The exact opposite phenotype is observed when plants are exposed to ultraviolet (UV)-B light: reduced growth and elongation and increased axillary branching result in a more compact plant stature (reviewed by Caldwell *et al.*, 1998). UV-B light is mostly absorbed by green plant tissue, and can therefore function as a signal for direct sunlight. After identification of the UV-B receptor UV RESISTANCE LOCUS 8 (UVR8; Rizinni *et al.* 2011), the UV-B signalling pathway has been studied intensively (reviewed by Tilbrook *et al.*, 2013; Jenkins 2014). Upon absorption of UV-B radiation, inactive UVR8 dimers quickly monomerise and bind to the E3-ubiquitin ligase CONSTITUTIVE PHOTOMORPHOGENESIS 1 (COP1). The reduced COP1 activity results in stabilisation of the bZIP transcription factor ELONGATED HYPOCOTYL 5 (HY5) and consequent activation of UV-B-responsive genes (Heijde and Ulm 2012).

UV-B and low R:FR thus cause opposite phenotypes, but what happens when plants receive both signals at the same time? Given how quickly and accurately plants respond to changes in their light environment, we expect that plants will integrate these signals at the signal transduction level. Exposing plants to UV-B and low R:FR simultaneously could help to provide new insights into the signal transduction networks behind plant responses to a changing light environment. Therefore, we investigate here whether the R:FR and UV-B signalling pathways interact and explore which of their components are involved in the integration of UV-B and low R:FR light signals.

Methods

Plant growth conditions

We used the following *Arabidopsis thaliana* mutants and their respective wild type backgrounds: *uvr8-7* (Favory *et al.*, 2009), *hy5 hyh* (Holm *et al.*, 2002) and Wassilewskija (Ws); *uvr8-1* (Kliebenstein *et al.*, 2002), the *DELLA* quadruple knock-out *gai-16 rga-24 rgl1-1 rgl2-1* (Achard *et al.*, 2006) and Landsberg *erecta* (*Ler*); *uvr8-6* (SALK_033468, Alonso *et al.*, 2003; Favory *et al.*, 2009), *pif4 pif5* (Lorrain *et al.*, 2008), *pif4 pif5 pif7* (created by and seeds kindly provided by C. Fankhauser, University of Lausanne, Switzerland), *pif1 pif3 pif4 pif5* (Leivar *et al.*, 2008), *par1* (PAR1-RNAi; Roig-Villanova *et al.*, 2007), *pk2* (Lariguet *et al.*, 2003), *pIAA19::GUS* (Tatematsu *et al.*, 2004) and Columbia (Col-0).

For experiments with adult *A. thaliana* plants, seeds were dark stratified for four days at 4 °C on moist Primasta soil (mix Z2254, Primasta B.V., Asten, the Netherlands). Germinated seedlings were transplanted at the two-leaf stage into individual 70 mL pots. We used four week old *Ler* and *uvr8-1* plants for growth measurements. We used 24-day old Col-0 and *uvr8-6* plants for qRT-PCR and for experiments with dense stands. For dense stands, seedlings were transplanted in individual pots of 19 mL in a checkerboard design of 7x7 plants (2066 plants m⁻²). Plants were grown under a short-day light regime (8h light, 16h dark) in climate chambers at 20 °C, 160-180 μmol m⁻² s⁻¹ photosynthetically active radiation (PAR) and 70 % relative humidity.

For experiments with *A. thaliana* seedlings, seeds were surface-sterilised and sown on plates containing 8 g l⁻¹ agar and 1 g l⁻¹ Murashige and Skoog (Duchefa Biochemie B.V., Haarlem, the Netherlands). After six days of dark stratification at 4 °C, plates were moved to climate chambers with a long-day light regime (16h light, 8h dark) at 20 °C, 160-180 μmol m⁻² s⁻¹ PAR and 70 % relative humidity. After a two-hour light pulse on the first day in the climate chamber, plates were in the light from the second day onwards. Treatment started on the fourth day, when cotyledons were completely unfolded. Seeds that had not germinated by then were excluded from the experiment.

Tomato (*Solanum lycopersicum*) cv. Moneymaker were grown on Primasta soil (mix Z2254, Primasta B.V., Asten, the Netherlands) under a long-day light regime (16h light, 8h dark) in climate chambers at 20 °C, 160-180 μmol m⁻² s⁻¹ PAR and 70 % relative humidity. Seeds were sown on moist soil, equally large seedlings were transplanted into individual pots after 1 week. Experiments were performed when plants were 2.5 weeks old, with their third leaf emerging.

Light treatments

Light treatments were performed in custom-made light boxes in the climate chamber where the plants were grown. Broad-spectrum UV-B lamps (UV21, 9 W, Waldmann, Tiel, the Netherlands) were placed above the plants to create the desired UV-B radiation levels (measured at leaf level with a handheld UV meter from Waldmann, Tiel, the Netherlands). Adult plants were exposed to 0.4 W m⁻² UV-B for four hours for growth and GUS measurements or two hours for qRT-PCR and dense stands. This resulted in a total daily dose of 5.8 or 2.9 kJ m⁻² h⁻¹, respectively. UV-B treatments were applied around solar noon. Plates with seedlings were exposed to 1 W m⁻² UV-B for the duration of the light period, resulting in a total daily dose of 57.6 kJ m⁻² h⁻¹. UV-B doses were adjusted per experiment to cause an effect on growth but not damage the plants so much that growth was completely arrested. Low R:FR treatments started with the UV-B treatment and lasted the entire light period. Low R:FR levels (R:FR 0.2) were obtained using supplemental far-red LEDs (730 nm; Philips Green Power, Eindhoven, the Netherlands) in addition to a control white light background (R:FR 2.2; Philips HPI-T Plus, 400 W, Philips, Eindhoven, the Netherlands). PAR levels inside all light boxes were around 120 μmol m⁻² s⁻¹. Light spectra of control and FR-enriched boxes are shown in Supplemental figure S5.1.

Hormone treatments

A. thaliana *Ler* seedlings were treated with 10 μM indole-3-acetic acid (IAA) in 0.1% ethanol, 20 μM gibberellic acid (GA₃) in 0.01% ethanol, 10 μM 24-epibrassinolide (EBL, inducing a brassinosteroid (BR) response; Keuskamp *et al.*, 2011) in 0.1% dimethyl sulfoxide (DMSO), or mock solution (IAA, GA, ethanol and DMSO: Duchefa Biochemie B.V., Haarlem, the Netherlands; EBL: Bio-Connect Diagnostics B.V., Huissen, the Netherlands). Hormones were added to the agar medium at the start of the light treatment. 150 μL of a concentrated solution was applied as a film on top of the agar and allowed to diffuse through the medium.

Growth measurements

Seedling hypocotyl lengths were measured after three days of treatment using a CanoScan 9000F MarkII Flatbed scanner (Canon, Tokio, Japan) and the open-source software package ImageJ (Abràmoff *et al.*, 2004). Hypocotyl experiments were repeated at least two times. Petiole lengths of individual *A. thaliana* plants were measured from photographs using ImageJ. Petiole lengths of *A. thaliana* in dense stands and first internode lengths of tomato plants were measured with a digital calliper. Relative elongation was calculated as $(\text{length}_{\text{end}} - \text{length}_{\text{start}}) / \text{length}_{\text{start}}$. Dense stand *A. thaliana* plants were harvested after eleven days of treatment, using only the nine inner plants of the stand to avoid edge effects. Leaf area per plant was measured using a scanner and ImageJ, like for hypocotyl length. Shoot dry weight was determined after drying the plant material in an oven at 70 °C for at least 48 hours.

GUS staining

Transgenic *pIAA19::GUS* plants, expressing the β -glucuronidase (GUS) enzyme driven by the *IAA19* promoter, were used to study auxin activity (Tatematsu *et al.*, 2004). Plant shoots were harvested 24 hours after start of treatment. GUS activity was determined by incubating shoots 24 hours at 37 °C in a staining solution containing 500 mg L⁻¹ X-Gluc (5-bromo-4-chloro-3-indolyl-D-glucuronide), 2.5 mM K₄Fe(CN)₆, 2.5 mM K₃Fe(CN)₆, 2.5 mM EDTA, 0.1% Triton X-100 (all from Duchefa Biochemie B.V., Haarlem, the Netherlands) and 100 mM sodium phosphate buffer with pH 8.0 (Merck, Darmstadt, Germany). Afterwards, shoots were bleached with 70% ethanol and the material was photographed.

QRT-PCR

For gene expression analyses either one adult shoot or 20 seedling shoots were sampled in an Eppendorf tube and snap frozen in liquid nitrogen. RNA extraction and DNase treatment were done with the RNeasy Mini Kit and RNase-Free DNase Set (Qiagen Benelux B.V., Venlo, the Netherlands). cDNA was synthesised with random hexamer primers and SuperScript III Reverse Transcriptase from Invitrogen (Bleiswijk, the Netherlands) and dNTP's and Ribolock RNase Inhibitor from ThermoScientific (Landsmeer, the Netherlands). Quantitative RT-PCR was performed in a ViiA™ 7 Real-Time PCR System (Life Technologies Europe B.V., Bleiswijk, the Netherlands) using iTaq universal SYBR Green Supermix (Bio-Rad, Veenendaal, the Netherlands) with gene specific primers (listed in Supplemental table S5.1).

Statistical analyses

We analysed microarray data obtained from adult *A. thaliana* Col plants that were either treated with low R:FR (De Wit *et al.*, 2013, GEO link GSE35700) or UV-B (Killian *et al.*, 2007, GEO link GSE5620 and GSE5626). These datasets are publicly available via www.ncbi.nlm.nih.gov/gds. From the former, we used the high R:FR and low R:FR samples from the mock JA sample set. From the latter, we used control and UV-B shoot samples from the three-hour time point. Significantly regulated genes ($p \leq 0.05$) with an absolute log₂ fold change larger than 1 were identified using the Bioconductor packages in R (www.bioconductor.org). Experimental data were analysed with a two-way ANOVA with post-hoc LSD for pairwise comparisons using SPSS Statistics version 22 (IBM, Amsterdam, the Netherlands), or a Student's t-tests using Microsoft Excel.

Results

UV-B and R:FR signalling pathways interact via UVR8

Figure 5.1A shows that UV-B represses low R:FR-induced elongation in wild type *Arabidopsis thaliana* plants. We found similar results for tomato, where UV-B completely represses low R:FR-induced elongation after 4 hours and partially after 2 and 7 days (Supplemental figure S5.2). Figure 5.1B shows that this repression of low R:FR-induced elongation is partially relieved in the *A. thaliana uvr8* mutant.

These data demonstrate that the R:FR and UV-B signalling pathways interact and that the repression of low R:FR-induced elongation by UV-B is UVR8-dependent.

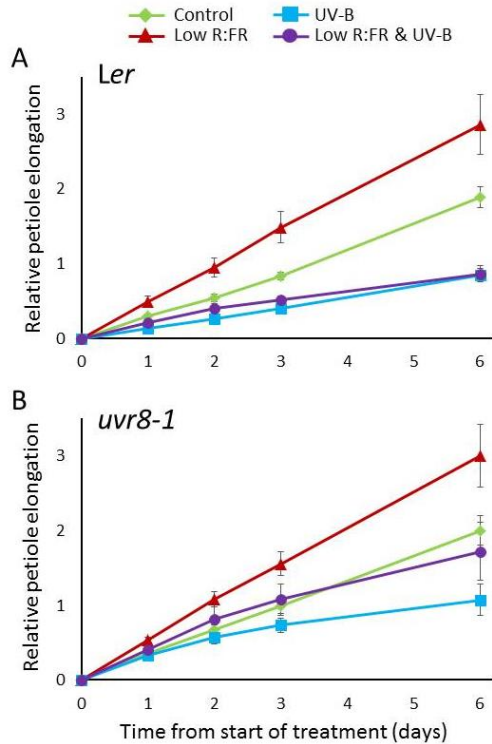


Figure 5.1 UV-B represses low R:FR-induced petiole elongation in wild type (A), but not in *uvr8* mutant plants (B). Four-week old *Arabidopsis thaliana* Ler and *uvr8-1* mutant plants were used. For low R:FR treatments, R:FR ratios were reduced from 2.0 to 0.2 using supplemental FR LEDs throughout the light period. For UV-B treatments, plants were exposed to 0.4 W m⁻² UV-B for four hours per day around solar noon, resulting in a daily UV-B dose of 5.8 kJ m⁻² h⁻¹. Effects of low R:FR and UV-B are significant (repeated measures ANOVA, $p \leq 0.05$). Data shown are averages \pm SE, $n = 6$.

R:FR signalling components involved in UV-FR interaction

We studied hypocotyl elongation of *A. thaliana* mutants to investigate what other components of their pathways are involved in the interaction between UV-B and R:FR signalling. Figure 5.2 shows that UV-B represses low R:FR-induced hypocotyl elongation of the *A. thaliana* Ler, Ws and Col accessions. Figure 5.2A and 5.2B show that, similar to adult plants, this repression is relieved in the *uvr8* mutants of these accessions. This confirms that UV-B represses low R:FR-induced elongation via UVR8. Figure 5.2C and 5.2D show that the repression is also relieved in *hy5 hyh* and *DELLA* quadruple mutants. This indicates that both the transcription factor HY5 and growth repressing DELLA proteins are involved in the UV-FR interaction. Figure 5.2E displays the response of *pif* mutants to low R:FR and UV-B. As expected, the *pif4 pif5 pif7* triple mutant shows no low R:FR-induced elongation. Therefore, we cannot use this mutant to investigate the effect of UV-B on low R:FR-induced elongation. However, the *pif4 pif5* double and *pif1 pif3 pif4 pif5* quadruple mutants do elongate under low R:FR, also in UV-B, indicating a role of the corresponding PIF proteins in the interaction between UV-B and R:FR signalling.

Existing datasets point to potential points of interaction

To find additional components of the UV-B and R:FR signalling pathways that are potentially involved in the interaction, we compared gene expression data from existing micro-array datasets. We selected a low R:FR dataset from De Wit *et al.* (2013) and a UV-B dataset from Kilian *et al.* (2007) because they are similar to our experiments in terms of plant accession and age, growth conditions and light treatments. Figure 5.3A shows the number of genes regulated in low R:FR and UV-B in these datasets. Our comparison reveals 200 genes regulated in low R:FR and 2506 in UV-B, of which 74 overlapped. Since we found that UV-B represses low R:FR-induced responses (Fig 5.1 and 5.2), we identified genes that were up-regulated in low R:FR while being down-regulated in UV-B as potential points of interaction between the pathways. We found 44 genes with this regulatory pattern (Fig 5.3A) and list their names, AGI codes and expression levels in figure 5.3B. Interestingly, many of these genes are associated with the shade

Chapter 5

avoidance syndrome directly, or with the growth regulating hormones auxin, gibberellic acid (GA) or brassinosteroids (BR).

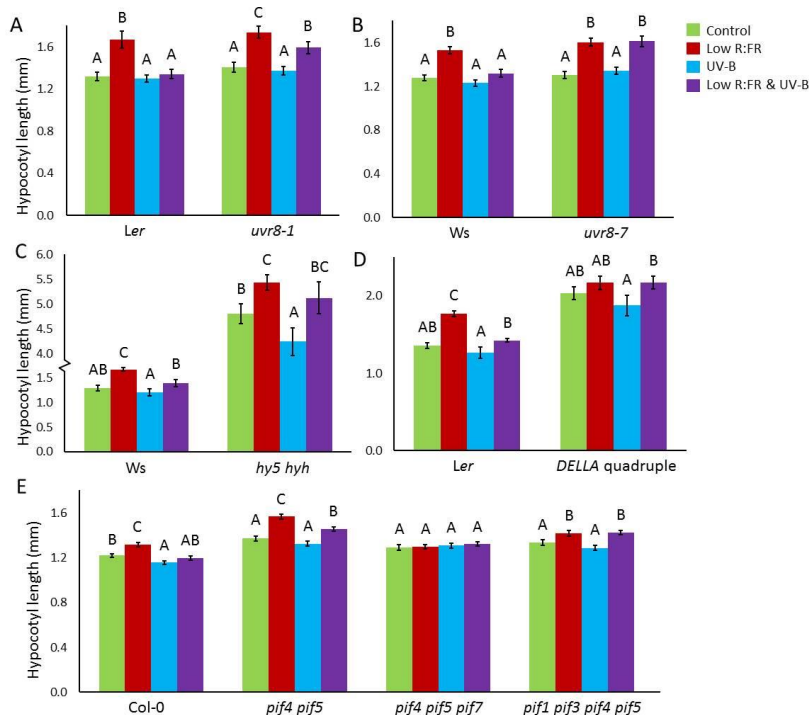


Figure 5.2 UV-B represses low R:FR-induced hypocotyl elongation in *Arabidopsis thaliana* wild type seedlings, but this repression is relieved in *uvr8-1*, *uvr8-7*, *hy5 hyh*, *gai-16 rga-24 rgl1-1 rgl2-1* (*DELLA* quadruple), *pif4 pif5* (partially) and *pif1 pif3 pif4 pif5* mutants. Hypocotyl length of mutants and their wild type backgrounds was measured after three days of treatment. For low R:FR treatments, R:FR ratios were reduced from 2.0 to 0.2 using supplemental FR LEDs throughout the light period. For UV-B treatments, plants were exposed to 1 W m⁻² UV-B throughout the 16-hour light period, resulting in a daily UV-B dose of 57.6 kJ m⁻² h⁻¹. Effects of genotype, low R:FR and UV-B are significant in all experiments shown (two-way ANOVA, $p \leq 0.05$). Letters above the columns indicate significant differences based on pairwise comparisons within genotype (Student's t-test, $p \leq 0.05$). Data shown are averages \pm SE, $n \geq 18$.

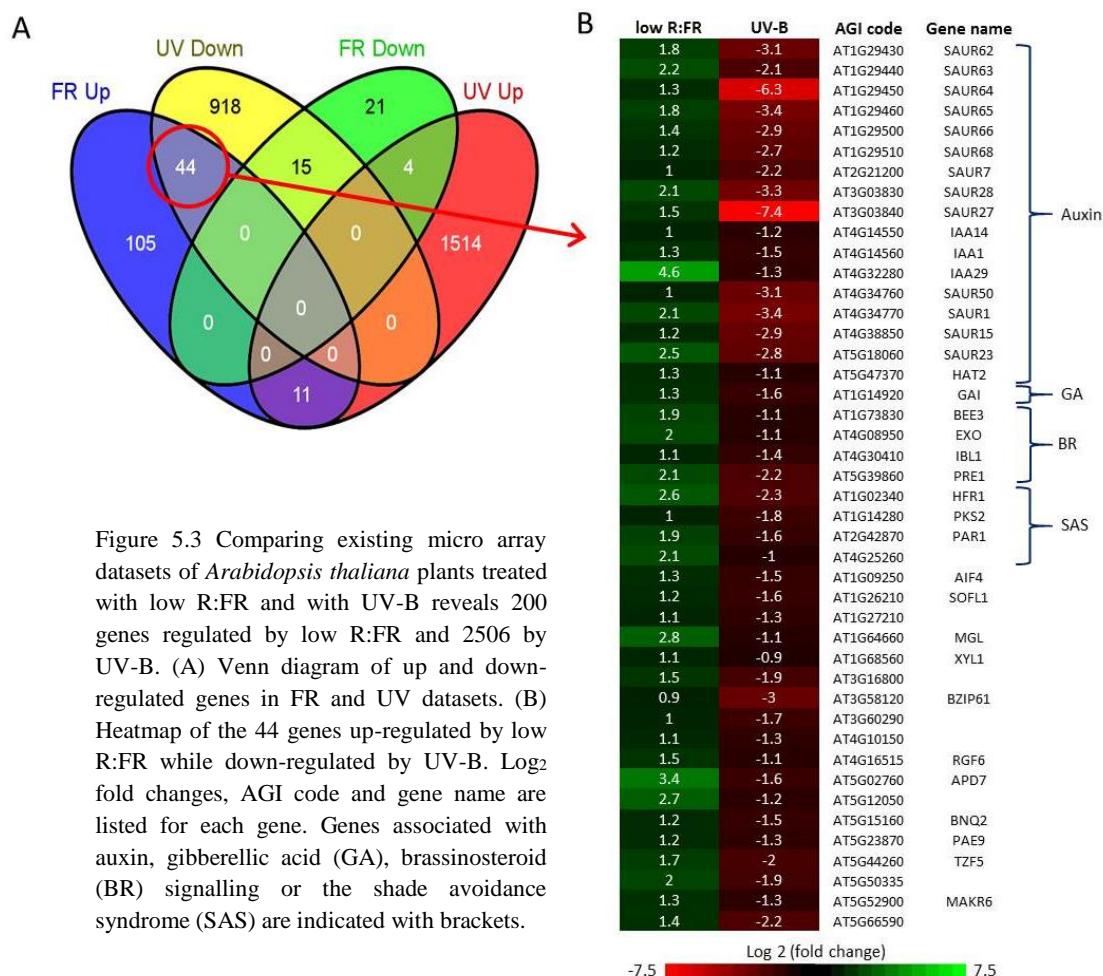


Figure 5.3 Comparing existing micro array datasets of *Arabidopsis thaliana* plants treated with low R:FR and with UV-B reveals 200 genes regulated by low R:FR and 2506 by UV-B. (A) Venn diagram of up and down-regulated genes in FR and UV datasets. (B) Heatmap of the 44 genes up-regulated by low R:FR while down-regulated by UV-B. Log₂ fold changes, AGI code and gene name are listed for each gene. Genes associated with auxin, gibberellic acid (GA), brassinosteroid (BR) signalling or the shade avoidance syndrome (SAS) are indicated with brackets.

Role of auxin, GA and BR in the UV-FR interaction

Because of the strong auxin signature in the transcriptome comparison (Fig 5.3B) and the known role of auxin in SAS (Casal 2012), we first investigated the involvement of auxin in the interaction between UV-B and shade avoidance responses. Figure 5.4 shows that low R:FR induces an auxin response in transgenic *pIAA19::GUS* plants, where blue staining is an indicator of auxin activity. However, although UV-B almost completely represses the staining of *pIAA19::GUS* plants exposed to control R:FR conditions, the low R:FR-induced auxin response is not affected by UV-B. We further investigated the role of hormones

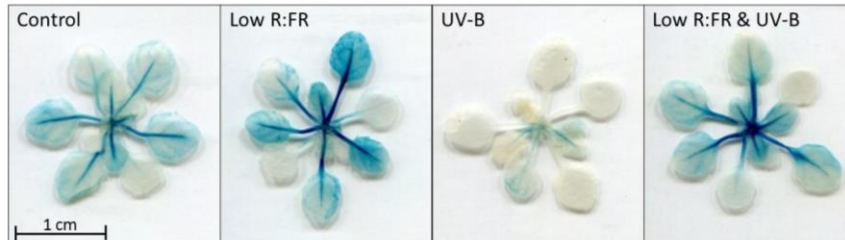


Figure 5.4 Gas chromatograms from birch. For every profile a running mean over five points is used. The blue lines are sampled from the non-ozonated reaction chamber, black lines are background measurements (purified air). (A) m/z 81.069 corresponds to monoterpenes, alcohols and aldehydes; (B) m/z 137.133 corresponds to monoterpenes only.

in the UV-FR interaction by adding indole-3-acetic acid (IAA, an auxin), gibberellic acid (GA), 24-epibrassinolide (EBL, inducing a brassinosteroid (BR) response) or mock solution to seedlings before exposing them to low R:FR and UV-B. Figure 5.5 shows that these hormones all increase hypocotyl growth under control light conditions while maintaining low R:FR-induced elongation, which indicates that the elongation response is not saturated. However, repression of low R:FR-induced elongation by UV-B is overcome only by EBL and not by GA or IAA. This suggests that UV-B represses low R:FR-induced brassinosteroids, rather than auxin and/or GA, thereby repressing low R:FR-induced elongation. We went on to investigate expression of the BR reporter genes *BR-ENHANCED EXPRESSION (BEE)1* and *ROTUNDIFOLIA (ROT)3* in *A. thaliana* seedlings (Cifuentes-Esquevel *et al.*, 2013; Polko *et al.*, 2013). Figure 5.6 shows that expression of *BEE1* is enhanced by UV-B as well as low R:FR and even more so by their combination, whereas *ROT3* expression is significantly stimulated only by the combined treatment. These data suggest that there is an interactive effect of UV-B and low R:FR on BR responses.

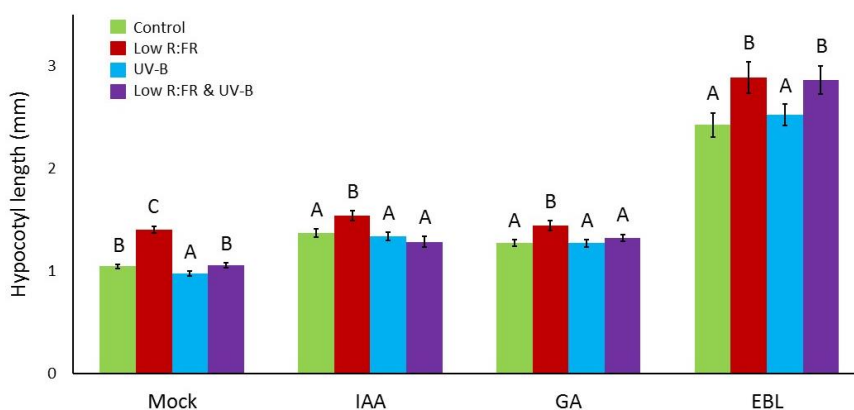


Figure 5.5 Effect of hormones on hypocotyl elongation of *Arabidopsis thaliana* Ler seedlings in low R:FR and UV-B light treatments. Mock control treatment, 10 μ M indole-3-acetic acid (IAA), 20 μ M gibberellic acid (GA) or 10 μ M 24-epibrassinolide (EBL) were applied before light treatments started. For low R:FR treatments, R:FR ratios were reduced from 2.0 to 0.2. For UV-B treatments, plants were exposed to 1 $W m^{-2}$ UV-B throughout the 16-hour light period, resulting in a daily UV-B dose of 57.6 $kJ m^{-2} h^{-1}$. Hypocotyls were measured after three days of treatment. Effects of hormone and both light treatments are significant (two-way ANOVA, $p \leq 0.05$). Letters above the columns indicate significant differences based on pairwise comparisons within genotype (Student's *t*-test, $p \leq 0.05$). Data shown are averages \pm SE, $n \geq 34$.

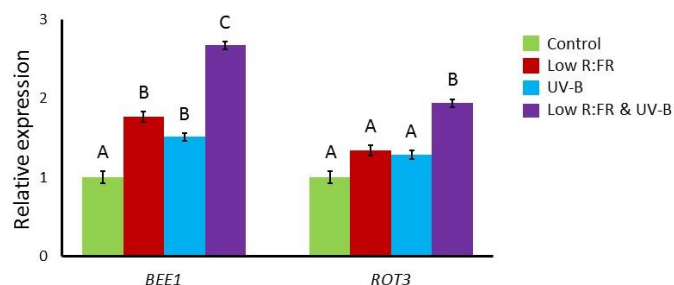


Figure 5.6 Effect of low R:FR and UV-B on expression of BR reporter genes *BR-ENHANCED EXPRESSION (BEE)1* and *ROTUNDIFOLIA (ROT)3* in *Arabidopsis thaliana* seedlings. For low R:FR treatments, R:FR ratios were reduced from 2.0 to 0.2. For UV-B treatments, plants were exposed to 1 W m^{-2} UV-B throughout the 16-hour light period, resulting in a daily UV-B dose of $57.6 \text{ kJ m}^{-2} \text{ h}^{-1}$. Seedling shoots were harvested after three days of treatment, 20 seedlings were pooled per sample. Letters above the columns indicate significant differences based on pairwise comparisons within genotype (Student's t-test, $p \leq 0.05$). Data shown are averages \pm SE, $n = 6$.

PAR1 and PKS2 are involved in the UV-FR interaction

Our transcriptome comparison identified the SAS-related genes *PHYTOCHROME RAPIDLY REGULATED (PAR)1* and *PHYTOCHROME KINASE SUBSTRATE (PKS)2* as contrastingly regulated by UV-B enrichment and low R:FR conditions (Fig 5.3). Therefore, we studied hypocotyl elongation under low R:FR and UV-B in *par1* and *pks2* mutants. Figure 5.7 shows that in *par1* and *pks2* mutants the repression of low R:FR-induced elongation by UV-B is (partially) relieved, indicating that PAR1 and PKS2 may indeed play a role in the interaction between the UV-B and R:FR signalling pathways.

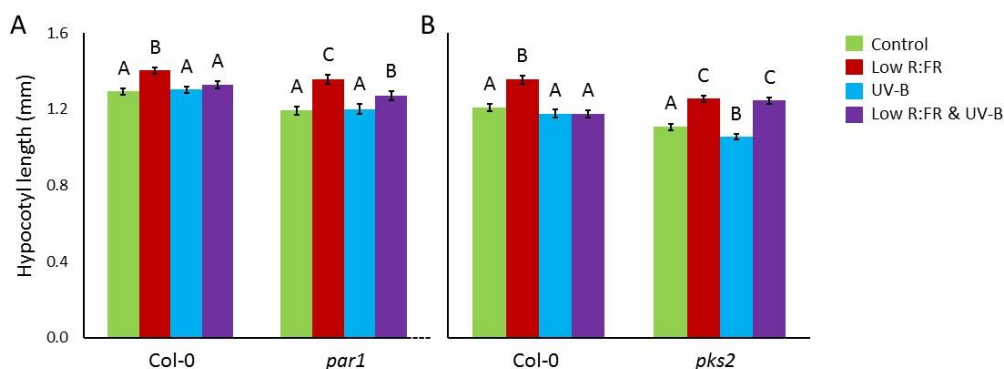


Figure 5.7 Repression of low R:FR-induced elongation by UV-B is relieved in *Arabidopsis thaliana par1* and *pks2* mutants. Hypocotyl length of mutants and their wild type background Col-0 were measured after three days of treatment. For low R:FR treatments, R:FR ratios were reduced from 2.0 to 0.2. For UV-B treatments, plants were exposed to 1 W m^{-2} UV-B throughout the 16-hour light period, resulting in a daily UV-B dose of $57.6 \text{ kJ m}^{-2} \text{ h}^{-1}$. Effects of genotype, low R:FR and UV-B are significant in both experiments (two-way ANOVA, $p \leq 0.05$). Letters above the columns indicate significant differences based on pairwise comparisons within genotype (Student's t-test, $p \leq 0.05$). Data shown are averages \pm SE, $n \geq 37$.

UV-B inhibits low R:FR-induced expression of PRE1 and HFRI

Figure 5.8 shows gene expression under low R:FR and UV-B of a selection of the 44 genes identified as potential points of interaction by the transcriptome comparison (Fig 5.3B). After two hours of treatment, low R:FR significantly induces all genes while UV-B has no effect. After 22 hours, responses of the investigated genes are more varied. Specifically, figures 5.8A and 5.8B show that *IAA INDUCIBLE (IAA)29* is induced by low R:FR but not affected by UV-B. Figures 5.8C and 5.8D show that *GIBBERELLIC ACID INSENSITIVE (GAI)* is not affected by either light treatment after 22 hours. These data are consistent with auxin and GA not being able to restore the repression of shade avoidance responses by UV-B (Fig 5.5). Figures 5.8E and 5.8F show that *PACLOBUTRAZOL RESISTANCE (PRE)1*,

Crosstalk between UV-B and R:FR signalling regulates elongation

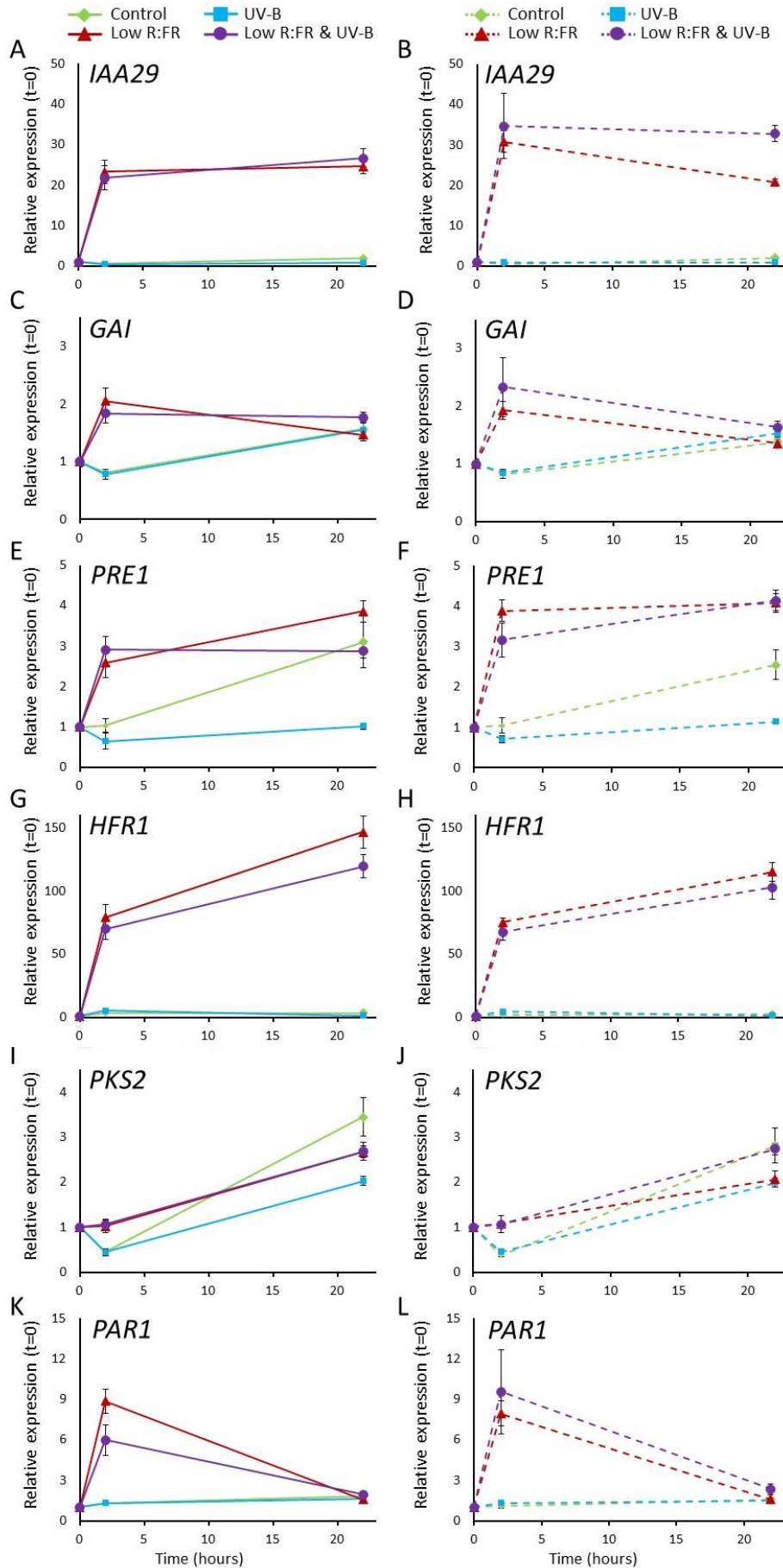


Figure 5.8 Effect of low R:FR and UV-B on gene expression in 24-day old *Arabidopsis thaliana* wild type (continuous lines, left panels) and *uvr8* mutant (dashed lines, right panels) plants. (A&B) *IAA INDUCIBLE (IAA)29*. (C&D) *GIBBERELLIC ACID INSENSITIVE (GAI)*. (E&F) *PACLOBUTRAZOL RESISTANCE (PRE)1*. (G&H) *LONG HYPOCOTYL IN FR (HFR)1*. (I&J) *PHYTOCHROME KINASE SUBSTRATE (PKS)2*. (K&L) *PHYTOCHROME RAPIDLY REGULATED (PAR)1*. For low R:FR treatments, R:FR ratios were reduced from 2.0 to 0.2. For UV-B treatments, plants were exposed to 0.4 W m⁻² UV-B for two hours per day around solar noon, resulting in a daily UV-B dose of 2.9 kJ m⁻² h⁻¹. Shoots were sampled at start of treatment, after two hours, and after 22 hours. Data shown are averages ± SE, n=7.

encoding a BR-inducible transcription factor, is induced by low R:FR and inhibited by UV-B after 22 hours. Moreover, UV-B inhibits the low R:FR-mediated induction of *PRE1* in wild type plants, while this effect is prevented in the *uvr8* mutant. This confirms a potential role for BR signalling in UVR8-mediated UV-FR interaction. Figures 5.8G and 5.8H show a similar expression pattern for the SAS-related, atypical basic-helix-loop-helix (bHLH) protein *LONG HYPOCOTYL IN FR (HFR)1*: after 22 hours, UV-B inhibits low R:FR-induction of *HFR1*, which is prevented in the *uvr8* mutant. The effect is small, but significant, hinting towards a role for *HFR1* in the UVR8-mediated repression of low R:FR signalling by UV-B. Finally, figures 5.8I to L show that the SAS-related genes *PKS2* and *PAR1* are induced by low R:FR after two hours but not after 22 hours, while UV-B has no significant effect at either time point, giving no indication of involvement of *PKS2* and *PAR1* in the UV-FR interaction at the transcriptional level.

UV-B reduces plant growth in dense stands independent of UVR8

We used dense *A. thaliana* stands to assess whether UV-B also represses shade avoidance responses when neighbouring plants are actually competing for light. In addition, we used *uvr8* mutants in monoculture and mixed stands to investigate if plants that are unable detect UV-B would have an advantage in such settings. Figure 5.9A shows representative photographs of monoculture and mixed stands exposed to white light or white light supplemented with UV-B. During the experiments, R:FR ratios gradually decreased, as the canopy closed and plant-plant competition increased (see Supplemental figure S5.3). Figure 5.10A shows that UV-B significantly reduces petiole elongation of wild type as well as *uvr8* mutant plants growing in monoculture stands. Although dry weight was not significantly affected there was a trend towards UV-B-induced inhibition of growth (Fig 5.10B), which would be consistent with the significantly reduced leaf area under UV-B (Fig 5.10C). Figures 5.10D to F show that UV-B significantly reduces petiole elongation, dry weight and leaf area in wild type and mutant plants of mixed culture stands, with no difference between the genotypes. These results indicate that UV-B reduces plant growth in dense stands independent of UVR8 and suggest that plant-plant competition for light is not impaired by sensing UV-B via UVR8.

Discussion & conclusion

UV-B represses low R:FR responses via the UVR8 pathway

To survive in a competitive environment, it is essential for plants to integrate information about light quality and quantity. We found that UV-B radiation can repress low R:FR responses in adult plants and seedlings of *Arabidopsis thaliana* (Fig 5.1 & 5.2). Studies with mutants lacking the UV-B receptor UVR8 demonstrate that this interaction depends on the detection of UV-B by this receptor (Fig 5.1, 5.2A and 5.2B). Besides being UVR8-dependent, the interaction between UV-B and low R:FR responses also depends on HY5 (Fig 5.2C). This bZIP transcription factor is known to act early in UVR8 signalling: it is stabilised immediately after UVR8 activation to promote UV-B-related gene expression (Brown *et al.*, 2005; Heijde and Ulm 2012). This confirms that UV-B represses low R:FR-induced elongation via the UVR8 signalling pathway.

Brassinosteroids, but not auxin and GA, are involved in the UV-FR interaction

Since auxin, gibberellic acid and brassinosteroids are essential components of the shade avoidance response (reviewed in Casal 2012), affecting their levels or signalling would be a way for UV-B to repress SAS. Although the transcriptome comparison shows a distinctly contrasting auxin profile for low R:FR and UV-B (Fig 5.3B), UV-B did not repress the low R:FR-induced induction of auxin response visualised through the *pIAA19::GUS* reporter (Fig 5.4). Moreover, addition of auxin to *A. thaliana* seedlings did not relieve the repression of low R:FR-induced elongation by UV-B (Fig 5.5). Finally, UV-B did not affect low R:FR-induced *IAA29* expression in wild type or *uvr8* mutant plants (Fig 5.8A and 5.8B). Thus, there is no suggestion from our data that UV-B represses low R:FR signalling by affecting auxin levels or auxin-dependent signalling. Our micro array comparison also pointed to GA and BR-related genes involved in

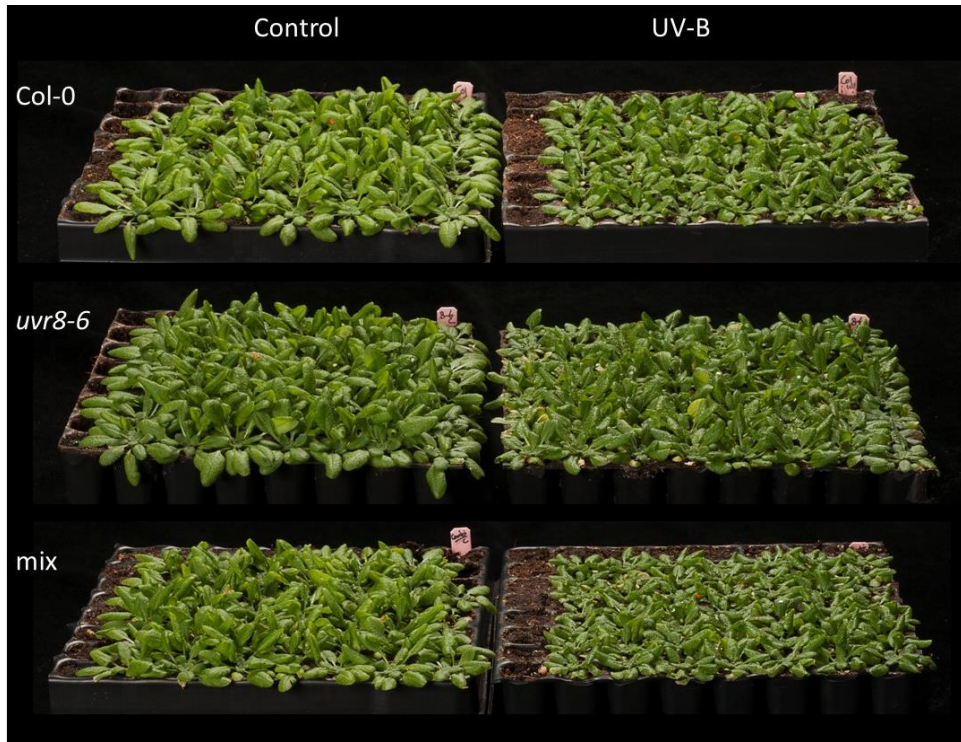


Figure 5.9 UV-B reduces growth of *Arabidopsis thaliana* in dense stands. Col-0 and *uvr8-6* plants were grown in mono and mixed culture stands of 7x7 plants. For UV-B treatments, 24-day old plants were exposed to 0.4 W m^{-2} UV-B for two hours per day around solar noon, resulting in a daily UV-B dose of $2.9 \text{ kJ m}^{-2} \text{ h}^{-1}$ UV-B. Pictures of representative stands were taken after 11 days of treatment.

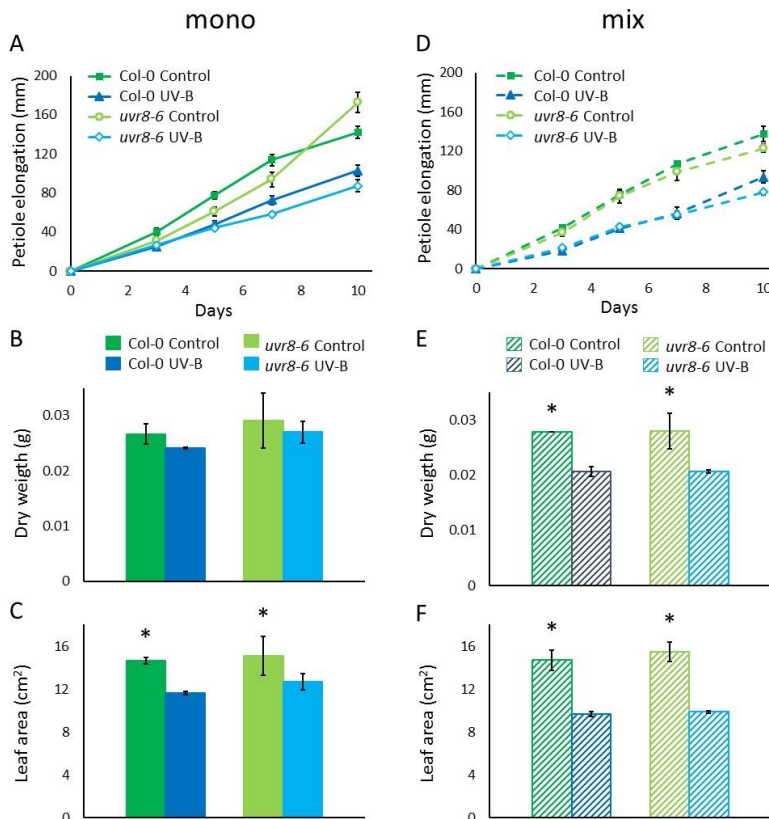


Figure 5.10 UV-B reduces petiole elongation (A&D), dry weight (B&E) and leaf area (C&F) of *Arabidopsis thaliana* in dense stands. Col-0 and *uvr8-6* plants were grown in mono and mixed culture stands of 7x7 plants. Results from monoculture stands are on the left (A-C), from mixed culture stands on the right (D-F). For UV-B treatments, 24-day old plants were exposed to 0.4 W m^{-2} UV-B for two hours per day around solar noon, resulting in a daily UV-B dose of $2.9 \text{ kJ m}^{-2} \text{ h}^{-1}$. Petiole length was measured throughout the experiment. UV-B significantly reduced petiole elongation in monoculture and mixed stands (repeated ANOVA, $p \leq 0.05$). Data shown are averages \pm SE of representative stands ($n = 9$ for monoculture, $n = 4$ or 5 for wild type or mutants in mixed culture stands, resp.). Shoots of the nine inner plants of each dense stand were harvested after 11 days of treatment to determine dry weight and leaf area. Asterisks indicate significant differences based on pairwise comparisons within genotype (two-way ANOVA, $p \leq 0.05$). Data shown are per plant averages of stands from independent experiments \pm SE ($n=3$ for monoculture, $n=2$ for mixed culture stands).

the UV-FR interaction. Our finding that DELLA proteins may be involved in the repression of low R:FR-induced elongation by UV-B (Fig 5.2A) suggests involvement of GA in the interaction, since DELLA degradation is regulated by GA. However, UV-B did not affect *GAI* expression in wild type or mutant plants (Fig 5.8C and 5.8D) and addition of GA to seedlings did not relieve the repression of low R:FR-induced elongation by UV-B (Fig 5.5). Thus, our data on GA-DELLA involvement are not conclusively supporting a role for GA in UV-B-mediated repression of low R:FR-induced responses. These findings partly contrast those of Hayes *et al.* (2014), who reported that UV-B inhibits shade avoidance responses by antagonizing auxin and GA. In order to substantiate the GA-DELLA data, follow-up experiments should involve studying DELLA protein stability in UV-B and GA treated plants, e.g. by using existing DELLA:GFP lines (Djakovic-Petrovic *et al.*, 2007). In contrast to auxin and GA, our data suggest that BR could be involved in the interaction between UV-B and shade avoidance responses. Adding EBL to *A. thaliana* seedlings relieved the repression of low R:FR-induced elongation by UV-B, suggesting that UV-B could act through suppression of BR levels (Fig 5.5). In addition, expression of the BR reporter genes *BEE1* and *ROT3* also showed an interaction between UV-B and low R:FR (Fig 5.6). Finally, UV-B inhibits low R:FR-induced *PRE1* expression in a UVR8-dependent manner (Fig 5.8E and 5.8F). Since *PRE1* is a BR-inducible transcription factor that is a positive regulator of BR-mediated cell elongation (Zhang 2009), this suggests that UV-B might repress shade avoidance responses via UVR8, BR and *PRE1*. Direct BR measurements as well as BR reporter line and mutant studies are needed to further elucidate the role of BR in the UV-FR interaction.

Early R:FR signalling network components involved in UV-FR interaction

Mutant studies demonstrated that the early R:FR signalling components PAR1, PKS2, DELLAs and PIFs are involved in the repression of low R:FR responses by UV-B (Fig 5.2 and 5.7). PIF proteins are positive regulators of low R:FR-induced elongation (Lorrain *et al.*, 2008). The repression of low R:FR-induced elongation by UV-B was prevented completely in *pif1 pif3 pif4 pif5* quadruple, but only partially in *pif4 pif5* double mutants (Fig 5.2E). Apparently, UV-B has to target several PIFs to overcome their redundancy and successfully repress SAS. Moreover, our results identify PIF1 and PIF3 as potential players in the UV-FR interaction besides PIF4 and PIF5, which were already reported recently by Hayes *et al.* (2014) to be necessary for UV-B to repress SAS. DELLA and PAR1 proteins both negatively regulate SAS by binding PIF proteins (Casal 2012; Hao *et al.*, 2012). It is therefore possible that UV-B represses shade avoidance responses by promoting or stabilizing DELLA-PIF and PAR-PIF interactions and/or affecting more downstream PIF targets via PAR1. PKS2 is likely to provide an additional mode of interaction between the pathways. This protein was already shown to interact with blue light receptors phototropin 1 and 2 as well as with phytochromes (Fankhauser *et al.*, 1999). Confirming its suggested role in signal integration from photoreceptors (Lariguet *et al.*, 2006), our results suggest involvement of PKS2 in UV-B repression of R:FR responses. Taken together, our results indicate that the interaction between UV-B and R:FR signalling occurs early in the R:FR signalling pathway. Possibly, the initial interaction takes place at the protein level, allowing fast integration of the light signals. This would be consistent with the lack of transcriptional control by UV-B after two hours of treatment (Fig 5.8). Rapid integration of light signal information would permit a plant to adjust quickly to a changing light environment, optimizing its photon harvest while avoiding damage. In addition, gene expression studies suggest that *PRE1* and *HFR1* might play a role in the UVR8-dependent repression of low R:FR-induced responses by UV-B, but perhaps at a later stage since UV-B only affects their expression levels on the day after UV-B treatment (Fig 5.8E to H). *PRE1* and *HFR1* are transcriptional cofactors that have been shown to heterodimerise with each other as well as with other components involved in the UV-FR interactions; *PRE1* binds to PAR1 (Hao *et al.*, 2012), while *HFR1* binds to PIF4 and PIF5 (Hornitschek *et al.*, 2009). It is possible that *PRE1* and *HFR1* consolidate the UV-FR interaction initially established through PAR1, DELLAs and PIFs. Studies on the protein and gene expression level at different time points after the start of UV-B and low R:FR exposure, including protein-protein and protein-photoreceptor interaction studies, are needed to further elucidate the roles of PIFs, DELLAs, PAR1, PKS2, *PRE1* and *HFR1* in the UV-FR interaction.

UV-B and UVR8 signalling do not affect plant-plant competition

Our data from individual plants show that UV-B represses shade avoidance. This implies that UV-B radiation limits a plant's ability to compete for light with its neighbours. However, *A. thaliana* plants still showed the SAS phenotype when competing with their neighbours for light in dense stands under UV-B (Fig 5.9), even though UV-B reduced growth (Fig 5.10). Moreover, wild type and *uvr8* mutant plants had similar elongation rates under UV-B in mixed stands (Fig 5.10D), suggesting that UVR8 signalling does not affect shade avoidance in dense stands. Plant-plant competition in a canopy differs in multiple ways from exposing individually growing plants to low R:FR. In a canopy the R:FR ratio varies with height, whereas individual plants in low R:FR experience the same R:FR ratio throughout. Moreover, other signals exist inside a canopy (touch, low B, low PAR) that might also interact with UV-B signalling. Thus, although individual plants are a useful model to investigate the integration of light signals by signalling networks, more realistic settings of plant-plant competition may provide essential information on how plants actually encounter these light signals in nature.

Conclusion & future research

In conclusion, our findings suggest that UV-B represses low R:FR signalling via the UVR8 pathway and that this interaction involves several early components of the R:FR signalling network. Brassinosteroids might have a role in the UV-FR interaction, whereas we found no evidence that auxin and GA play a role. Future studies on protein and hormone levels, protein-protein interactions and the identification of novel targets of the UVR8 pathway are likely to provide further insight into the entanglement of the UV-B and R:FR signalling networks.

Acknowledgements

This project is funded by a strategic funding scheme (Focus and Mass) of Utrecht University. We thank Roman Ulm, Keara Franklin and Christian Fankhauser for kindly providing seeds of the *uvr8* mutants and Debatosh Das for help with analysing the micro array data.

Supplemental figures

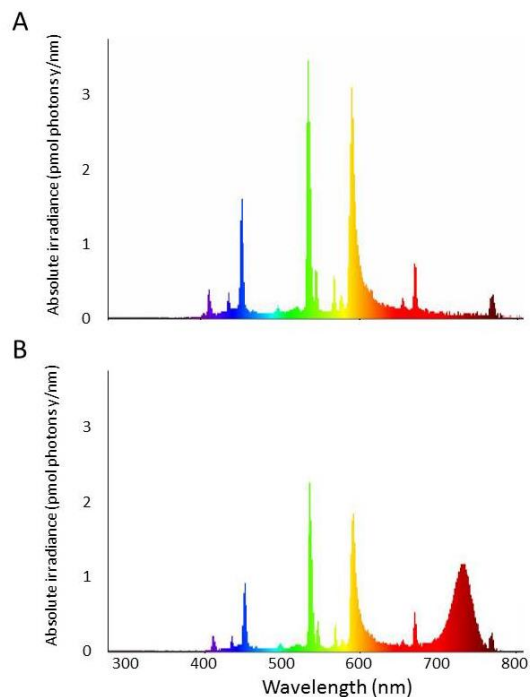


Figure S5.1 Spectra of (A) control and (B) FR-enriched light boxes, where supplemental far-red LEDs lowered the R:FR ratio from 2.0 to 0.2.

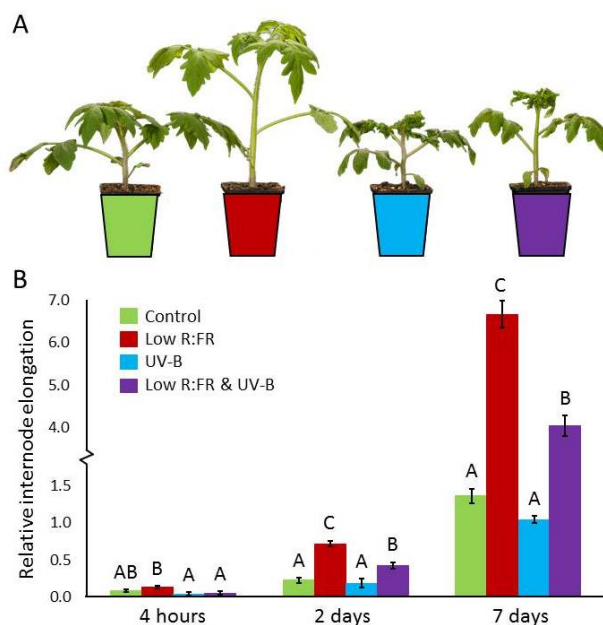


Figure S5.2 Effect of low R:FR and UV-B on 2.5-week old tomato plants. (A) Picture of representative plants after seven days of treatment. (B) Internode elongation after 4 hours, 2 days and 7 days of treatment. For low R:FR treatments, R:FR ratios were reduced from 2.0 to 0.2 using supplemental FR LEDs throughout the light period. For UV-B treatments, plants were exposed to 0.4 W m^{-2} UV-B for four hours per day around solar noon, resulting in a daily UV-B dose of $5.8 \text{ kJ m}^{-2} \text{ h}^{-1}$. Effects of both light treatments are significant (repeated measures ANOVA, $p \leq 0.05$). Letters above the columns indicate significant differences based on pairwise comparisons at that time point (Student's t-test, $p \leq 0.05$). Data shown are averages \pm SE, $n = 10$.

Crosstalk between UV-B and R:FR signalling regulates elongation

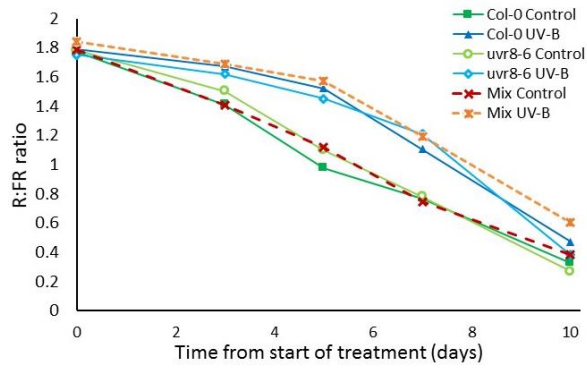


Figure S5.3 R:FR ratios in dense stands during treatment. R:FR ratios are measured at four points in four directions at ground level between the nine inner plants of each dense stand. Averages of a representative set of dense stands (the same as in Fig 9) are shown, n = 4.

Table S5.1 Gene specific primers used for qRT-PCR

Primer target	Direction	Sequence (5' to 3')
<i>BEE1</i>	Forward	TAAGGCTATGGGAATGGCTACG
	Reverse	TTGCTGCAGTGAGTTTCATCG
<i>ROT3</i>	Forward	AGATTTTCGTCAGCGGAAAGA
	Reverse	CCAAAGGGTGTGAAGCAAAT
<i>IAA29</i>	Forward	ATCACCATCATTGCCCGTAT
	Reverse	ATTGCCACACCATCCATCTT
<i>GAI</i>	Forward	CTGTGGTTGAGCAGGAATCG
	Reverse	AACCTCCGACATGACCTTGT
<i>PRE1</i>	Forward	CTGATAAGGTATCAGCCTCGAAAG
	Reverse	GGCTTCAGGGCTATCTTCATCG
<i>HFR1</i>	Forward	AATGGGGCTACGGCTACTTT
	Reverse	CCAATAAATCCTCCTTCGCA
<i>PKS2</i>	Forward	CCAGATGGTTATGCACCAAGTG
	Reverse	GGATTTCGAGGAATCTGAAAAGACC
<i>PAR1</i>	Forward	TCTCTGTCACCGTCATGCTC
	Reverse	GCTTCTTCTCGGTCTTCACG
<i>TUBULIN-6</i>	Forward	ATAGCTCCCCGAGGTCTCTC
	Reverse	TCCATCTCGTCCATTCCTC

General discussion

Abbreviations

UVR8	UV RESISTANCE LOCUS 8
HY5	ELONGATED HYPOCOTYL 5
PIF	PHYTOCHROME-INTERACTING FACTOR
PAR1	PHYTOCHROME RAPIDLY REGULATED 1
PKS2	PHYTOCHROME KINASE SUBSTRATE 2
PRE1	PACLOBUTRAZOL RESISTANCE 1
HFR1	LONG HYPOCOTYL IN FR 1
BR	brassinosteroids
GA	gibberellic acid
PAR	photosynthetically active radiation

Plants detect and integrate an assortment of signals from their environment, and use these signals to maximise their performance by adjusting their growth and development as well as their secondary metabolite production. In this thesis, we investigated how plants integrate visual and olfactory signals. First, a system to measure plant volatile organic compounds (VOCs) was set up (chapter 2). Second, the effect of UV-B radiation on tomato and *Arabidopsis thaliana* VOC emissions was described and its regulation via *TERPENE SYNTHASE* gene expression and the UV-B photoreceptor UVR8 examined (chapter 3 and 4). Third, the interaction between UV-B and low red to far-red (R:FR) responses was investigated at the physiological and signal transduction level (chapter 5). The current chapter reiterates our findings, places them into perspective and identifies outstanding questions and future research opportunities.

Before discussing the findings of this thesis, it is important to note that plant responses to UV-B greatly depend on the UV-B level plants are exposed to. This is well known in the UV-B research community and is clear from gene expression and metabolite studies (Brown and Jenkins 2008, Morales *et al.*, 2013). In our VOC experiments, the daily UV-B dose applied matched natural levels, as illustrated by figure 1.3. In our low R:FR experiments, these doses were lowered to prevent growth arrest. Interestingly, we found that tomato VOC emissions show a duration threshold for induction by UV-B (Fig 3.3), adding a temporal dimension to UV-B-dose dependency.

UV-B controls VOC emissions

UV-B differentially affects VOC emissions independent of UVR8

In tomato, UV-B induced VOC emissions with differential timing: a first class of VOCs increased immediately upon UV-B exposure, a second class of compounds had a delayed response and a third class increased only after UV-B exposure stopped (Fig 3.2). This third class included monoterpenes and methyl salicylate (MeSA), compounds known to function as signals in ecological interactions (Frag and Paré 2002; Leitner *et al.*, 2005; Blande *et al.*, 2010). We identified six different monoterpenes that were induced by UV-B (Fig 3.5), but found no correlation between their induced emission and up-regulation of their *TERPENE SYNTHASE* (*TPS*) genes, except for β -phellandrene and *TPS4* expression in leaves (Fig 3.6 and 3.7). Using *Arabidopsis thaliana*, we demonstrated that UV-B induces VOC emissions independent of the UV-B photoreceptor UVR8 (Fig 4.2 and 4.3). In fact, these are the first data showing that some secondary metabolites are regulated by UV-B exposure in a UVR8-independent manner. In addition, comparing UV-

B-mediated VOC emissions of tomato and *A. thaliana* revealed that (i) the timing of UV-B-induced monoterpene emissions and (ii) UV-B-induced MeSA emissions are species specific.

Our findings that UV-B increased VOC emission in tomato and *A. thaliana* are consistent with earlier reports of UV-B-enhanced VOC emissions in oak, basil, peatland and Mediterranean scrubs (Harley *et al.*, 1996; Johnson *et al.*, 1999; Tiiva *et al.*, 2007; Llusia *et al.*, 2012). Furthermore, species-specific UV-B effects as well as differential effects on individual VOC compounds were also reported, consistent with our findings on species specificity (Blande *et al.*, 2009; Llusia *et al.*, 2012). Thus, UV-B seems to generally induce VOC emissions, and these effects are likely to be species specific, also in terms of timing and induction of individual volatile compounds.

Regulation of VOC emission upon UV-B

Our findings suggest that UV-B controls VOC emissions in a UVR8-independent way that induces volatile emissions without up-regulating their specific terpene synthesis genes. Alternative modes of regulation could be (i) enhancing precursor pools, (ii) boosting TPS enzyme activity, or (iii) releasing terpenes from storage. The latter is unlikely, however, since there is only limited storage capacity for volatile terpenes in these species (Niinemets *et al.*, 2004). Larger precursor pools could also arise when UV-B activates the production of secondary metabolites that use the same precursor pools, such as chlorophylls and membrane sterols needed to counteract UV-B damage, or terpenoid hormones (e.g. BR) involved in UV-B responses (Lange and Ghassemian 2003). Future studies on the regulation of UV-B-mediated VOC emissions should focus on UVR8-independent signalling pathways, taking into account such secondary effects of other UV-B responses. In addition, since we found that closely related *TPS* genes were similarly regulated (Fig 3.6), and related genes may have similar promoter sequences, analyses of promoter regions of UV-B-regulated genes could also aid this research direction.

Unravelling the regulation of VOC emissions can help to improve crops by enhancing their indirect defences. Protective plant traits have often been lost during years of breeding for other desirable traits, like palatability (Li *et al.*, 1993). Crop improvement via VOC remodelling has been nicely shown in tomato, where wild accessions are better protected against herbivores through their emitted volatiles (Bleeker *et al.*, 2009) and the responsible genes can be used to improve herbivore resistance in their cultivated relatives (Bleeker *et al.*, 2012). Such practices have the potential to reduce pesticide use and increase yields.

Functional consequences of VOC emission upon UV-B

As reviewed in chapter 1, volatile terpenes can function as quenchers of radical oxygen species that arise during abiotic stress (Peñuelas and Llusia 2003; Vickers *et al.*, 2009). However, our results suggest that this is not their main function in UV-B stress, since (i) in tomato, the observed monoterpene emission patterns (a gradual induction after UV-B exposure stopped) did not match the pattern expected when monoterpenes would function as quenchers during UV-B exposure (Fig 3.3), and (ii) in *A. thaliana*, a much weaker VOC emitter than tomato, monoterpenes were emitted during UV-B exposure and could therefore not have reacted with radicals (Fig 4.2). Another possibility is that VOC emissions function as signals, either within or between plants, or between plants and higher trophic levels (reviewed by Heil 2008). UV-B-mediated alterations of VOC blends would then either constitute an information cue or disrupt an existing cue. Future studies with appropriate bioassays are needed to determine whether UV-B-induced VOC emissions affect ecological interactions. When they do, this may provide interesting clues on how UV-B can be more effectively utilised in pest control.

VOC studies aid climate change models

Plant VOC emissions make up a substantial part of the global carbon cycle and regulate crucial features of atmospheric chemistry (Fehsenfeld *et al.*, 1992; Kesselmeier *et al.*, 2002; Lerda and Slobodkin 2002).

Although essential, researchers modelling carbon cycles and climate change have been struggling to input these emissions into their calculations, because of insufficient knowledge on emission patterns, species specificity and the content of VOC blends (Kesselmeier *et al.*, 2002). Recently, Monson *et al.* (2012) argued that plant VOC emissions should be modelled based on plant biology instead of atmospheric chemistry principles. However, even with simplified versions of such plant-biology-based models, the call for more observations remains (Harrison *et al.*, 2013). This thesis provides input for VOC models by showing the differential induction of VOC types by UV-B and their order of magnitude. An important contribution of our work is the notion that UV-B effects on VOC emissions are species specific and that VOCs may even be induced by abiotic factors with temporal variability. Moreover, our data as well as those from Kegge *et al.* (2013) on R:FR-mediated VOC emissions indicate that VOC emissions may vary on the small spatial scales at which light quality varies within dense stands. Functional-structural plant (FSP) models simulate plant growth in dense stands based on this spatial heterogeneity of light quality (Bongers *et al.*, 2014). We therefore suggest that integrating FSP models into VOC emission models may help to substantially improve carbon budget and climate change projections.

UV-B interacts with R:FR signalling

UV-B represses low R:FR responses and signalling

By exposing *A. thaliana* to UV-B and low R:FR simultaneously, we demonstrated that UV-B represses low R:FR responses via the UVR8 pathway and that this interaction involves several components of the R:FR signalling network (chapter 5). Mutant studies indicated involvement in the UV-FR interaction of the early UVR8-signalling component HY5, growth-repressing DELLA proteins, central shade avoidance regulators PIF4 and PIF5, but possibly also PIF1 and PIF3, auxin-related and PIF-inhibiting PAR1, and photoreceptor-interacting PKS2 (Fig 5.2 and 5.7). In addition, gene expression studies suggested a role for the PAR1-binding and BR-inducible transcription factor PRE1, as well as for HFR1, which inhibits PIF4 and PIF5 action (Fig 5.8). The repression of low R:FR responses by UV-B was also reported by Hayes *et al.* (2014) and Mazza and Ballaré (2015) in *A. thaliana*. Our results are consistent with Hayes *et al.* (2014), who also showed the involvement of UVR8, HY5, DELLAs, PIF4 and PIF5 in the interaction between UV-B and R:FR signalling. But, in addition to Hayes *et al.* (2014), our study demonstrates for the first time the involvement of PAR1, PKS2, PRE1, HFR1 and possibly PIF1 and PIF3 in the UV-FR interaction. Determining the role of UV-B and R:FR signalling components in the interaction between these pathways promises novel insights into both UV-B and shade avoidance responses.

Concerning the involvement of hormones in the UV-FR interaction, we found that BR might be important, whereas we found no such evidence for auxin and GA (Fig 5.4, 5.5 and 5.6). This is consistent with the observation that BR-deficient mutants have reduced expression levels of UV-B-inducible genes (Sävenstrand *et al.*, 2004). In contrast, Hayes *et al.* (2014) reported that UV-B inhibits shade avoidance by increasing GA catabolism and repressing auxin biosynthetic and responsive genes. Also, Hectors *et al.*, (2012) reported increased UV-B sensitivity of auxin mutants. Direct hormone measurements as well as reporter line and mutant studies are needed to pinpoint the exact roles that these hormones play in the UV-FR interaction.

Light signals in a canopy

By repressing low R:FR responses, UVR8 may prevent excessive shade avoidance in canopy gaps. However, when *A. thaliana* plants were competing for light in dense stands, UV-B repressed growth, but did not seem to inhibit shade avoidance responses (Fig 5.9). Moreover, when wild type and *uvr8* mutant plants were competing in mixed stands, one genotype did not outcompete the other (Fig 5.10). Apparently, low R:FR can overrule UV-B repression when competition pressure increases, arguably because the low R:FR signal is reinforced by other shade signals like low blue, low PAR or the touching of leaf tips. This

indicates how the interaction between UV-B and R:FR signalling may lead to ecological advantageous acclimatisation to a variable light environment, as was also argued by Mazza and Ballaré (2015).

Synthesis: integrating signals in a patchy environment

This thesis demonstrates that plant responses to distinct environmental cues interact, and that there is cross-talk between the intrinsic signalling pathways a plant uses to assess and respond to light quality changes. This is especially relevant when considering plant responses in patchy environments.

Most plants grow close together, whether in an agricultural field, grassland or forest. Such environments are patchy in terms of light quality and quantity, with differing conditions at the top of the canopy compared to closer to the ground (Casal 2012). Since VOC emissions are reduced by low R:FR ratios and actual proximity of conspecifics (Kegge *et al.*, 2013, Kigathi *et al.*, 2013), while being increased by UV-B (chapter 3 and 4), dense stands may also be patchy in terms of VOCs. Interestingly, such close-quarter-environments might be exactly where VOCs could play a signalling role. Assessing whether light quality changes could affect VOC emissions on the leaf level *within* a single plant would provide exciting new insights into the dynamics of plant-plant interactions as well as into within and between plant signalling via VOCs.

Another promising direction for future research is the interaction between light responses and (herbivore) defence. While UV-B responses were already known to have common elements with direct herbivore defence responses (Mackerness *et al.*, 1999; Demkura *et al.*, 2010; Izaguirre *et al.*, 2003; Killian *et al.*, 2007), this thesis is the first to demonstrate the overlap with putative indirect defence responses. Such overlap and the underpinning integration of (a)biotic stress responses will be *the* area of study in plant biology the next decades (Atkinson and Urwin 2012; Rymen and Sugimoto 2012; Ballaré 2014; Pierik & Testerink 2014; Mazza and Ballaré 2015). Although current genetic techniques make constructing large datasets easy, a coordinated effort with accurately chosen experimental conditions is needed to produce valuable insights into these processes. In addition, and especially for the application of obtained insights in agricultural settings, experiments in more natural settings such as dense stands remain essential.

Conclusion

In summary, we have shown that UV-B induced VOC emissions in tomato and *A. thaliana*, and that volatile emissions are thus dependent on light quality. Also, for the first time, we reported (i) differential and species-specific timing of UV-B-mediated induction of VOC emissions, (ii) UVR8-independent induction of these secondary metabolites by UV-B, and (iii) overlap between VOC responses to UV-B and herbivory. Importantly, insights into the regulation of VOC emissions upon UV-B could provide new approaches for improvement of crops and agricultural practices. In addition, we found that UV-B can repress responses to low R:FR ratios that indicate proximate neighbours, with the UV-B and R:FR signalling pathways interacting via UVR8 and multiple components of the R:FR network. Together, these findings illustrate that plants respond to their environment by integrating distinct signals, allowing local acclimations to patchy environments. To advance our understanding of these processes, a combination of (i) powerful genetic tools used in well-designed and coordinated experiments, (ii) improved modelling of plant responses, and (iii) validation of obtained insights in dense stands is needed. Measurements of VOC responses to local, within-plant variation in light quality could provide a first step in this direction.

References

- Abràmoff MD, Magelhães PJ, Ram SJ (2004) Image processing with ImageJ. *Biophotonics International* 11: 36-42
- Achard P, Vriezen WH, Van Der Straeten D, Harberd NP (2003) Ethylene regulates *Arabidopsis* development via the modulation of DELLA protein growth repressor function. *Plant Cell* 15: 2816-2825
- Achard P, Cheng H, De Grauwe L, Decat J, Schoutteten H, Moritz T, Van der Straeten D, Peng JR, Harberd NP (2006) Integration of plant responses to environmentally activated phytohormonal signals. *Science* 311: 91-94
- Achard P, Liao L, Jiang C, Desnos T, Bartlett J, Fu X, Harberd NP (2007) DELLAs contribute to plant photomorphogenesis. *Plant Physiology* 143: 1163-1172
- Aharoni A, Giri AP, Deuerlein S, Griepink F, de Kogel WJ, Verstappen FWA, Verhoeven HA, Jongsma MA, Schwab W, Bouwmeester HJ (2003) Terpenoid metabolism in wild-type and transgenic *Arabidopsis* plants. *Plant Cell* 15: 2866-2884
- Albert KR, Mikkelsen TN, Ro-Poulsen H, Arndal MF, Boesgaard K, Michelsen A, Bruhn D, Schmidt NM (2012) Solar UV-B effects on PSII performance in *Betula nana* are influenced by PAR level and reduced by EDU: results of a 3-year experiment in the High Arctic. *Physiologia Plantarum* 145: 485-500
- Alonso JM, Stepanova AN, Lisse TJ, Kim CJ, Chen H, Shinn P, Stevenson DK, Zimmerman J, Barajas P, Cheuk R, Gadrinab C, Heller C, Jeske A, Koesema E, Meyers CC, Parker H, Prednis L, Ansari Y, Choy N, Deen H, Geralt M, Hazari N, Hom E, Karnes M, Mulholland C, Ndubaku R, Schmidt I, Guzman P, Aguilar-Henonin L, Schmid M, Weigel D, Carter DE, Marchand T, Risseeuw E, Brogden D, Zeko A, Crosby WL, Berry CC, Ecker JR (2003) Genome-wide insertional mutagenesis of *Arabidopsis thaliana*. *Science* 301: 653-657
- Ament K, Kant MR, Sabelis MW, Haring MA, Schuurink RC (2004) Jasmonic acid is a key regulator of spider mite-induced volatile terpenoid and methyl salicylate emission in tomato. *Plant Physiology* 135: 2025-2037
- Ament K, Van Schie CC, Bouwmeester HJ, Haring MA, Schuurink RC (2006) Induction of a leaf specific geranylgeranyl pyrophosphate synthase and emission of (E,E)-4,8,12-trimethyltrideca-1,3,7,11-tetraene in tomato are dependent on both jasmonic acid and salicylic acid signaling pathways. *Planta* 224: 1197-1208
- Andreae MO, Crutzen PJ (1997) Atmospheric aerosols: Biogeochemical sources and role in atmospheric chemistry. *Science* 276: 1052-1058
- Arimura G, Ozawa R, Shimoda T, Nishioka T, Boland W, Takabayashi J (2000) Herbivory-induced volatiles elicit defence genes in lima bean leaves. *Nature* 406: 512-515
- Arimura G, Ozawa R, Horiuchi J, Nishioka T, Takabayashi J (2001) Plant-plant interactions mediated by volatiles emitted from plants infested by spider mites. *Biochemical Systematics and Ecology* 29: 1049-1061
- Arimura G, Huber DPW, Bohlmann J (2004a) Forest tent caterpillars (*Malacosoma disstria*) induce local and systemic diurnal emissions of terpenoid volatiles in hybrid poplar (*Populus trichocarpa* x *deltoides*): cDNA cloning, functional characterization, and patterns of gene expression of (-)-germacrene D synthase, PtdTPS1. *The Plant Journal* 37: 603-616
- Arimura G, Ozawa R, Kugimiya S, Takabayashi J, Bohlmann J (2004b) Herbivore-induced defense response in a model legume. Two-spotted spider mites induce emission of (E)- β -ocimene and transcript accumulation of (E)- β -ocimene synthase in *Lotus japonicus*. *Plant Physiology* 135: 1976-1983
- Arimura G, Kost C, Boland W (2005) Herbivore-induced, indirect plant defences. *Biochimica et Biophysica Acta* 1734: 91-111
- Arimura G, Köpke S, Kunert M, Volpe V, David A, Brand P, Dabrowska P, Maffei ME, Boland W (2008) Effects of feeding *Spodoptera littoralis* on lima bean leaves: IV. Diurnal and nocturnal damage differentially initiate plant volatile emission. *Plant Physiology* 146: 965-973
- Atkinson NJ, Urwin PE (2012) The interaction of plant biotic and abiotic stresses: from genes to the field. *Journal of Experimental Botany* 63: 3523-3543
- Ballaré CL, Scopel AL, Sanchez RA (1990) Far-red radiation reflected from adjacent leaves: an early signal of competition in plant canopies. *Science* 247: 329-332

References

- Ballaré CL, Barnes PW, Flint SD, Price S (1995) Inhibition of hypocotyl elongation by ultraviolet-B radiation in de-etiolating tomato seedlings. II. Time-course, comparison with flavonoid responses and adaptive significance. *Physiologia Plantarum* 93: 593-601
- Ballaré CL, Caldwell MM, Flint SD, Robinson A, Bornman JF (2011) Effects of solar ultraviolet radiation on terrestrial ecosystems. Patterns, mechanisms, and interactions with climate change. *Photochemical & Photobiological Science* 10: 226-241
- Ballaré CL (2014) Light regulation of plant defense. *Plant Biology* 65: 335-363
- Bate NJ, Rothstein SJ (1998) C6-volatiles derived from the lipoxygenase pathway induce a subset of defense-related genes. *The Plant Journal* 16: 561-569
- Bernasconi ML, Turlings TCJ, Ambrosetti L, Bassetti P, Dorn S (1998) Herbivore-induced emission of maize volatiles repel the corn leaf aphid *Rhopalosiphum maidis*. *Entomologia Experimentalis et Applicata* 87: 133-142
- Björn LO, Callaghan TV, Gehrke C, Gwynn-Jones D, Lee JA, Johanson U, Sonesson M, Buck ND (1999) Effects of ozone depletion and increased ultraviolet-B radiation on northern vegetation. *Polar Research* 18: 331-337
- Blande JD, Turunen K, Holopainen JK (2009) Pine weevil feeding on Norway spruce bark has a stronger impact on needle VOC emissions than enhanced ultraviolet-B radiation. *Environmental Pollution* 157: 174-180
- Blande JD, Kojus M, Holopainen JK (2010) Foliar methyl salicylate emissions indicate prolonged aphid infestation on silver birch and black alder. *Tree Physiology* 30: 404-416
- Bleeker PM, Diergaarde PJ, Ament K, Guerra J, Weidner M, Schütz S, de Both MT, Haring MA, Schuurink RC (2009) The role of specific tomato volatiles in tomato-whitefly interaction. *Plant Physiology* 151: 925-935
- Bleeker PM, Spyropoulou EA, Diergaarde PJ, Volpin H, De Both MT, Zerbe P, Bohlmann J, Falara V, Matsuba Y, Pichersky E, Haring MA, Schuurink RC (2011) RNA-seq discovery, functional characterization, and comparison of sesquiterpene synthases from *Solanum lycopersicum* and *Solanum habrochaites* trichomes. *Plant Molecular Biology* 77: 323-336
- Bleeker PM, Mirabella R, Diergaarde PJ, VanDoorn A, Tissier A, Kant MR, Prins M, de Vos M, Haring MA, Schuurink RC (2012) Improved herbivore resistance in cultivated tomato with the sesquiterpene biosynthetic pathway from a wild relative. *Proceedings of the National Academy of Sciences* 109: 20124-20129
- Bongers FJ, Evers JB, Anten NP, Pierik R (2014) From shade avoidance responses to plant performance at vegetation level: using virtual plant modelling as a tool. *New Phytologist* 204: 268-272
- Britt AB (1996) DNA damage and repair in plants. *Annual Review of Plant Physiology and Plant Molecular Biology* 47: 75-100
- Britt AB (2004) Repair of DNA damage induced by solar UV. *Photosynthesis Research* 81: 105-112
- Brown BA, Cloix C, Jiang GH, Kaiserli E, Herzyk P, Kliebenstein DJ, Jenkins GI (2005) A UV-B-specific signaling component orchestrates plant UV protection. *Proceedings of the National Academy of Sciences* 102: 18225-18230
- Brown BA, Jenkins GI (2008) UV-B signaling pathways with different fluence-rate response profiles are distinguished in mature *Arabidopsis* leaf tissue by requirement for UVR8, HY5, and HYH. *Plant Physiology* 146: 576-588
- Bruin J, Dicke M, Sabelis MW (1992) Plants are better protected against spider-mites after exposure to volatiles from infested conspecifics. *Experientia* 48: 525-529
- Burke CC, Croteau R (2002a) Geranyl diphosphate synthase from *Abies grandis*: cDNA isolation, functional expression, and characterization. *Archives of Biochemistry and Biophysics* 405: 130-136
- Burke CC, Croteau R (2002b) Interaction with the small subunit of geranyl diphosphate synthase modifies the chain length specificity of geranylgeranyl diphosphate synthase to produce geranyl diphosphate. *Journal of Biological Chemistry* 277: 3141-3149
- Buttery RG, Ling LC, Light DM (1987) Tomato leaf volatile aroma components. *Journal of Agricultural and Food Chemistry* 35: 1039-1042
- Caldwell MM, Teramura AH, Tevini M (1989) The changing solar ultraviolet climate and the ecological consequences for higher plants. *Trends in Ecology & Evolution* 4: 363-367
- Caldwell MM, Björn LO, Bornman JF, Flint SD, Kulandaivelu G, Teramura AH, Tevini M (1998) Effects of increased solar ultraviolet radiation on terrestrial ecosystems. *Journal of Photochemistry and Photobiology B: Biology* 46: 40-52

- Caldwell MM, Bornman JF, Ballaré CL, Flint SD, Kulandaivelu G (2007) Terrestrial ecosystems, increased solar ultraviolet radiation, and interactions with other climate change factors. *Photochemical & Photobiological Science* 6: 252-266
- Calogirou A, Larsen BR, Kotzias D (1999) Gas-phase terpene oxidation products: a review. *Atmospheric Environment* 33: 1423-1439
- Casal JJ (2012) Shade avoidance. *The Arabidopsis book*, 10
- Casal JJ (2013) Photoreceptor signaling networks in plant responses to shade. *Annual Review of Plant Biology* 64: 403-27
- Cardoza YJ, Alborn HT, Tumlinson JH (2002) In vivo volatile emissions from peanut plants induced by simultaneous fungal infection and insect damage. *Journal of Chemical Ecology* 28: 161-174
- Cifuentes-Esquivel N, Bou-Torrent J, Galstyan A, Gallemí M, Sessa G, Salla Martret M, Roig-Villanova I, Ruberti I, Martínez-García JF (2013) The bHLH proteins BEE and BIM positively modulate the shade avoidance syndrome in *Arabidopsis* seedlings. *The Plant Journal* 75: 989-1002
- Christie JM, Arvai AS, Baxter KJ, Heilmann M, Pratt AJ, O'Hara A, Kelly SM, Hothorn M, Smith BO, Hitomi K, Jenkins GI, Getzoff ED (2012) Plant UVR8 photoreceptor senses UV-B by tryptophan-mediated disruption of cross-dimer salt bridges. *Science* 335: 1492-1496
- Conrath U, Beckers GJ, Flors V, García-Agustín P, Jakab G, Mauch F, Newman MA, Pieterse CM, Poinssot B, Pozo MJ, Pugin A, Schaffrath U, Ton J, Wendehenne D, Zimmerli L, Mauch-Mani B (2006) Priming: getting ready for battle. *Molecular Plant-Microbe Interactions* 19: 1062-1071
- Croft KPC, Jüttner F, Slusarenko AJ (1993) Volatile products of the lipoxygenase pathway evolved from *Phaseolus vulgaris* (L.) leaves inoculated with *Pseudomonas syringae* pv. phaseolicola. *Plant Physiology* 101: 13-24
- Deckmyn G, Impens I (1997) The ratio UV-B/photosynthetically active radiation (PAR) determines the sensitivity of rye to increased UV-B radiation. *Environmental and Experimental Botany* 37: 3-12
- Degenhardt J, Köllner TG, Gershenzon J (2009) Monoterpene and sesquiterpene synthases and the origin of terpene skeletal diversity in plants. *Phytochemistry* 70: 1621-1637
- Delphia CM, Mescher MC, De Moraes CM (2007) Induction of plant volatiles by herbivores with different feeding habits and the effects of induced defenses on host-plant selection by thrips. *Journal of Chemical Ecology* 33: 997-1012
- Demkura PV, Abdala G, Baldwin IT, Ballaré CL (2010) Jasmonate-dependent and -independent pathways mediate specific effects of solar ultraviolet B radiation on leaf phenolics and antiherbivore defense. *Plant Physiology* 152: 1084-1095
- Demkura PV, and Ballaré CL (2012) UVR8 mediates UV-B-induced *Arabidopsis* defense responses against *Botrytis cinerea* by controlling sinapate accumulation. *Molecular Plant* 5: 642-652
- Denman KL, Brasseur G, Chidthaisong A, Ciais P, Cox PM, Dickinson RE, Hauglustaine D, Heinze C, Holland E, Jacob D, Lohmann U, Ramachandran S, Da Silva Dias PL, Wofsy SC, Zhang X (2007) *Climate Change 2007: The Physical Science Basis. Contribution of Working Group I to the Fourth Assessment Report of the Intergovernmental Panel on Climate Change*. Cambridge University Press
- Devlin PF, Yanovsky MJ, Kay SA (2003) A genomic analysis of the shade avoidance response in *Arabidopsis*. *Plant Physiology* 133: 1617-1629
- Dicke M, Sabelis MW (1988) How plants obtain predatory mites as bodyguards. *Netherlands Journal of Zoology* 38: 148-165
- Dicke M, Dijkman H (1992) Induced defence in detached uninfested plant-leaves – effects on behavior of herbivores and their predators. *Oecologia* 91: 554-560
- Dicke M (1999) Are herbivore-induced plant volatiles reliable indicators of herbivore identity to foraging carnivorous arthropods? *Entomologia Experimentalis et Applicata* 91: 131-142
- Dicke M, van Loon JJA (2000) Multitrophic effects of herbivore-induced plant volatiles in an evolutionary context. *Entomologia Experimentalis et Applicata* 97: 237-249
- Dicke M, Agrawal AA, Bruin J (2003) Plants talk, but are they deaf? *Trends in Plant Science* 8: 403-405
- Dicke M, Baldwin IT (2010) The evolutionary context for herbivore-induced plant volatiles: beyond the 'cry for help'. *Trends in Plant Science* 15: 167-175
- Djakovic-Petrovic T, De Wit M, Voesenek LACJ, Pierik R (2007) DELLA protein function in growth responses to canopy signals. *The Plant Journal* 51: 117-126
- Drukker B, Bruin J, Jacobs G, Kroon A, Sabelis MW (2000) How predatory mites learn to cope with variability in volatile plant signals in the environment of their herbivorous prey. *Experimental and Applied Acarology* 24: 881-895

References

- Dudareva N, Murfitt LM, Mann CJ, Gorenstein N, Kolosova N, Kish CM, Bonham C, Wood K (2000) Developmental regulation of methyl benzoate biosynthesis and emission in snapdragon flowers. *Plant Cell* 12: 949-961
- Dudareva N, Pichersky E, Gershenzon J (2004) Biochemistry of plant volatiles. *Plant Physiology* 135: 1893-1902
- Dudareva N, Klempien A, Muhlemann JK, Kaplan I (2013) Biosynthesis, function and metabolic engineering of plant volatile organic compounds. *New Phytologist* 198: 16-32
- Engelberth J, Alborn HT, Schmelz EA, Tumlinson JH (2004) Airborne signals prime plants against insect herbivore attack. *Proceedings of the National Academy of Sciences* 101: 1781-1785
- Falara V, Akhtar TA, Nguyen TTH, Spyropoulou EA, Bleeker PM, Schauvinhold I, Matsuba Y, Bonini ME, Schillmiller AL, Last RL, Schuurink RC, Pichersky E (2011) The tomato terpene synthase gene family. *Plant Physiology* 157: 770-789
- Fankhauser C, Yeh KC, Lagarias JC, Zhang H, Elich TD, Chory J (1999) PKS1, a substrate phosphorylated by phytochrome that modulates light signaling in *Arabidopsis*. *Science* 284: 1539-1541
- Farag MA, Paré PW (2002) C6-Green leaf volatiles trigger local and systemic VOC emissions in tomato. *Phytochemistry* 61: 545-554
- Favory JJ, Stec A, Gruber H, Rizzini L, Oravec A, Funk M, Albert A, Cloix C, Jenkins GI, Oakeley EJ, Seidlitz HK, Nagy F, Ulm R (2009) Interaction of COP1 and UVR8 regulates UV-B-induced photomorphogenesis and stress acclimation in *Arabidopsis*. *The EMBO Journal* 28: 591-601
- Fehsenfeld F, Calvert J, Fall R, Goldan P, Guenther AB, Hewitt CN, Lamb B, Liu S, Trainer M, Westberg H, Zimmerman P (1992) Emissions of volatile organic compounds from vegetation and the implications for atmospheric chemistry. *Global Biogeochemical Cycles* 6: 389-430
- Fernie AR, Tohge T (2014) Location, location, location – no more! The unravelling of chromatin remodeling regulatory aspects of plant metabolic gene clusters. *New Phytologist* 205: 458-460
- Franklin KA (2008) Shade avoidance. *New Phytologist* 179: 930-944
- Frost CJ, Appel HM, Carlson JE, De Moraes CM, Mescher MC, Schultz JC (2007) Within-plant signalling via volatiles overcomes vascular constraints on systemic signalling and primes responses against herbivores. *Ecology Letters* 10: 490-498
- Frost CJ, Mescher MC, Carlson JE, De Moraes CM (2008) Plant defense priming against herbivores: getting ready for a different battle. *Plant Physiology* 146: 818-824
- Fu X, Harberd NP (2003) Auxin promotes *Arabidopsis* root growth by modulating gibberellin response. *Nature* 421: 740-743
- Galstyan A, Cifuentes-Esquivel N, Bou-Torrent J, Martinez-Garcia JF (2011) The shade avoidance syndrome in *Arabidopsis*: a fundamental role for atypical basic helix-loop-helix proteins as transcriptional cofactors. *The Plant Journal* 66: 258-267
- Gardner HW, Dornbos DLJ, Desjardins AE (1990) Hexanal, trans-2-hexenal, and trans-2-nonenal inhibit soybean, *Glycine max*, seed germination. *Journal of Agricultural and Food Chemistry* 38: 1316-1320
- Goldstein AH, Galbally IE (2007) Known and unexplored organic constituents in the Earth's Atmosphere. *Environmental Science & Technology* 41: 1514-1521
- Goodner KL (2008) Practical retention index models of OV-101, DB-1, DB-5, and DB-Wax for flavor and fragrance compounds. *Food Science and Technology* 41: 951-958
- Gonzalez-Besteiro MA, Bartels S, Albert A, Ulm R (2011) *Arabidopsis* MAP kinase phosphatase 1 and its target MAP kinases 3 and 6 antagonistically determine UV-B stress tolerance, independent of the UVR8 photoreceptor pathway. *The Plant Journal* 68: 727-737
- Gouinguéné SP, Turlings TCJ (2002) The effects of abiotic factors on induced volatile emissions in corn plants. *Plant Physiology* 129: 1296-1307
- Graus M, Muller M, Hansel A (2010) High resolution PTRTOF quantification and formula confirmation of VOC in real time. *J. Am. Soc. Mass Spectr.* 21: 1037-1044
- Guenther A, Karl T, Harley P, Wiedinmyer C, Palmer PI, Geron C (2006) Estimates of global terrestrial isoprene emissions using MEGAN (Model of Emissions of Gases and Aerosols from Nature). *Atmospheric Chemistry and Physics* 6: 3181-3210
- Hao X, Hale BA, Ormrod DP, Papadopoulos AP (2000) Effects of pre-exposure to ultraviolet-B radiation on responses of tomato (*Lycopersicon esculentum* cv. New Yorker) to ozone in ambient and elevated carbon dioxide. *Environmental Pollution* 110: 217-224
- Hao Y, Oh E, Choi G, Liang Z, Wang ZY (2012) Interactions between HLH and bHLH factors modulate light-regulated plant development. *Molecular Plant* 5: 688-97
- Harley P, Deem G, Flint S, Caldwell M (1996) Effects of growth under elevated UV-B on photosynthesis and isoprene emission in *Quercus gambelii* and *Mucuna pruriens*. *Global Change Biology* 1: 149-154

- Harrison RM, Yin J (2000) Particulate matter in the atmosphere: which particle properties are important for its effects on health? *Science of The Total Environment* 249: 85-101
- Harrison SP, Morfopoulos C, Dani KG, Prentice IC, Arneth A, Atwell BJ, Barkley MP, Leishman MR, Loreto F, Medlyn BE, Niinemets Ü, Possell M, Peñuelas J, Wright IJ (2013) Volatile isoprenoid emissions from plastid to planet. *New Phytologist* 197: 49-57
- Hartikainen K, Riikonen J, Nerg A, Kivimäenpää M, Ahonen V, Tervahauta A, Kärenlampi S, Mäenpää M, Rousi M, Kontunen-Soppela S, Oksanen E, Holopainen T (2012) Impact of elevated temperature and ozone on the emission of volatile organic compounds and gas exchange of silver birch (*Betula pendula* Roth). *Environmental and Experimental Botany* 84: 33-43
- Hartmann, DL, Wallace JM, Limpasuvan V, Thompson DWJ, Holton JR (2000) Can ozone depletion and global warming interact to produce rapid climate change? *Proceedings of the National Academy of Sciences* 97: 1412-1417
- Hayes C, Velanis CN, Jenkins GI, Franklin KA (2014) UV-B detected by the UVR8 photoreceptor antagonizes auxin signaling and plant shade avoidance. *Proceedings of the National Academy of Sciences* 111: 11894–11899
- Hectors K, van Oevelen S, Guisez Y, Prinsen E, Jansen MAK (2012) The phytohormone auxin is a component of the regulatory system that controls UV-mediated accumulation of flavonoids and UV-induced morphogenesis. *Physiologia Plantarum* 145: 594-603
- Heijari J, Blande JD, Holopainen JK (2011) Feeding of large pine weevil on Scots pine stem triggers localised bark and systemic shoot emission of volatile organic compounds. *Environmental and Experimental Botany* 71: 390-398
- Heijde M, Ulm R (2012) UV-B photoreceptor-mediated signalling in plants. *Trends in Plant Science* 17: 230-237
- Heijde M, Ulm R (2013) Reversion of the Arabidopsis UV-B photoreceptor UVR8 to the homodimeric ground state. *Proceedings of the National Academy of Sciences* 110: 1113-1118
- Heil M, Silva Bueno JC (2002) Within-plant signaling by volatiles leads to induction and priming of an indirect plant defense in nature. *Proceedings of the National Academy of Sciences* 104: 5467-5472
- Heil M (2008) Indirect defence via tritrophic interactions. *New Phytologist* 178: 41-61
- Heil M, Karban R (2009) Explaining evolution of plant communication by airborne signals. *Trends in Ecology & Evolution* 25: 137-44
- Hemmerlin A, Hoeffler JF, Meyer O, Tritsch D, Kagan IA, Grosdemange-Billiard C, Rohmer M, Bach TJ (2003) Cross-talk between the cytosolic mevalonate and the plastidial methylerythritol phosphate pathways in tobacco bright yellow-2 cells. *Journal of Biological Chemistry* 278: 26666-26676
- Hemmerlin A, Harwood JL, Bach TJ (2012) A *raison d'être* for two distinct pathways in the early steps of plant isoprenoid biosynthesis? *Progress in Lipid Research* 51: 95-148
- Hildebrand DF, Brown GC, Jackson DM, Hamilton-Kemp TR (1993) Effects of some leaf-emitted volatile compounds on aphid population increase. *Journal of Chemical Ecology* 19: 1875-1887
- Hisamatsu T, King RW, Helliwell CA, Koshioka M (2005) The involvement of gibberellin 20-oxidase genes in phytochrome-regulated petiole elongation of *Arabidopsis*. *Plant Physiology* 138: 1106-1116
- Holm M, Ma L, Qu L, Deng X (2002) Two interacting bZIP proteins are direct targets of COP1-mediated control of light-dependent gene expression in *Arabidopsis*. *Genes & Development* 16: 1247-1259
- Holzinger R, Kasper-Giebl A, Staudinger M, Schauer G, Röckmann T (2010a) Analysis of the chemical composition of organic aerosol at the Mt. Sonnblick observatory using a novel high mass resolution thermal-desorption proton-transfer-reaction mass-spectrometer (hr-TD-PTR-MS). *Atmospheric Chemistry and Physics* 10: 10111–10128
- Holzinger R, Williams J, Herrmann F, Lelieveld J, Donahue NM, Röckmann T (2010b) Aerosol analysis using a Thermal-Desorption Proton-Transfer-Reaction Mass Spectrometer (TD-PTR-MS): a new approach to study processing of organic aerosols. *Atmospheric Chemistry and Physics* 10: 2257–2267
- Hornitschek P, Lorrain S, Zoete V, Michielin O, Fankhauser C (2009) Inhibition of the shade avoidance response by formation of non-DNA binding bHLH heterodimers. *The EMBO Journal* 28: 3893-3902
- Huang S, Dai Q, Peng S, Chavez AQ, Miranda MLL, Visperas RM, Vergara BS (1997) Influence of supplemental ultraviolet-B on indoleacetic acid and calmodulin in the leaves of rice (*Oryza sativa* L.). *Plant Growth Regulation* 21: 59-64
- Huang J, Cardoza YJ, Schmelz EA, Raina R, Engelberth J, Tumlinson JH (2003) Differential volatile emissions and salicylic acid levels from tobacco plants in response to different strains of *Pseudomonas syringae*. *Planta* 217: 767-775
- Hui D, Iqbal J, Lehmann K, Gase K, Saluz HP, Baldwin IT (2003) Molecular interactions between the specialist herbivore *Manduca sexta* (Lepidoptera, Sphingidae) and its natural host *Nicotiana attenuata*:

References

- V. microarray analysis and further characterization of large-scale changes in herbivore-induced mRNAs. *Plant Physiology* 131: 1877-1893
- Hui R, Li X, Chen C, Zhao X, Jia R, Liu L, Wei Y (2013) Responses of photosynthetic properties and chloroplast ultrastructure of *Bryum argenteum* from a desert biological soil crust to elevated ultraviolet-B radiation. *Physiologia Plantarum* 147: 489-501
- IPCC (2007) *Climate Change 2007: The Physical Science Basis. Contribution of Working Group I to the Fourth Assessment Report of the Intergovernmental Panel on Climate Change.* Solomon S, Qin D, Manning M, Chen Z, Marquis M, Averyt KB, Tignor M, Miller HL (eds.). Cambridge University Press, Cambridge, United Kingdom
- Izaguirre MM, Scopel AL, Baldwin IT, Ballaré CL (2003) Convergent responses to stress. Solar ultraviolet-B radiation and *Manduca sexta* herbivory elicit overlapping transcriptional responses in field-grown plants of *Nicotiana longiflora*. *Plant Physiology* 132: 1755-1767
- Jansen MA, Gaba V, Greenberg BM (1998) Higher plants and UV-B radiation: balancing damage, repair and acclimation. *Trends in Plant Science* 3: 131-135
- Jansen MAK, Hectors K, O'Brien NM, Guisez Y, Potters G (2008) Plant stress and human health: Do human consumers benefit from UV-B acclimated crops? *Plant Science* 175: 449-458
- Jenkins GI (2014) The UV-B photoreceptor UVR8: from structure to physiology. *The Plant Cell* 26: 21-37
- Johnson CB, Kirby J, Naxakis G, Pearson S (1999) Substantial UV-B-mediated induction of essential oils in sweet basil (*Ocimum basilicum* L.). *Phytochemistry* 51: 507-510
- Jordan A, Haidacher S, Hanel G, Hartungen E, Märk L, Seehauser H, Schottkowsky R, Sulzer P, Mark TD (2009) A high resolution and high sensitivity proton-transfer-reaction time-of-flight mass spectrometer (PTR-TOF-MS). *International Journal of Mass Spectrometry* 286: 122-128
- Kami C, Allenbach L, Zourelidou M, Ljung K, Schütz F, Isono E, Watahiki MK, Yamamoto KT, Schwechheimer C, Fankhauser C (2014) Reduced phototropism in *pks* mutants may be due to altered auxin-regulated gene expression or reduced lateral auxin transport. *The Plant Journal* 77: 393-403
- Kant MR, Ament K, Sabelis MW, Haring MA, Schuurink RC (2004) Differential timing of spider mite-induced direct and indirect defenses in tomato plants. *Plant Physiology* 135: 483-495
- Karban R, Baldwin IT, Baxter KJ, Laue G, Felton GW (2000) Communication between plants: induced resistance in wild tobacco plants following clipping of neighboring sagebrush. *Oecologia* 125: 66-71
- Karban R (2007) Experimental clipping of sagebrush inhibits seed germination of neighbours. *Ecology Letters* 10: 791-797
- Kegge W, Pierik R (2010) Biogenic volatile organic compounds and plant competition. *Trends in Plant Science* 15: 126-132
- Kegge W, Weldegergis BT, Soler R, Vergeer-Van Eijk M, Dicke M, Voesenek LACJ, Pierik R (2013) Canopy light cues affect emission of constitutive and methyl jasmonate-induced volatile organic compounds in *Arabidopsis thaliana*. *New Phytologist* 200: 861-874
- Kesselmeier J, Ciccioli P, Kuhn U, Stefani P, Biesenthal T, Rottenberger S, Wolf A, Vitullo M, Valentini R, Nobre A, Kabat P, Andreae MO (2002) Volatile organic compound emissions in relation to plant carbon fixation and the terrestrial carbon budget. *Global Biochemical Cycles* 16: 73-1-73-9
- Kessler A, Halitschke R, Diezel C, Baldwin IT (2006) Priming of plant defense responses in nature by airborne signaling between *Artemisia tridentata* and *Nicotiana attenuata*. *Oecologia* 148: 280-292
- Keuskamp DH, Pollmann S, Voesenek LACJ, Peeters AJM, Pierik R (2010) Auxin transport through PIN-FORMED 3 (PIN3) controls shade avoidance and fitness during competition. *Proceedings of the National Academy of Sciences* 107: 22740-22744
- Keuskamp DH, Sasidharan R, Vos I, Peeters AJM, Voesenek LACJ, Pierik R (2011) Blue-light-mediated shade avoidance requires combined auxin and brassinosteroid action in *Arabidopsis* seedlings. *The Plant Journal* 67: 208-217
- Kigathi RN, Weisser WW, Veit D, Gershenson J, Unsicker SB (2013) Plants suppress their emission of volatiles when growing with conspecifics. *Journal of Chemical Ecology* 39: 537-545
- Kilian J, Whitehead D, Horak J, Wanke D, Weigl S, Batistic O, D'Angelo C, Bornberg-Bauer E, Kudla J, Harter K (2007) The AtGenExpress global stress expression data set: protocols, evaluation and model data analysis of UV-B light, drought and cold stress responses. *The Plant Journal* 50: 347-363
- Kishimoto K, Matsui K, Ozawa R, Takabayashi J (2005) Volatile C6-aldehydes and Allo-ocimene activate defense genes and induce resistance against *Botrytis cinerea* in *Arabidopsis thaliana*. *Plant and Cell Physiology* 46: 1093-1102
- Kliebenstein DJ, Lim JE, Landry LG, Last RL (2002) *Arabidopsis* UVR8 regulates ultraviolet-B signal transduction and tolerance and contains sequence similarity to human regulator of chromatin condensation 1. *Plant Physiology* 130: 234-243

- König G, Brunda M, Puxbaum H, Hewitt CN, Duckham SC, Rudolph J (1995) Relative contribution of oxygenated hydrocarbons to the total biogenic VOC emissions of selected mid-European agricultural and natural plant species. *Atmospheric Environment* 29: 861–874
- Kozuka T, Kobayashi J, Horiguchi G, Demura T, Sakakibara H, Tsukaya H, Nagatani A (2010) Involvement of auxin and brassinosteroid in the regulation of petiole elongation under the shade. *Plant Physiology* 153: 1608–1618
- Kulmala M (2003) How particles nucleate and grow. *Science* 302: 1000–1001
- Kusano M, Tohge T, Fukushima A, Kobayashi M, Hayashi N, Otsuki H, Kondou Y, Goto H, Kawashima M, Matsuda F, Niida R, Matsui M, Saito K, Fernie AR (2011) Metabolomics reveals comprehensive reprogramming involving two independent metabolic responses of *Arabidopsis* to UV-B light. *The Plant Journal* 67: 354–369
- Lange BM, Ghassemian M (2003) Genome organization in *Arabidopsis thaliana*: a survey for genes involved in isoprenoid and chlorophyll metabolism. *Plant Molecular Biology* 51: 925–948
- Lariguet P, Boccalandro HE, Alonso JM, Ecker JR, Chory J, Casal JJ, Fankhauser C (2003) A growth regulatory loop that provides homeostasis to phytochrome A signaling. *The Plant Cell* 15: 2966–2978
- Lariguet P, Schepens I, Hodgson D, Pedmale UV, Trevisan M, Kami C, de Carbonnel M, Alonso JM, Ecker JR, Liscum E, Fankhauser C (2006) PHYTOCHROME KINASE SUBSTRATE 1 is a phototropin 1 binding protein required for phototropism. *Proceedings of the National Academy of Sciences* 103: 10134–10139
- Leitner M, Boland W, Mithofer A (2005) Direct and indirect defences induced by piercing-sucking and chewing herbivores in *Medicago truncatula*. *New Phytologist* 167: 597–606
- Leitner M, Kaiser R, Rasmussen MO, Driguez H, Boland W, Mithofer A (2008) Microbial oligosaccharides differentially induce volatiles and signaling components in *Medicago truncatula*. *Phytochemistry* 69: 2029–2040
- Leivar P, Monte E, Oka Y, Liu T, Carle C, Castillon A, Huq E, Quail PH (2008) Multiple phytochrome-interacting bHLH transcription factors repress premature seedling photomorphogenesis in darkness. *Current Biology* 18: 1815–1823
- Lerdau M, Slobodkin L (2002) Trace gas emissions and species-dependent ecosystem services. *TRENDS in Ecology and Evolution* 17: 309–312
- Li J, Ou-Lee TM, Raba R, Amundson RG, Last RL (1993) *Arabidopsis* flavonoid mutants are hypersensitive to UV-B irradiation. *Plant Cell* 5: 171–179
- Li L, Ljung K, Breton G, Schmitz RJ, Pruneda-Paz J, Cowing-Zitron C, Cole BJ, Ivans LJ, Pedmale UV, Jung HS, Ecker JR, Kay SA, Chory J (2012) Linking photoreceptor excitation to changes in plant architecture. *Genes & Development* 26: 785–790
- Lichtenthaler HK (1999) The 1-deoxy-D-xylulose-5-phosphate pathway of isoprenoid biosynthesis in plants. *Annual Review of Plant Physiology and Plant Molecular Biology* 50: 47–65
- Llusià J, Peñuelas J (1998) Changes in terpene content and emission in potted Mediterranean woody plants under severe drought. *Canadian Journal of Botany* 76: 1366–1373
- Llusià J, Llorens L, Bernal M, Verdaguer D, Peñuelas J (2012) Effects of UV radiation and water limitation on the volatile terpene emission rates, photosynthesis rates, and stomatal conductance in four Mediterranean species. *Acta Physiologiae Plantarum* 34: 757–769
- Loreto F, Pinelli P, Manes F, Kollist H (2004) Impact of ozone on monoterpene emissions and evidence for and isoprene-like antioxidant action of monoterpenes by *Quercus ilex* leaves. *Tree Physiology* 24: 361–367
- Loreto F, Schnitzler JP (2010) Abiotic stresses and induced BVOCs. *Trends in Plant Science* 15: 154–166
- Lorrain S, Allen T, Duek PD, Whitelam GC, Fankhauser C (2008) Phytochrome-mediated inhibition of shade avoidance involves degradation of growth-promoting bHLH transcription factors. *The Plant Journal* 53: 312–323
- Loughrin JH, A Manukian, RR Heath, TC Turlings, JH Tumlinson (1994) Diurnal cycle of emission of induced volatile terpenoids by herbivore-injured cotton plant. *Proceedings of the National Academy of Sciences* 91: 11836–11840
- De Lucas M, Daviere JM, Rodríguez-Falcón M, Pontin M, Iglesias-Pedraz JM, Lorrain S, Fankhauser C, Blázquez MA, Titarenko E, Prat S (2008) A molecular framework for light and gibberellin control of cell elongation. *Nature* 451: 480–484
- Mackerness SAH, Surplus SL, Blake P, John CF, Buchanan-Wollaston V, Jordan BR, Thomas B (1999) Ultraviolet-B-induced stress and changes in gene expression in *Arabidopsis thaliana*: role of signalling pathways controlled by jasmonic acid, ethylene and reactive oxygen species. *Plant, Cell and Environment* 22: 1413–1423

References

- Mäntylä E, Alessio GA, Blande JD, Heijari J, Holopainen JK, Laaksonen T, Piirtola P, Klemola T (2008) From plants to birds: higher avian predation rates in trees responding to insect herbivory. *PLoS ONE* 3: e2832
- Maes K, Vercammen J, Pham-Tuan H, Sandra P, Debergh PC (2001) Critical aspects for the reliable headspace analysis of plants cultivated in vitro. *Phytochemical Analysis* 12: 153-158
- Mark U, Saile-Mark M, Tevini M (1996) Effects of solar UVB radiation on growth, flowering and yield of Central and Southern European maize cultivars (*Zea mays* L.) *Photochemistry and Photobiology* 64: 457-463
- Mark U, Tevini M (1997) Effects of solar ultraviolet-B radiation, temperature and CO₂ on growth and physiology of sunflower and maize seedlings. *Plant Ecology* 128: 225-234
- Matsushita Y, Kang W, Charlwood BV (1996) Cloning and analysis of a cDNA encoding farnesyl diphosphate synthase from *Artemisia annua*. *Gene* 172: 207-209
- Mazza CA, Ballaré CL (2015) Photoreceptors UVR8 and phytochrome B cooperate to optimize plant growth and defense in patchy canopies. *New Phytologist* 207: 4-9
- McConkey ME, Gershenzon J, Croteau RB (2000) Developmental regulation of monoterpene biosynthesis in the glandular trichomes of peppermint. *Plant Physiology* 122: 215-224
- McGarvey DJ, Croteau R (1995) Terpenoid metabolism. *Plant Cell* 7: 1015-1026
- McKenzie RL, Aucamp PJ, Bais AF, Björn LO, Ilyas M, Madronich S (2011) Ozone depletion and climate change: impacts on UV radiation. *Photochemical & Photobiological Science* 10: 182-198
- Mepsted R, Paul ND, Stephen J, Corlett JE, Nogués S, Baker NR, Jones HG, Ayres PG (1996) Effects of enhanced UV-B radiation on pea (*Pisum sativum* L.) grown under field conditions in the UK. *Global Change Biology* 2: 325-334
- Miller B, Madilao LL, Ralph S, Bohlmann J (2005) Insect-induced conifer defense: White pine weevil and methyl jasmonate induce traumatic resinosis, *de novo* formed volatile emissions, and accumulation of terpenoid synthase and octadecanoid pathway transcripts in Sitka spruce. *Plant Physiology* 137: 369-382
- De Moraes CM, Lewis WJ, Paré PW, Alborn HT, Tumlinson JH (1998) Herbivore-infested plants selectively attract parasitoids. *Nature* 393: 570-573
- De Moraes CM, Mescher MC, Tumlinson JH (2001) Caterpillar-induced nocturnal plant volatiles repel conspecific females. *Nature* 410: 577-580
- Morales LO, Brosché M, Vainonen J, Jenkins GI, Wargent JJ, Sipari N, Strid Å, Lindfors AV, Tegelberg R, Aphalo PJ (2013) Multiple roles for UV RESISTANCE LOCUS8 in regulating gene expression and metabolite accumulation in *Arabidopsis* under solar ultraviolet radiation. *Plant Physiology* 161: 744-759
- Monson RK, Grote R, Niinemets Ü, Schnitzler JP (2012) Modeling the isoprene emission rate from leaves. *New Phytologist* 195: 541-559
- Monson RK1, Jones RT, Rosenstiel TN, Schnitzler JP (2013) Why only some plants emit isoprene. *Plant, Cell and Environment* 36: 503-516
- Moon YR, Lee MH, Tovuu A, Lee CH, Chung BY, Park YI, Kim JH (2011) Acute exposure to UV-B sensitizes cucumber, tomato, and *Arabidopsis* plants to photooxidative stress by inhibiting thermal energy dissipation and antioxidant defense. *Journal of Radiation Research* 52: 238-248
- Muhlemann JK, Maeda H, Chang CY, San Miguel P, Baxter I, Cooper B, Perera MA, Nikolau BJ, Vitek O, Morgan JA, Dudareva N (2012) Developmental changes in the metabolic network of snapdragon flowers. *PLoS ONE* 7: e40381
- Neilson EH, Goodger JQD, Woodrow IE, Møller BL (2013) Plant chemical defense: at what cost? *Trends in Plant Science* 18: 250-258
- Niinemetts Ü, Loreto F, Reichstein M (2004) Physiological and physicochemical controls on foliar volatile organic compound emissions. *Trends in Plant Science* 9: 1360-1385
- Oravec A, Baumann A, Máté Z, Brzezinska A, Molinier J, Oakeley EJ, Adám E, Schäfer E, Nagy F, Ulm R (2006) CONSTITUTIVELY PHOTOMORPHOGENIC1 is required for the UV-B response in *Arabidopsis*. *Plant Cell* 18: 1975-1990
- Paré PW, Tumlinson JH (1997) *De novo* biosynthesis of volatiles induced by insect herbivory in cotton plants. *Plant Physiology* 114: 1161-1167
- Peñuelas J, Llusà J (2003) BVOCs: plant defense against climate warming? *Trends in Plant Science* 8: 105-109
- Pettersson J, Ninkovic V, Ahmed E (1999) Volatiles from different barley cultivars affect aphid acceptance of neighbouring plants. *Acta Agriculturae Scandinavica B - Plant Soil Science* 49: 152-157

- Pierik R, Djakovic-Petrovic T, Keuskamp DH, de Wit M, Voeselek LACJ (2009) Auxin and ethylene regulate elongation responses to neighbor proximity signals independent of gibberellin and DELLA proteins in *Arabidopsis*. *Plant Physiology* 149: 1701-1712
- Pierik R, de Wit M (2013) Shade avoidance: phytochrome signalling and other aboveground neighbour detection cues. *Journal of Experimental Botany* 65: 2815-2824
- Pierik R, Testerink C (2014) The art of being flexible: how to escape from shade, salt, and drought. *Plant Physiology* 166: 5-22
- Polko JK, van Zanten M, van Rooij JA, Marée AF, Voeselek LA, Peeters AJ, Pierik R (2012) Ethylene-induced differential petiole growth in *Arabidopsis thaliana* involves local microtubule reorientation and cell expansion. *New Phytologist* 193: 339-348
- Polko JK, Pierik R, Van Zanten M, Tarkowská D, Strnad M, Voeselek LACJ, Peeters AJM (2013) Ethylene promotes hyponastic growth through interaction with ROTUNDIFOLIA3/CYP90C1 in *Arabidopsis*. *Journal of Experimental Botany* 64: 613-624
- Porra R, Thompson W (1989) Determination of accurate extinction coefficients and simultaneous equations for assaying chlorophylls *a* and *b* extracted with four different solvents: verification of the concentration of chlorophyll standards by atomic absorption spectroscopy. *Biochimica et Biophysica Acta* 975: 384-394
- Quail PH (2002) Phytochrome photosensory signalling networks. *Nature Reviews Molecular Cell Biology* 3: 85-93
- Raguso RA (2008) Wake up and smell the roses: the ecology and evolution of floral scent. *Annual Review of Ecology, Evolution, and Systematics* 39: 549-569
- Reed JW, Foster KR, Morgan PW, Chory J (1996) Phytochrome B affects responsiveness to gibberellins in *Arabidopsis*. *Plant Physiology* 112: 337-342
- Ries G, Heller W, Puchta H, Sandermann H, Seidlitz HK, Hohn B (2000) Elevated UV-B radiation reduces genome stability in plants. *Nature* 406: 98-101
- Riipinen I, Pierce JR, Yli-Juuti T, Nieminen T, Häkkinen S, Ehn M, Junninen H, Lehtipalo K, Petaja T, Slowik J, Chang R, Shantz NC, Abbatt J, Leaitch WR, Kerminen VM, Worsnop DR, Pandis SN, Donahue NM, Kulmala M (2011) Organic condensation: a vital link connecting aerosol formation to cloud condensation nuclei (CCN) concentrations. *Atmospheric Chemistry and Physics* 11: 3865-3878
- Rizzini L, Favory JJ, Cloix C, Faggionato D, O'Hara A, Kaiserli E, Baumeister R, Schafer E, Nagy F, Jenkins GI, Ulm R (2011) Perception of UV-B by the *Arabidopsis* UVR8 protein. *Science* 332: 103-106
- Rodriguez-Saona CR, Rodriguez-Saona LE, Frost CJ (2009) Herbivore-induced volatiles in the perennial shrub, *Vaccinium corymbosum*, and their role in inter-branch signaling. *Journal of Chemical Ecology* 35: 163-175
- Roig-Villanova I, Bou-Torrent J, Galstyan A, Carretero-Paulet L, Portolés S, Rodríguez-Concepción M, Martínez-García JF (2007) Interaction of shade avoidance and auxin responses: a role for two novel atypical bHLH proteins. *The EMBO Journal* 26: 4756-4767
- Runyon JB, Mescher MC, De Moraes CM (2006) Volatile chemical cues guide host location and host selection by parasitic plants. *Science* 313: 1964-1967
- Rymen B, Sugimoto K (2012) Tuning growth to the environmental demands. *Current Opinion in Plant Biology* 15: 683-690
- Sabelis MW, Van de Baan HE (1983) Location of distant spider mite colonies by phytoseiid predators: demonstration of specific kairomones emitted by *Tetranychus urticae* and *Panonychus ulmi*. *Entomologia Experimentalis et Applicata* 33: 303-314
- Sahu LK (2012) Volatile organic compounds and their measurements in the troposphere. *Current Science India* 102: 1645-1649
- Saile-Mark M, Tevini M (1997) Effects of solar UV-B radiation on growth, flowering and yield of central and southern European bush bean cultivars (*Phaseolus vulgaris* L.). *Plant Ecology* 128: 115-125
- Sävenstrand H, Brosche M, Strid A (2004) Ultraviolet-B signalling: *Arabidopsis* brassinosteroid mutants are defective in UV-B regulated defence gene expression. *Plant Physiology and Biochemistry* 42: 687-694
- Schnee C, Kollner TG, Gershenzon J, Degenhardt J (2002) The maize gene terpene synthase 1 encodes a sesquiterpene synthase catalyzing the formation of (E)-beta-farnesene, (E)-nerolidol, and (E,E)-farnesol after herbivore damage. *Plant Physiology* 130: 2049-2060
- Scutareanu P, Bruin J, Posthumus MA, Drukker B (2003) Constitutive and herbivore-induced volatiles in pear, alder and hawthorn trees. *Chemoecology* 13: 63-74

References

- Searles PS, Caldwell MM, Winter K (1995) The response of five tropical dicotyledon species to solar ultraviolet-B radiation. *American Journal of Botany* 82: 445-453
- Sessa G, Carabelli M, Sassi M, Ciolfi A, Possenti M, Mittempergher F, Becker J, Morelli G, Ruberti I (2005) A dynamic balance between gene activation and repression regulates the shade avoidance response in *Arabidopsis*. *Genes & Development* 19: 2811-2815
- Shen B, Zheng Z, Dooner HK (2000) A maize sesquiterpene cyclase gene induced by insect herbivory and volicitin: Characterization of wild-type and mutant alleles. *Proceedings of the National Academy of Sciences* 97: 14807-14812
- Smith H, Casal JJ, Jackson GM (1990) Reflection signals and the perception by phytochrome of the proximity of neighbouring vegetation. *Plant, Cell and Environment* 13: 73-78
- Snoeren TAL, Mumm R, Poelman EH, Yang Y, Pichersky E, Dicke M (2010) The herbivore-induced plant volatile methyl salicylate negatively affects attraction of the parasitoid *Diadegma semiclausum*. *Journal of Chemical Ecology* 36: 479-489
- Solomon S (1990) Progress towards a quantitative understanding of Antarctic ozone depletion. *Nature* 347: 347-354
- Staudt M, Bertin N (1998) Light and temperature dependence of the emission of cyclic and acyclic monoterpenes from holm oak (*Quercus ilex L.*) leaves. *Plant, Cell and Environment* 21: 385-395
- Stepanova AN, Robertson-Hoyt J, Yun J, Benavente LM, Xie DY, Dolezal K, Schlereth A, Jurgens G, Alonso JM (2008) TAA1-mediated auxin biosynthesis is essential for hormone crosstalk and plant development. *Cell* 133: 177-191
- Summerfelt ST, Hochheimer JN (1997) Review of ozone processes and applications as an oxidizing agent in aquaculture. *The Progressive Fish-Culturist* 59: 94-105
- Takabayashi J, Dicke M, Posthumus MA (1991) Variation in composition of predator-attracting allelochemicals emitted by herbivore-infested plants: relative influence of plant and herbivore. *Chemoecology* 2: 1-6
- Takabayashi J, Dicke M, Posthumus MA (1994a) Volatile herbivore induced terpenoids in plant mite interactions - variation caused by biotic and abiotic factors. *Journal of Chemical Ecology* 20: 1329-1354
- Takabayashi J, Dicke M, Takahashi S, Posthumus MA, Vanbeek TA (1994b) Leaf age affects composition of herbivore-induced synomones and attraction of predatory mites. *Journal of Chemical Ecology* 20: 373-386
- Tao Y, Ferrer JL, Ljung K, Pojer F, Hong F, Long JA, Li L, Moreno JE, Bowman ME, Ivans LJ, Cheng Y, Lim J, Zhao Y, Ballaré CL, Sandberg G, Noel JP, Chory J (2008) Rapid synthesis of auxin via a new tryptophan-dependent pathway is required for shade avoidance in plants. *Cell* 133: 164-176
- Tatematsu K, Kumagai S, Muto H, Sato A, Watahiki MK, Harper RM, Liscum E, Yamamoto KT (2004) MASSUGU2 encodes Aux/IAA19, an auxin-regulated protein that functions together with the transcriptional activator NPH4/ARF7 to regulate differential growth responses of hypocotyl and formation of lateral roots in *Arabidopsis thaliana*. *Plant Cell* 16: 379-393
- Tiiva P, Rinnan R, Faubert P, Räsänen J, Holopainen T, Kyrö E, Holopainen JK (2007) Isoprene emission from a subarctic peatland under enhanced UV-B radiation. *New Phytologist* 176: 346-355
- Tilbrook K, Arongaus AB, Binkert M, Heijde M, Yin R, Ulm R (2013) The UVR8 UV-B photoreceptor: Perception, signaling and response. *The Arabidopsis Book* 11
- Timkovsky J, Gankema P, Pierik R, Holzinger R (2014) A plant chamber system with downstream reaction chamber to study the effects of pollution on biogenic emissions. *Environmental Science: Processes & Impacts* 16: 2301-2312
- Ton J, D'Alessandro M, Jourdie V, Jakab G, Karlen D, Held M, Mauch-Mani B, Turlings TC (2006) Priming by airborne signals boosts direct and indirect resistance in maize. *The Plant Journal* 49: 16-26
- Turlings TCJ, Loughrin JH, McCall PJ, Röse USR, Lewis WJ, Tumlinson JH (1995) How caterpillar-damaged plants protect themselves by attracting parasitic wasps. *Proceedings of the National Academy of Sciences* 92: 4169-4174
- Ulm R, Baumann A, Oravecz A, Máté Z, Adám E, Oakeley EJ, Schäfer E, Nagy F (2004) Genome-wide analysis of gene expression reveals function of the bZIP transcription factor HY5 in the UV-B response of *Arabidopsis*. *Proceedings of the National Academy of Sciences* 101: 1397-1402
- UNEP (2011) Environmental effects of ozone depletion and its interactions with climate change: 2010 assessment. *Photochemical & Photobiological Sciences* 10: 178-181
- Unsicker SB, Kunert G, Gershenzon J (2009) Protective perfumes: the role of vegetative volatiles in plant defense against herbivores. *Current Opinion in Plant Biology* 12: 479-485

- Van de Staaij JWM, Lenssen GM, Stroetenga M, Rozema J (1993) The combined effects of elevated CO₂ levels and UV-B radiation on growth characteristics of *Elymus athericus* (= *E. pycnanathus*). *Vegetatio* 104/105: 433
- Van Poecke RMP, Posthumus MA, Dicke M (2001) Herbivore-induced volatile production by *Arabidopsis thaliana* leads to attraction of the parasitoid *Cotesia rubecula*: chemical, behavioral, and gene-expression analysis. *Journal of Chemical Ecology* 27: 1911-1928
- Van Schie CCN, Haring MA, Schuurink RC (2007) Tomato linalool synthase is induced in trichomes by jasmonic acid. *Plant Molecular Biology* 64: 251-263
- Vickers CE, Gershenzon J, Lerdau MT, Loreto F (2009) A unified mechanism of action for volatile isoprenoids in plant abiotic stress. *Nature Chemical Biology* 5: 283-291
- Voityuk AA, Marcus RA, Michel-Beyerle ME (2014) On the mechanism of photoinduced dimer dissociation in the plant UVR8 photoreceptor. *Proceedings of the National Academy of Sciences* 111: 5219-5224
- Von Dahl CC, Havecker M, Schlogl R, Baldwin IT (2006) Caterpillar elicited methanol emission: a new signal in plant-herbivore interactions? *The Plant Journal* 46: 948-960
- Walling LL (2000) The myriad plant responses to herbivores. *Journal of Plant Growth Regulation* 19: 195-216
- Wargent JJ, Jordan BR (2013) From ozone depletion to agriculture: understanding the role of UV radiation in sustainable crop production. *New Phytologist* 197: 1058-1076
- Wegener R, Schulz S, Meiners T, Hadwich K, Hilker M (2000) Analysis of volatiles induced by oviposition of elm leaf beetle *Xanthogaleruca luteola* on *Ulmus minor*. *Journal of Chemical Ecology* 27: 499-515
- Winter TR, Rostás M (2008) Ambient ultraviolet radiation induces protective responses in soybean but does not attenuate indirect defense. *Environmental Pollution* 155: 290-297
- De Wit M, Kegge W, Evers JB, Vergeer-van Eijk MH, Gankema P, Voeselek LACJ, Pierik R (2012) Plant neighbor detection through touching leaf tips precedes phytochrome signals. *Proceedings of the National Academy of Sciences* 109: 14705-14710
- De Wit M, Spoel SH, Sanchez-Perez GF, Gommers CM, Pieterse CM, Voeselek LA, Pierik R (2013) Perception of low red:far-red ratio compromises both salicylic acid- and jasmonic acid-dependent pathogen defences in *Arabidopsis*. *The Plant Journal* 75: 90-103
- Wu D, Hu Q, Yan Z, Chen W, Yan C, Huang X, Zhang J, Yang P, Deng H, Wang J, Deng X, Shi Y (2012) Structural basis of ultraviolet-B perception by UVR8. *Nature* 484: 214-219
- Zhang LY, Bai MY, Wu J, Zhu JY, Wang H, Zhang Z, Wang W, Sun Y, Zhao J, Sun X, Yang H, Xu Y, Kim SH, Fujioka S, Lin WH, Chong K, Lu T, Wang ZY (2009) Antagonistic HLH/bHLH transcription factors mediate brassinosteroid regulation of cell elongation and plant development in rice and *Arabidopsis*. *Plant Cell* 21: 3767-3780
- Ziska L, Teramura AH, Sullivan JH (1992) Physiological sensitivity of plants along an elevational gradient to UV-B radiation. *American Journal of Botany* 79: 863-871

Nederlandse samenvatting

Planten groeien veelal dicht bij andere planten. Als burenen concurreren ze met elkaar om grondstoffen zoals licht, water en mineralen. Om optimaal te presteren onder uiteenlopende omstandigheden hebben planten complexe interne communicatienetwerken ontwikkeld die bestaan uit sensoren en signaalstoffen, die er samen voor zorgen dat de plant steeds de beste strategie volgt. Planten kunnen o.a. kleuren en lichtsterkte waarnemen en hierop reageren. Ook verspreiden ze een specifieke melange van vluchtige stoffen die afhangt van omgevingsfactoren. Hieronder volgt eerst een toelichting over deze licht- en geursignalen, voordat de bevindingen van dit proefschrift uiteen worden gezet.

“Volatile organic compounds”

Vluchtige stoffen van planten (in het Engels afgekort tot BVOCs of VOCs) zijn belangrijke signaalstoffen die ook invloed hebben op klimaat en gezondheid. Welke vluchtige stoffen een plant precies uitstoot hangt af van de soort plant, de leeftijd van de bladeren en van omgevingsfactoren zoals licht, temperatuur en aanvallen door herbivoren of ziekteverwekkers. Bovendien kan de uitstoot toe- of afnemen door stress. Hierdoor bevat de melange van vluchtige stoffen die een plant uitstoot veel informatie voor eenieder die deze chemische mix kan 'lezen'. Vluchtige stoffen werken bijvoorbeeld als signaal in plant-insect interacties; wanneer een tomatenplant aangevreten wordt door spintmijten, gaat de plant geurstoffen produceren waardoor hij aantrekkelijk wordt voor roofmijten, de vijanden van de spintmijt. Recent onderzoek laat bovendien zien dat vluchtige stoffen kunnen werken als signaal tussen verschillende delen van een plant (takken) of zelfs tussen buurplanten.

Lichtsignalen: UV-B en 'groene schaduw'

Planten hebben speciale sensoren om verschillende kleuren licht waar te nemen, waaronder voor ultraviolet-B (UV-B) en voor de verhouding tussen rood en verrood (zie het spectrum van figuur 1.2). UV-B veroorzaakt schade aan de plant en vermindert de groei (figuur 3.1), maar kan ook de interactie tussen planten en herbivoren beïnvloeden. De rood:verrood-verhouding is een signaal voor 'groene schaduw', oftewel de nabijheid van buurplanten. De groene bladeren van een buurplant absorberen namelijk rood licht, terwijl ze verrood licht weerkaatsen. Daardoor daalt de rood:verrood-verhouding in een vegetatie sterk. De plant neemt dit waar en strekt zich uit naar het licht om de concurrentie voor te zijn. Dit ontwijken van schaduw heet in het Engels “shade avoidance”.

Opbouw van dit proefschrift

Dit proefschrift beschrijft hoe ultraviolet(UV)-B straling de emissie van vluchtige stoffen en het ontwijken van schaduw door planten verandert. Hoofdstuk 1 geeft een overzicht van de huidige kennis van deze processen. Hoofdstuk 6 bediscussieert de bevindingen van dit proefschrift in de context van eerdere bevindingen. De tussenliggende hoofdstukken beschrijven de methode en resultaten van het onderzoek.

Bevindingen van dit proefschrift

Om de vluchtige stoffen van planten te meten hebben we een opstelling gebouwd met twee plantenkamers en een reactiekamer (figuur 2.1). Hoofdstuk 2 laat zien hoe deze opstelling eruit ziet en hoe deze werkt. Met de twee plantenkamers kunnen we de emissies van planten vergelijken die een verschillende behandeling krijgen. Met de reactiekamer kunnen we onderzoeken hoe de vluchtige stoffen zich gedragen in de atmosfeer, onder verschillende omstandigheden, zonder de planten bloot te stellen aan deze omstandigheden. Uniek aan deze opstelling is de zeer gevoelige meetapparatuur, waarmee we de verandering van emissies over tijd kunnen bestuderen.

Hoofdstuk 3 laat zien dat UV-B de uitstoot van vluchtige stoffen door tomatenplanten verhoogt (figuur 3.2 en 3.3). Opvallend is dat de timing hiervan per stof verschilt. De uitstoot van sommige stoffen

neemt meteen toe, bij sommige duurt het even voor een verschil zichtbaar is, en bij een derde groep stijgt de emissie pas als de UV-B-blootstelling voorbij is (figuur 3.2). Deze derde groep bevat o.a. een aantal monoterpenen. Omdat dit bekende signaalstoffen zijn in plant-insect interacties, hebben we deze groep verder onderzocht. Voor een enkele stof, β -phellandreen, vonden we een relatie tussen de verhoogde uitstoot en een verhoogde activiteit van het gen dat codeert voor het enzym dat β -phellandreen maakt. Voor andere monoterpenen vonden we dit echter niet.

Hoofdstuk 4 laat zien dat eenzelfde verhoging van de uitstoot van vluchtige stoffen in UV-B plaatsvindt bij de modelsoort *Arabidopsis thaliana* (zandraket). De timing is echter anders dan bij tomatenplanten, en is dus soortafhankelijk (figuur 4.2). Verrassend genoeg is deze reactie van de plant op UV-B onafhankelijk van de UV-B sensor UVR8 (figuur 4.2 en 4.3). Er moet dus een andere sensor of mechanisme in de plant zijn die de verandering in uitstoot door UV-B veroorzaakt.

In hoofdstuk 5 onderzoeken we de interactie tussen de reacties van de plant op de twee bovengenoemde lichtsignalen; UV-B en de rood:verrood-verhouding. Door *Arabidopsis thaliana* planten tegelijk bloot te stellen aan UV-B en een zeer lage rood:verrood-verhouding, laten we zien dat UV-B het ontwijken van schaduw kan onderdrukken (figuur 5.1 en 5.2). Ook laten we zien dat deze onderdrukking afhankelijk is van de UV-B receptor UVR8. Om meer te weten te komen over de interactie tussen de communicatienetwerken die geactiveerd worden door UV-B of een lage rood:verrood-verhouding, onderzochten we een aantal eiwitten waarvan bekend is dat ze werken als signaalstoffen in één of beide netwerken. Voor enkele van deze eiwitten vonden we aanwijzingen dat ze een rol spelen in de interactie. Ook onderzochten we de rol van plantenhormonen en vonden dat zogenaamde brassinosteroiden waarschijnlijk een rol spelen in de interactie, terwijl we dit bewijs niet vonden voor de plantenhormonen auxine en gibberelline. De precieze rol van deze eiwitten en hormonen moet nu verder onderzocht worden. De bevindingen van dit proefschrift geven echter al belangrijke nieuwe inzichten in de verwevenheid van de communicatienetwerken die planten gebruiken om zich aan te passen aan hun omgeving.

Dankwoord

Een bijzonder moment is daar. Het boekje is af, ik mag mensen gaan bedanken. Dat doe je niet vaak op zo'n mooie plek, dus ik betrek hierbij graag iedereen bij die mij op welke manier dan ook heeft geholpen en geïnspireerd.

Allereerst en bovenal ben ik dank verschuldigd aan mijn promotor en copromotor. Rens en Ronald, ik ben en zal jullie altijd dankbaar zijn voor de kans die ik kreeg om te promoveren, en bovendien voor de zeer prettige omstandigheden waaronder ik dat mocht doen. Ecofysiologie van Planten (EvP) is dankzij jullie een wetenschappelijk hoogstaande en uitdagende groep met een uitzonderlijk fijne en collegiale sfeer. Het is niet voor niets dat buitenlandse medewerkers bij EvP als eerste het woord 'gezellig' leren. Ik kreeg van jullie veel vrijheid om dit project aan te gaan, maar kon ook altijd binnen lopen met mijn vragen. Ik heb heel veel van jullie geleerd, en dankzij jullie snelle reacties was het boekje op tijd klaar voor de commissie. Ik ben trots met jullie gewerkt te hebben aan dit mooie resultaat.

Scientifically, the next ones to thank should certainly be the people from IMAU, with whom we did this plant-volatile-atmospheric project. Thomas, thank you for providing the opportunity and being in my committee. Rupert, thanks for your patience in explaining me all this atmospheric chemistry stuff, I learned a lot! Joseph, both in and outside of science I learned a lot from our collaboration. We had a lot of fun practicing Dutch and once the system worked I think we were a pretty good day-and-night volatile team. Thank you for working together with me. Also thanks a lot to the technicians (Carina, Henk, Michel, Marcel) and other IMAU colleagues, I felt very welcome on the 6th floor of the BBL.

My colleagues from EvP, you are like family. You don't pick your family, and I realize how lucky I was to have you and share many great moments with you. I am grateful to have met you and proud to have worked with you. If you are ever in Amsterdam - not the most unlikely place to visit - you are always welcome at our home.

Hans en Lot, met jullie heb ik ontelbare leuke, grappige en emotionele momenten meegemaakt. Hans, jij bent een van de weinigen die mijn project van zo dichtbij heeft meegemaakt en kent mij daardoor als geen ander. Ik kon altijd bij je terecht met mijn frustraties, die we na uitgeraad te zijn heerlijk samen weglachten. Lot, je bent een zonnetje. Het was heerlijk om jouw energie om me heen te hebben. Ik ben trots dat ik zulke goede wetenschappers en lieve vrienden als paranimfen heb.

Kate, you not only helped me with scientific advice but you were also great to have next to me on the dance floor, I hope we can do that again some time. I miss you and John now that you are so far away.

Rashmi, ook jij bent verantwoordelijk voor de bovengenoemde kwaliteiten van deze groep. Bedankt voor je vriendschap en de gedeelde moeder verhalen en babykleertjes.

Debatosh, you came to us from a different world and I've never seen someone adapt so much in such a short time. I hope you get everything from life that you want, you surely deserve it. And good luck with your defence, you're up next!

Franca, ik bewonder je vermogen om altijd goede vragen te stellen en je bijna fanatieke enthousiasme voor de wetenschap. Blijf zo, ik hoop je nog vaak te zien.

Elaine and Chrysa, it was great to share the room with you. Kasper, het was kort maar krachtig, bedankt voor alle lol. Maarten, bedankt voor het delen van je protocollen, ik hoop dat ik het Italiaans goed

ontcijferd heb. Chiakai, I am glad you chose Utrecht over Wageningen. Sara, thanks for your great smile. Thijs en Henri, jullie levenslange inzet voor de wetenschap bewonder ik en ik ben blij met jullie de fascinatie voor het leven te hebben mogen delen.

Some great colleagues left the group a while before I finished. Diederik, het was meteen gezellig met jou, bedankt voor de gedeelde verhalen en biertjes. Mieke, jij bent een super wetenschapper. Asia, you know everything and you are funny, more people should learn how to do that. Wouter, bedankt dat je me verslaafd hebt gemaakt aan Radio Tour de France. Divya, thanks for many great moments. Anna, bedankt voor je warme energie. Ton, we hebben maar kort samengewerkt, maar het was altijd leuk je later weer tegen het lijf te lopen. Bedankt!

Ons oh-zo-belangrijke “ondersteunend personeel”, ze zouden jullie “essentieel personeel” moeten noemen. Emilie, Ankie, Rob en Judith, en eerder Marleen, Yvonne en Joke, laat ze jullie nooit anders vertellen, jullie zijn onmisbaar! Overstromingen, hittegolven, luizenplagen, of RNA-kit-verslindende studenten, niets krijgt jullie eronder. Zelfs geen bergen taart. Bovendien zijn jullie erg gezellig. Bedankt daarvoor en voor alle hulp.

Hulp kwam ook van de fotografen Ronald en Frits die o.a. mijn mooie coverfoto's maakten. Van de mannen van de glasblazerij en de werkplaats, zonder wie de plantenkamer op de foto niet bestaan had. Bedankt, heren!

Ook in mijn eigen woonplaats, op de Universiteit van Amsterdam, vond ik hulp bij mijn onderzoek. Bart Schimmel, Merijn Kant en Arne Janssen, bedankt voor jullie hulp bij de spintmijtproeven die ik bij jullie mocht doen. Arjen van Doorn, Michel de Vries en Petra Bleeker, jullie hebben me erg geholpen bij het denken over en meten van volatiles. Zowel de spintmijten als de analyses hebben het boekje niet gehaald, maar ach, jullie weten hoe dat gaat. Dank voor de samenwerking!

Studenten begeleiden was een uitdagend maar vooral leuk en voor mij ook leerzaam onderdeel van mijn promotie-tijd. Fons, Anne, Iko, Marize, Jan, Jesse, Graeme, Kirsten en Manon, en nogmaals Jesse, bedankt voor jullie enthousiasme voor en bijdrage aan dit project. Ik hoop dat de biologie jullie nog lang zal boeien!

Tja, en dan waren er in de andere gangen van het Kruid nog een paar biologen verstopt, met wie je op gezette tijden heel goed een biertje kon drinken, een praatje maken, of wat chemicaliën lenen. De hele bliksemse bende van PMI, waaronder Chiel, Pim, Dmitry, Roeland, Sas, Corné, Guido, Peter, Nora, Lotte, Tom, Ivan, Ainhua, Giannis en Irene, Nicole van MPF, Joost en Peter van Ecologie: bedankt!

De fascinatie voor de biologie begon natuurlijk al voor mijn promotie-tijd. Speciaal wil ik Nico van Straalen, Hans Cornelissen, Matty Berg, Nico de Wit, Marcel van der Heijden, Henk Schat en ook Anneke Wagner bedanken voor de inspirerende college's, excursies en practica op de VU. Daarbij waren Marit, Joki, Tjeu, Nadia, Jennifer en Rogier mijn liefste mede-studenten en -enthousiastelingen die die hele studie eigenlijk alleen maar leuk maakten. Ik moet zeggen dat de mensen van Gyrinus en in de Stelling daar ook zeker aan hebben bijgedragen. Lieverds en leukerds, bedankt! Very special memories I have to my internship at BCI, and I want to say very many thanks to the whole BCI population and to Allen, Scott and Aafke especially.

Lasting memories are also created when scientists meet at conferences (dull as that sounds). Scott, thanks for sharing great times and scientific discoveries. Carlos & Amy, you made me feel welcome at conferences around the world. Bas en Chris, het was super jullie steeds weer tegen te komen. Michel

(Haring) en Marcel (Dicke), heel fijn hoe benaderbaar jullie als ‘grote jongens’ zijn, ik hoop nog eens een biertje te drinken samen.

Dan de mensen buiten de biologie. Jullie bijdrage aan mijn geestelijke gezondheid en dus aan de totstandkoming van dit boekje dient niet onderschat te worden. Mijn lieve vrienden Merel, Nadia, Lehman en Paul, ik geniet enorm van alle dingen die we delen en hoop dat dat nog lang door mag gaan. Vrienden ‘van Gijs’; Guusje (surfdudette, bedankt voor de cover!), Martijn (altijd pret), Markus en Femke, Derk en Susan, Duco en Karin, Jona, Matthijs en Bianca, Died en Eva, Bert en Hinke, het is altijd heerlijk om te eten en te drinken, te kletsen en de dansen in jullie gezelschap. Dansen doe ik ook heel graag met de ‘Party-people’; met Miguel, Claudia, Ruben, Sander, Guido, Vlien, Annemarie, Pauline, Edgar, Tiago, Juanma, Laura en de rest, maar vooral met Bart en Janneke, wiens groeiende vriendschap mij zeer dierbaar is.

Tenslotte wil ik bedanken bij wie het allemaal begon en bij wie het elke dag weer eindigt, mijn familie. Pap en mam, bedankt dat jullie me altijd de vrijheid, maar vooral ook het vertrouwen hebben gegeven mijn eigen weg te gaan. Zonder jullie was me dit niet gelukt. Frank, broeder, je hebt een onvervangbare plek in mijn hart. Mijn lieve Gijs, we zijn een uitermate goed team, ik hoop dat we dat altijd zullen blijven. Heel erg bedankt voor je steun en begrip in de afgelopen jaren.

Als allerlaatste bedank ik nog de aarde en haar leven, zonder wier oneindige schoonheid en complexiteit de verwondering en de liefde niet zouden bestaan.

Bedankt! Thank you!

Paulien

Curriculum vitae

Paulien Gankema was born on the 22nd of August, 1984 in Emmen, the Netherlands. After finishing her secondary education at the Esdal College in Emmen in 2002, she started studying Biology at VU University in Amsterdam. During her studies, she was an active member of the academic community. She served as a board member of her students association for a year, was the president of the excursion committee for several years and started an advisory committee. On top, she served for two years in the faculty's student board and was a teaching assistant for several biology and biochemistry courses. As a part of her master program, she did internships at the University of Amsterdam (UvA) and at the Smithsonian Tropical Research Institute (STRI) in Panama. Her project at the UvA focused on direct and indirect defences of tomato plants against herbivores, and involved molecular as well as physiological techniques. Her project at STRI focused on differential effects of arbuscular mycorrhizal fungi on growth of a pioneer tree species in the tropical moist forest of Barro Colorado Island (BCI). This involved setting up and conducting a field experiment on BCI as well as identifying fungal species with molecular techniques at the laboratory of Animal Ecology at VU University in Amsterdam. After obtaining her MSc degree in 2008, Paulien returned to Panama for a second sampling effort, and wrote a research proposal to continue working on this project. When this was unsuccessful, she continued her scientific career as a PhD student in the Plant Ecophysiology group at Utrecht University, the Netherlands, under supervision of prof.dr. L.A.C.J. Voesenek and prof.dr. R. Pierik. The result of this project is described in this thesis. Paulien currently works as a campaigner on sustainable food for Friends of the Earth the Netherlands (Milieudefensie) in Amsterdam.